Sandia National Laboratories
Waste Isolation Pilot Plant

Analysis Report for the CRA-2004 PABC Culebra Flow and Transport Calculations

Task Number
1.4.1.1

Author: Thomas S Lowry (6115) for Thomas Lowry 10/19/05
Print Signature Date

Author: Joseph F. Kanney (6821) 10/19/05
Print Signature Date

Technical Review: Joshua S Stein (6852) Mario Chavez for 10/19/05
Print Signature Date

QA Review: Mario J. Chavez (6820) Mario Chavez 10/19/05
Print Signature Date

Management Review: David S. Kessel (6821) David Kessel 10/19/05
Print Signature Date

CONTENTS

FIGURES

TABLES

1 Introduction

The Waste Isolation Pilot Plant (WIPP) is a deep geologic repository developed by the U.S. Department of Energy (DOE) for the disposal of transuranic (TRU) radioactive waste. Containment of TRU waste at the WIPP is regulated by the U.S. Environmental Protection Agency (EPA) according to the regulations set forth in Title 40 of the Code of Federal Regulations (CFR), Parts 191 and 194. The DOE demonstrates compliance with the containment requirements in the regulations by means of performance assessment (PA) calculations.

PA calculations were included in DOE's 1996 WIPP Compliance Certification Application (CCA, U.S. DOE 1996), and in a subsequent Performance Assessment Verification Test (PAVT, MacKinnon and Freeze 1997a, 1997b, 1997c). Based, in part, on the CCA and PAVT PA calculations, the EPA certified that the WIPP met the containment criteria in the regulations and was approved for disposal of transuranic waste in May 1998. PA calculations were also an integral part of DOE's 2004 WIPP Compliance Recertification Application (CRA-2004, U.S. DOE 2004). The CRA-2004 is currently being reviewed by the EPA.

WIPP PA calculations estimate the probability and consequence of radionuclide releases from the repository to the accessible environment for a regulatory period of 10,000 years after facility closure. For the purposes of WIPP PA, the accessible environment is considered to be the ground surface and/or the lateral limits of subsurface within the land withdrawal boundary (LWB). Among other release mechanisms, WIPP PA assesses the probability and consequence of radionuclide releases from the repository to the accessible environment due to the movement of radionuclide contaminated brines moving up a (sealed) shaft or oil/gas exploration borehole, and migrating laterally to the LWB in the Culebra Member of the Rustler Formation.

Radionuclide movement through the Culebra is a function of the groundwater flow field and the transport properties of the radionuclide species being considered. Groundwater flow velocity and direction is highly dependent upon the magnitude and the spatial variability of hydraulic transmissivity field (T-field). WIPP PA considers the potential for future potash mining in the McNutt potash zone of the Salado Formation underlying the Rustler to cause subsidence in the Culebra and hence increase Culebra transmissivity.

During their review of the CRA-2004, the EPA did not agree with the one aspect of DOE's approach to account for the potential effect of potash mining on Culebra T-fields. EPA disagreed with the use of a 1-mile-radius exclusion zone around existing oil and gas wells for potash resources outside the LWB (Cotsworth 2004, comment G-11). In response to comment G-11, the potash mining areas were redefined to consist of all mined and un-mined potash resources including where they fall within 1-mile exclusion zones around oil and gas wells. Based upon the new mining areas, the mining

modifications to the Culebra T-fields and the Culebra flow fields were re-calculated in Lowry (2004).

During their review of the CRA-2004, the EPA also requested an additional performance assessment calculation be conducted with modified assumptions and parameter values (Cotsworth 2005). This set of calculations is referred to as WIPP 2004 Compliance Recertification Application Performance Assessment Baseline Calculation (CRA-2004 PABC). The CRA-2004 PABC mainly repeats the CRA-2004 PA calculations with modifications to certain modeling assumptions, codes, and input data/parameters. See Kanney and Leigh (2005) for detailed information on the changes made for the CRA-2004 PABC. In Cotsworth (2005), EPA requested that the redefined process for mining modifications described in Lowry (2004) be used in the Culebra flow and transport calculations for the CRA-2004 PABC. Kanney (2005) describes the detailed plan for implementing this request.

1.1 Organization

The work reported herein was conducted under Analysis Plan for Culebra Transport Calculations: Post CRA Baseline Calculation (AP-121, Kanney 2005) and Analysis Plan for Post CRA PA Baseline Calculation (AP-122, Kanney and Leigh 2005).

Background information on groundwater flow and solute transport within the Culebra is presented in section 2. Calculation of the mining-modified Culebra T-fields and the subsequent flow-field calculations are described in section 3. The radionuclide transport simulations are reported in section 4. Results of the flow and transport calculations are summarized and conclusions are drawn in section 5.

2 Background

The WIPP repository is located approximately 26 miles (42 kilometers) southeast of Carlsbad, New Mexico. The disposal horizon of the WIPP is approximately 2,150 feet (655 meters) below the ground surface in the Salado Formation of the Delaware Basin. The Salado is regionally extensive, consisting predominantly of halite, a low permeability evaporite (Powers et al. 1978).

The Rustler Formation is located above the Salado and is of particular importance in estimating the potential for radionuclide releases from the WIPP because it contains the most transmissive units above the repository. In the vicinity of the WIPP, the Rustler consists of evaporite units interbedded with carbonates and siliciclastic units (Vine 1963, Holt and Powers 1988). The Culebra Dolomite Member has been identified as the most transmissive unit in the Rustler and consequently the most likely pathway for subsurface transport of radionuclides.

The Culebra is an approximately 7.7 meter thick fractured dolomite with nonuniform properties in both the horizontal and vertical directions (Holt 1997). There are multiple scales of porosity and permeability within the Culebra ranging from microfractures to potentially large vuggy zones. Flow occurs through fractures, vugs and, to some extent, through intergranular pores. The large permeability contrast between the different scales of inter-connected porosity suggests a dual porosity conceptualization consisting of advective porosity (also referred to as fracture porosity) and diffusional porosity (also known as matrix porosity). The advective porosity is thought to consist of the void space contained in the highly transmissive portions of the rock such as large open fractures and/or interconnected vugs. The diffusional porosity represents the intergranular and intragranular porosity and may also include microfractures and/or vugs. Tracer tests conducted at the WIPP site have demonstrated both advective transport and matrix diffusion (Meigs et al. 2000).

Although the Culebra properties vary in the vertical direction, the error introduced by modeling the Culebra in two rather than three dimensions has been determined to be negligible for the objective of groundwater flow and radionuclide transport calculations (Corbet 1996).

Potash mining in the WIPP area involves resource extraction below the Culebra dolomite in the McNutt Potash zone, which is part of the larger Salado Formation (Ramsey et al., 1996) that underlies the Rustler Formation. It is hypothesized that subsidence of the Culebra due to mining extraction causes fracturing and unconsolidation of the aquifer material that results in higher transmissivities. This increase in transmissivity may significantly change the regional groundwater flow pattern in the Culebra and additionally the transport of any nuclides entering the aquifer from the underlying repository. WIPP PA includes mining scenario calculations to estimate the impact potash mining may have on groundwater flow and radionuclide transport.

The key steps in estimating radionuclide transport through the Culebra include: 1) constructing conditioned geostatistical realizations of Culebra hydraulic transmissivity fields (T-fields); 2) modifying the T-fields to account for potential subsidence due to potash mining in formations beneath the Culebra; 3) calculating steady state groundwater flow fields for each mining-modified T-field; and 4) calculating radionuclide transport through the Culebra for each flow field. Culebra transport simulations calculate the cumulative discharge at the land withdrawal boundary over the 10,000-year regulatory period due to a source located at the center of the waste panel area. The source releases 1 kg for each of several radionuclides over the first 50 years of the simulation.

The work reported herein does not include constructing conditioned geostatistical realizations of Culebra T-fields (step 1) since T-fields produced for the CRA-2004 PA are re-used in this analysis. A detailed discussion of these T-Fields is available in the CRA-2004 (U.S. DOE 2004, Appendix PA, Attachement TFIELD).

3 Culebra T-Field Mining Modifications and Flow Field Calculations

3.1 Overview

The CRA-2004 PABC Culebra T-field mining modifications and flow field calculations will follow the procedure used in Lowry (2004), with the exception that a new set of sampled values for the random mining modification factor (CULEBRA:MINP_FAC) will be employed. Changes in the number of sampled parameters for the CRA-2004 PABC require that CULEBRA:MINP_FAC be re-sampled. This new set of calculations will also be performed using formal run control techniques. The procedure for this analysis is summarized below.

1. Obtain the sampled values for the random mining modification factor (100 vectors x 3 replicates).

2. Map potential areas of future potash mining onto the groundwater modeling domain for both full and partial mining scenarios.

3. Apply the mining modification factor to the 100 stochastically calibrated T-fields from Beauheim (2003) and McKenna and Hart (2003b). This will produce 600 mining-modfied T-fields (100 vectors x 2 mining scenarios x 3 replicates).

4. Perform steady-state flow simulations for each mining-modified T-field using MODFLOW 2000.

5. Perform particle tracking using the new mining-affected flow-fields to determine travel times to the LWB.

6. Refine the flow field to smaller grid size for use in the radionuclide transport calculations.

This analysis report represents the latest effort in characterizing mining effects in the Culebra and highlights the differences and additions relative to past calculations (Ramsey and Wallace 1996, Wallace 1996, Lowry 2003b, a, Lowry 2004). Specifically it will address the differences between Lowry (2004) that result from the CRA-2004 PABC sampling of the random mining modification factors. The reader is encouraged to review the past documents for further background information.

The CRA-2004 PABC models two categories of mining-impacted transmissivity fields: one with mining outside the land withdrawal boundary (LWB) only and the other with regions both inside and outside the LWB mined (partial and full-mining scenarios, respectively).

Flow modeling is performed starting with 100 stochastically calibrated T-fields from Beauheim (2003) and McKenna and Hart (2003b). Each T-field is modified to reflect the effects of mining by multiplying the transmissivity value in cells that lie within designated mining zones by a random factor between 1 and 1000. The range of this factor is set by the EPA in regulation 40CFR Part 194, p. 5229 (Federal Register/vol. 61, No. 28) and is reproduced in Wallace (1996). The scaling factor for each T-field is provided from Latin Hypercube Sampling (LHS).

A forward steady-state flow simulation is run for each new T-field under each mining scenario (full and partial) across three replicates of mining factors, resulting in 600 simulations. Particle tracking is performed on the modified flow fields to determine the flow path and groundwater travel time from a point above the center of the WIPP disposal panels to the LWB. Cumulative probability distribution functions (CDFs) are produced for each mining scenario and compared to the undisturbed scenario generated from Task 4 of AP-088 (McKenna and Hart 2003b), as well as to the full- and partial-mining scenarios from Lowry (2004). The CDFs describe the probability of a conservative tracer reaching the LWB at a given time. In addition to comparing travel times, particle-tracking directions are also examined to determine the effect on the regional flow direction in the WIPP area due to mining.

The flow fields generated from the mining scenarios are then refined as part of Tasks 4 of Kanney (2005) and passed to Tasks 7 and 8 of Kanney (2005), which performs radionuclide transport modeling in the Culebra. The detailed methodology involved in these tasks can be found in Lowry (2003b). Their inclusion in this report is only to provide context to the procedures and approach used in these calculations.

3.2 *Approach*

3.2.1 Modeling Assumptions

Besides assumptions inherent in all modeling exercises (e.g. physical processes can be adequately parameterized and estimated on a numerical grid) there are several assumptions that are specific and important to the CRA-2004 PABC analysis. Those assumptions are as follows:

1. It is assumed that the boundary conditions along the model domain boundary are known and are not dependent on mining. The reasoning for this assumption is described in Section 3.2.4.
2. It is assumed that the flow-field over the duration of the particle tracking and transport times can be adequately represented by steady-state conditions. This is related to the first assumption in that the boundary conditions are also assumed to remain constant over time. This assumption is necessary since data do not exist that can predict the transient conditions at the site over the time frames involved (>100,000 years).
3. It is assumed that the mining effects can be adequately represented with a single mining factor that increases the transmissivity uniformly across the potential mining

zones within the Culebra. This is directed by EPA regulation 40CFR Part 194, p. 5229 and is assumed adequate for this Task. The regulation is included as an appendix in Wallace (1996).

4. Mining will occur in the previously omitted 1 mile radius exclusion zones around existing oil and gas wells as well as all regions with identified potash resources.

Other assumptions related to this analysis can be found in McKenna and Hart (2003b).

3.2.2 Software and Run Control

The mining-modified Culebra flow fields were produced on the WIPP PA Pentium 4 Cluster using MODFLOW2000 (MF2K, Harbough et al. 2000), DTRKMF (WIPP PA 2002), and several utility codes. Note that this platform is different from that used in the previous CRA-2004 mining modification and flow field calculations. Migration of the codes to the WIPP PA Pentium Cluster and subsequent regression testing are described in Kirchner (2005a) and Hart (2005), respectively.

With the exception of preparing the mining maps, the calculations were performed under formal run control, using the scripts shown in Table 3.1. The run control scripts extracted executables and input files from access-controlled repositories, performed the calculations in access-controlled directories, and stored the output files in access-controlled repositories. The Run Control Coordinator performed the calculations using a reserved account (run_mast) on the cluster. Input and output files were archived using the Concurrent Version System (CVS) application. See Long and Kanney (2005) for a detailed description of the WIPP PA Pentium 4 Cluster , the run control procedures, and CVS.

At the highest level, the mining modification simulations were run using a general purpose Perl script (ARCONS). ARCONS performs five major functions: 1) set up of temporary directories and log files, 2) check out the model codes/scripts and input files from the CVS repositories, 3) execution of the codes/scripts on a single computer or on one or mode nodes of a cluster, 4) check the output and log files into the CVS repositories, and 5) clean up the temporary directories.

The ARCONS script input and output files are shown in Table 3.2. The ARCONS input control file is mining_pabc.ctrl. The check-in and check-out functions are controlled by the contents of the mining_pabc.checkin and mining_pabc.checkout files, respectively. These files specify the repository to be used, the repository flags, and the names of the files or directories to be checked in or out. For the Culebra flow calculations, ARCONS invokes the mining_pabc.execute bash script which actually runs the computational codes (the WIPP PA codes MF2K and DTRKMF, plus a number of Fortran utility codes and bash utility scripts).

Table 3.1 Culebra Mining Modification and Flow Calculation Run Control Scripts

Script	CVS Repository	CVS Module	CVS Tag
ARCONS	$CVSLIB/CRA1BC	Mining/RunControl/arcons_2.0	AP-122
mining_pabc.execute	$CVSLIB/CRA1BC	Mining/RunControl/mining_pabc.execute	AP-122

Table 3.2 ARCONS Script Input and Output Files

CVS Module	CVS Repository	CVS Tag
Mining/RunControl/mining_pabc.ctrl	$CVSLIB/CRA1BC	AP-122
Mining/RunControl/mining_pabc.checkout	$CVSLIB/CRA1BC	AP-122
Mining/RunControl/mining_pabc.checkin	$CVSLIB/CRA1BC	AP-122
Mining/RunControl/mining_pabc.log	$CVSLIB/CRA1BC	AP-122

The combined action of the ARCONS and mining_pabc.execute scripts are described below:

1. ARCONS reads its input control file (mining_pabc.ctrl).
2. ARCONS checks out the files and directories specified in the file mining_pabc.checkin.
    a. Extract the MF2K and DTRKMF executables from the MODFLOW2K repository ($CVSLIB/MODFLOW2K), as shown in Table 3.3.
    b. Extract the MF2K and DTRKMF input files for the 100x100m grid from the MODFLOW2K repository (see Table 3.4).
    c. Extract the MODFLOW2000 input files for the 50x50m grid from the MODFLOW2K repository (see Table 3.5).
    d. Extract input files used by utility codes and scripts from the CRA1BC repository ($CVSLIB/CRA1BC), as shown in Table 3.6.
    e. Extract the Fortran utility source files and bash utility scripts (see Table 3.7).

3. ARCONS invokes the mining_pabc.execute bash script, which performs the following steps:
    a. Uncompress the MF2K and DTRKMF input files (file.gz → file).
    b. Edit file paths in the MF2K input file (steady.nam) and the DTRKMF input files (dtrkmf.in and wippctrl.inp) in the 100x100 directory to point to run_mast home directory.
    c. Edit file paths in the MF2K input file steady.nam in the 50x50 directory to point to run_mast home directory.
    d. Compile and link the Fortran utility codes ba, min_fact, ptout, ptplot, and ref_qsub.
    e. Extract the 100 calibrated Culebra transmissivity fields (T-fields) from CVS repository $CVSLIB/MODFLOW2K. The T-field ID's (or runs) are contained in the file Good_runs.txt (see Table 3.8). These are on 100x100 m grids.
    f. Loop over replicates contained in the file Replicate.txt (i.e., R1, R2 R3). Loop over mining scenarios (full and partial) for each replicate. Loop

over T-fields for each replicate/scenario combination, constructing bash scripts R*r-s-run*.sh, where $r \in \{1, 2, 3\}$, $s \in \{\text{full, partial}\}$ and $run \in \{\text{Good\_runs.txt}\}$. Each script is submitted to the batch queue and routed to a compute node for execution. Each script performs the following functions:

i. Run the min_fact utility on the calibrated T-fields to produce mining-modified T-fields (100x100m grid). See Table 3.9 for input and output file names and locations.
ii. Run the ref_qsub utility to refine the 100x100m grid mining-modified T-fields to a 50x50m grid. See Table 3.10 for input and output file names and locations.
iii. Compute flow field on 100x100 grid with MF2K. See Table 3.11 for input and output file names and locations.
iv. Perform particle tracking on 100x100 grid using DTRKMF. See Table 3.12 for input and output file names and locations.
v. Compute flow field on 50x50 grid using MF2K. See Table 3.13 for input and output file names and locations.

g. Invoke the post.sh script to move the DTRKMF output files to a common directory. See Table 3.14 for input and output file names and locations.
h. Run the ptout utility to combine the DTRKMF output into two files. See Table 3.15 for input and output file names and locations.
i. Run the ptplot utility to put all the particle track (x,y) coordinate pairs into one file for plotting purposes. See Table 3.16 for input and output file names and locations.
j. Create ASCII budget files (for use in Culebra transport calculations) from MF2K 50x50 grid binary output budget file. The ba.sh script loops over replicates, mining scenarios, and T-field IDs running the ba utility on the 50x50 grid binary output budget file. See Table 3.17 for input and output file names and locations.
k. Rename budget files (assign flow field numbers). The pabc_mining.execute script loops over replicates, mining scenarios and T-field IDs, copying the ASCII budget files to files that follow the naming convention mf2k_cra1bc_*rep_scen_ff*.out, where $rep \in \{1, 2, 3\}$, $scen \in \{\text{mp,mf}\}$ for each rep, and $ff \in \{001, 002, ..., 100\}$ for each $scen$. See Table 3.18 for input and output and output file names and locations. Table 3.19 provides a mapping between vectors, T-fields, and flow fields for each replicate.

4. ARCONS checks in all the files in the directories specified in the file mining_pabc.checkin (see Table 3.20).

Table 3.3 MODFLOW2000 and DTRKMF binaries in CVS repository $CVSLIB/MODFLOW2K

Directory	File	Tag
bin/mf2k	mf2k_1.6.release[1]	Release
bin/dtrkmf	dtrkmf_v0100	qa

1. Note that the code name and build date listed in CRA-2004 PABC Analysis Plan (AP-122, Kanney and Leigh 2005) are incorrect. The correct code name is listed here. The correct code name and build date is listed in the CRA-2004 PABC Culebra Transport Calculation Analysis Plan (AP-121, Kanney 2005) and the PABC Run Control Report (Long and Kanney 2005).

Table 3.4 MODFLOW2000 and DTRKMF input files (100x100m grid)[1]

Directory	File1[1,2]	Tag	Remark
mining/100x100	steady.nam.gz	culebra	MF2K name file
	steady.ba6.gz	culebra	MF2K basic input file
	steady.bc6.gz	culebra	MF2K block-centered flow module input file
	steady.dis.gz	culebra	MF2K discretization input file
	steady.lmg.gz	culebra	MF2K linear solver input file
	steady.oc.gz	culebra	MF2K output control file
	culebra.ibd.gz	culebra	Culebra boundary conditions
	culebra.ihd.gz	culebra	Culebra initial heads
	culebra.top.gz	culebra	Culebra top elevations
	culebra.bot.gz	culebra	Culebra bottom elevations
	dtrkmf.in.gz	culebra	DTRKMF command line arguments
	wippctrl.inp.gz	culebra	DTRKMF input control file
	wippctrl_old.inp.gz	culebra	Not used in this analyses
	multi.in.gz	culebra	Not used in this analyses
	multi.inp.gz	culebra	Not used in this analyses

1. CVS repository $CVSLIB/MODFLOW2K
2. ".gz" extension indicates file compressed using the gzip file compression application. File uncompressed before use.

Table 3.5 MODFLOW2000 input files (50x50m grid)[1]

Directory	File[1,2]	Tag	Remark
mining/50x50	steady.nam.gz	culebra	MF2K name file
	steady.ba6.gz	culebra	MF2K basic input file
	steady.bc6.gz	culebra	MF2K block-centered flow module input file
	steady.dis.gz	culebra	MF2K discretization input file
	steady.lmg.gz	culebra	MF2K linear solver input file
	steady.oc.gz	culebra	MF2K output control file
	cNew.ibd.gz	culebra	Culebra boundary conditions
	cNew.ihd.gz	culebra	Culebra initial heads
	cNew.top.gz	culebra	Culebra top elevations
	cNew.bot.gz	culebra	Culebra bottom elevations

1. CVS repository $CVSLIB/MODFLOW2K
2. ".gz" extension indicates file compressed using the gzip file compression application. File uncompressed before use.

Table 3.6 Input files for mining_pabc.execute and other utilities

Directory	File	CVS Tag	Remark
Mining/Inputs	Good_runs_all.txt	AP-122	not used in this analyses (same as Good_runs.txt)
	Good_runs.txt	AP-122	list of T-field IDs
	mfR1.txt[2]	AP-122	T-field- mining factor pairs
	mfR2.txt[2]	AP-122	T-field- mining factor pairs
	mfR3.txt[2]	AP-122	T-field- mining factor pairs
	New_Full.dat	AP-122	Full-mining scenario mining zone map
	New_Part.dat	AP-122	Partial-mining scenario mining zone map
	Replicate.txt	AP-122	Replicates list
	sum1_st2d_cra1bc_r1.tbl	AP-122	Vector-mining factor-flow field mapping
	sum1_st2d_cra1bc_r2.tbl	AP-122	Vector-mining factor-flow field mapping
	sum1_st2d_cra1bc_r3.tbl	AP-122	Vector-mining factor-flow field mapping

1. CVS repository $CVSLIB/MODFLOW2K
2. T-field-mining factor pairs for each replicate constructed from Good_runs.txt and vector-mining factor-flow field mapping. Row number of T-field in Good_runs.txt matched with vector number in sum1_st2d_cra1bc_r*.tbl. The vector-mining factor-flow field mapping tables are produced in Step 4 of the Culebra transport calculations (see section 4) and transferred to the Pentium Cluster.

Table 3.7 Utility Fortran Codes and Bash Scripts Used by mining_pabc.execute Script

CVS Module	CVS Repository	CVS Tag
Mining/Src/ba.f90	$CVSLIB/CRA1BC	AP-122
Mining/Src/min_fact.f90	$CVSLIB/CRA1BC	AP-122
Mining/Src/ptout.f	$CVSLIB/CRA1BC	AP-122
Mining/Src/ptplot.f90	$CVSLIB/CRA1BC	AP-122
Mining/Src/ref_qsub.f90	$CVSLIB/CRA1BC	AP-122
Mining/Src/ba.sh	$CVSLIB/CRA1BC	AP-122
Mining/Src/post.sh	$CVSLIB/CRA1BC	AP-122

Table 3.8 Contents of Good_runs.txt file

Row	T-Field
1	d01r02
2	d01r04
3	d01r07
4	d01r10
5	d02r02
6	d03r01
7	d03r03
8	d03r06
9	d03r07
10	d03r08
11	d03r09
12	d04r01
13	d04r02
14	d04r03
15	d04r04
16	d04r05

Table 3.8 Contents of Good_runs.txt file

Row	T-Field
17	d04r06
18	d04r07
19	d04r08
20	d04r10
21	d05r03
22	d05r07
23	d06r02
24	d06r03
25	d06r04
26	d06r05
27	d06r06
28	d06r07
29	d06r10
30	d07r01
31	d07r02
32	d07r05
33	d07r06
34	d07r07
35	d07r08
36	d07r09
37	d07r10
38	d08r01
39	d08r02
40	d08r03
41	d08r04
42	d08r05
43	d08r06
44	d08r07
45	d09r02
46	d09r03
47	d09r04
48	d09r05
49	d09r06
50	d09r07
51	d09r08
52	d09r09
53	d09r10
54	d10r02
55	d10r03
56	d10r04
57	d10r06
58	d10r07
59	d10r08
60	d10r09

Table 3.8 Contents of Good_runs.txt file

Row	T-Field
61	d10r10
62	d11r01
63	d11r02
64	d11r06
65	d11r07
66	d11r08
67	d11r09
68	d11r10
69	d12r01
70	d12r02
71	d12r03
72	d12r05
73	d12r06
74	d12r07
75	d12r08
76	d12r09
77	d13r01
78	d13r02
79	d13r03
80	d13r05
81	d13r06
82	d13r07
83	d13r08
84	d13r09
85	d21r01
86	d21r02
87	d21r03
88	d21r04
89	d21r05
90	d21r06
91	d21r07
92	d21r10
93	d22r02
94	d22r03
95	d22r04
96	d22r06
97	d22r07
98	d22r08
99	d22r09
100	d22r10

Table 3.9 Input and output files for T-field mining modification (100x100m grid)

	File/Module[1,2,3]	CVS Repository	CVS Tag
Input	trans/runs/*run*/Tupdate.mod	$CVSLIB/MODFLOW2K	Done
Input	Mining/Inputs/mfR*r*.txt	$CVSLIB/CRA1BC	AP-122
Input	Mining/Inputs/New_Full.dat	$CVSLIB/CRA1BC	AP-122
Input	Mining/Inputs/New_Part.dat	$CVSLIB/CRA1BC	AP-122
Output	Mining/Outputs/R*r*/full/*run*/Cmine.mod	$CVSLIB/CRA1BC	AP-122
Output	Mining/Outputs/R*r*/partial/*run*/Cmine.mod	$CVSLIB/CRA1BC	AP-122

1. $r \in \{1, 2, 3\}$
2. *scen* $\in$ {full, partial} for each *r*
3. *run*$\in$ {Good_runs.txt} for each *scen*

Table 3.10 Input and output files for grid refinement of mining-modified T-fields

	File/Module[1,2,3]	CVS Repository	CVS Tag
ref_qsub			
Input	Mining/Outputs/R*r*/full/*run*/Cmine.mod	$CVSLIB/CRA1BC	AP-122
Input	Mining/Outputs/R*r*/partial/*run*/Cmine.mod	$CVSLIB/CRA1BC	AP-122
Output	Mining/Outputs/R*r*/full/*run*/Tnew.mod	$CVSLIB/CRA1BC	AP-122
Output	Mining/Outputs/R*r*/partial/*run*/Tnew.mod	$CVSLIB/CRA1BC	AP-122

1. $r \in \{1, 2, 3\}$
2. *scen*$\in$ {full, (part)ial} for each *r*
3. *run*$\in$ {Good_runs.txt} for each *scen*

Table 3.11 Input and output files for flow field calculations on 100x100m grid

	File/Module[1,2,3]	CVS Repository	CVS Tag
MF2K			
Input	steady.nam	NOT KEPT	NOT KEPT
Input	Mining/Outputs/R*r*/*scen*/*run*/steady100x100.bud	$CVSLIB/CRA1BC	AP-122
Input	mining/100x100/steady.dis	$CVSLIB/MODFLOW2K	culebra
Input	mining/100x100/culebra.ihd	$CVSLIB/MODFLOW2K	culebra
Input	mining/100x100/culebra.ibd	$CVSLIB/MODFLOW2K	culebra
Input	mining/100x100/culebra.top	$CVSLIB/MODFLOW2K	culebra
Input	mining/100x100/culebra.bot	$CVSLIB/MODFLOW2K	culebra
Input	mining/100x100/steady.ba6	$CVSLIB/MODFLOW2K	culebra
Input	mining/100x100/steady.bc6	$CVSLIB/MODFLOW2K	culebra
Input	mining/100x100/steady.oc	$CVSLIB/MODFLOW2K	culebra
Input	mining/100x100/steady.lmg	$CVSLIB/MODFLOW2K	culebra
Output	Mining/Outputs/R*r*/*scen*/*run*/steady100x100.bud	$CVSLIB/CRA1BC	AP-122
Output	Mining/Outputs/R*r*/*scen*/*run*/steady100x100.lst	NOT KEPT	NOT KEPT
Output	Mining/Outputs/R*r*/*scen*/*run*/steady100x100.hed	NOT KEPT	NOT KEPT

1. $r \in \{1, 2, 3\}$
2. *scen*$\in$ {full, (part)ial} for each *r*
3. *run*$\in$ {Good_runs.txt} for each *scen*

Table 3.12 Input and output files for particle tracking calculations (100x100m grid)

	Module[1,2,3,4]	CVS Repository	CVS Tag
Script ***(mining_pabc.execute)***			
Input	dtrkmf.in	NOT KEPT	NOT KEPT
DTRKMF			
Input	wipptctrl.inp	NOT KEPT	NOT KEPT
Input	Mining/Outputs/R*r*/*scen*/*run*/steady100x100.bud	$CVSLIB/CRA1BC	AP-122
Input	mining/100x100/steady.dis	$CVSLIB/MODFLOW2K	culebra
Output	Mining/Outputs/R*r*/*scen*/*run*/dtrk.out	$CVSLIB/CRA1BC	AP-122
Output	Mining/Outputs/R*r*/*scen*/*run*/dtrk.dbg	$CVSLIB/CRA1BC	AP-122

1. $r \in \{1, 2, 3\}$
2. *scen*$\in$(full, (part)ial) for each *r*
3. *run*$\in$(Good_runs.txt) for each *scen*
4. dtrkmf.in and wippctrl.inp files used here are produced from copies shown in Table 3.4 by editing file paths to point to the current working directory.

Table 3.13 Input and output files for flow field calculations on 50x50m grid

	File/Module[1,2,3]	CVS Repository	CVS Tag
MF2K			
Input	steady.nam	NOT KEPT	NOT KEPT
Input	Mining/Outputs/R*r*/*scen*/*run*/steady50x50.bud	$CVSLIB/CRA1BC	AP-122
Input	mining/50x50/steady.dis	$CVSLIB/MODFLOW2K	culebra
Input	mining/50x50/cNew.ihd	$CVSLIB/MODFLOW2K	culebra
Input	mining/50x50/cNew.ibd	$CVSLIB/MODFLOW2K	culebra
Input	mining/50x50/cNew.top	$CVSLIB/MODFLOW2K	culebra
Input	mining/50x50/cNew.bot	$CVSLIB/MODFLOW2K	culebra
Input	mining/50x50/steady.ba6	$CVSLIB/MODFLOW2K	culebra
Input	mining/50x50/steady.bc6	$CVSLIB/MODFLOW2K	culebra
Input	mining/50x50/steady.oc	$CVSLIB/MODFLOW2K	culebra
Input	mining/50x50/steady.lmg	$CVSLIB/MODFLOW2K	culebra
Output	Mining/Outputs/R*r*/*scen*/*run*/steady50x50.bud	$CVSLIB/CRA1BC	AP-122
Output	Mining/Outputs/R*r*/*scen*/*run*/steady50x50.lst	NOT KEPT	NOT KEPT
Output	Mining/Outputs/R*r*/*scen*/*run*/steady50x50.hed	NOT KEPT	NOT KEPT

1. $r \in \{1, 2, 3\}$
2. *scen* $\in$ (full, partial) for each *r*
3. *run*$\in$(Good_runs.txt) for each *scen*

Table 3.14 Input and Output files for post.sh script

	File/Module[1,2,3]	CVS Repository	CVS Tag
Script (post.sh)			
Input	Mining/Outputs/R*r*/*scen*/*run*/dtrk.out	$CVSLIB/CRA1BC	AP-122
Output	Mining/Outputs/R*r*/ptout/*run*-*scen*.out	$CVSLIB/CRA1BC	AP-122

1. $r \in \{1, 2, 3\}$
2. *scen* $\in$ {full, partial} for each *r*
3. *run* $\in$ {Good_runs.txt} for each *scen*

Table 3.15 Input and Output files for ptout utility

	File/Module[1,2,3]	CVS Repository	CVS Tag
ptout			
Input	Mining/Outputs/R*r*/ptout/*run*-scen.out	$CVSLIB/CRA1BC	AP-122
Output	Mining/Outputs/R*r*/ptout/ptout.out	$CVSLIB/CRA1BC	AP-122
Output	Mining/Outputs/R*r*/ptout/times.out	$CVSLIB/CRA1BC	AP-122

1. $r \in \{1, 2, 3\}$
2. *scen* $\in$ {full, partial} for each *r*
3. *run* $\in$ {Good_runs.txt} for each *scen*

Table 3.16 Input and Output files for ptplot utility

	File/Module[1,2,3]	CVS Repository	CVS Tag
ptplot			
Input	Mining/Outputs/R*r*/ptout/*run*-scen.out	$CVSLIB/CRA1BC	AP-122
Output	Mining/Outputs/R*r*/ptout/plot.out	$CVSLIB/CRA1BC	AP-122

1. $r \in \{1, 2, 3\}$
2. *scen* $\in$ {full, partial} for each *r*
3. *run* $\in$ {Good_runs.txt} for each *scen*

Table 3.17 Input and Output files for ba utility

	File/Module[1,2,3,4]	CVS Repository	CVS Tag
ba			
Input	Mining/Outputs/R*r*/*scen*/*run*/steady50x50.bud	$CVSLIB/CRA1BC	AP-122
Output	Mining/Outputs/R*r*/aff/*run*_*s*_R*r*.out	$CVSLIB/CRA1BC	AP-122

1. $r \in \{1, 2, 3\}$
2. *scen* $\in$ {full, partial} for each *r*
3. $s \in \{f, p\}$ for each *r*
4. *run* $\in$ {Good_runs.txt} for each *scen*, *s*

Table 3.18 Input and Output files for copying ASCII flow fields and assigning flow field numbers

	File/Module[1,2,3]	CVS Repository	CVS Tag
Script (pabc_mining.execute)			
Input	Mining/Outputs/R*r*/aff/*run_s_*R*r*.out	$CVSLIB/CRA1BC	AP-122
Output	Mining/Outputs/secotp/mf2k_cra1bc_*rr_ms_ffff*.out	$CVSLIB/CRA1BC	AP-122
	Mining/Outputs/secotp/joblist.txt	$CVSLIB/CRA1BC	AP-122

1. $r \in \{1, 2, 3\}$
2. $s \in \{f, p\}$ for each r
3. *run* and *fff* as shown in joblist.txt and **Error! Reference source not found.**

Table 3.19 Vector/T-field/mining factor/flow field mapping

Vector	T-field	Replicate R1		Replicate R2		Replicate R3	
		minp_fac	flow field	minp_fac	flow field	minp_fac	flow field
001	d01r02	9.83E+02	046	2.49E+02	073	6.39E+02	047
002	d01r04	9.09E+02	079	8.65E+02	086	7.28E+02	075
003	d01r07	5.32E+02	093	6.21E+01	091	2.14E+02	070
004	d01r10	5.84E+02	030	9.36E+02	075	1.26E+02	023
005	d02r02	3.74E+02	088	7.29E+02	024	3.47E+02	087
006	d03r01	8.03E+02	036	1.95E+02	041	9.22E+02	051
007	d03r03	3.85E+02	096	6.57E+02	077	6.89E+02	050
008	d03r06	7.44E+02	081	3.18E+02	069	3.32E+02	053
009	d03r07	7.83E+02	095	4.52E+02	036	5.17E+02	094
010	d03r08	7.05E+02	051	2.71E+02	001	5.49E+02	016
011	d03r09	5.79E+02	042	8.52E+02	080	1.54E+02	030
012	d04r01	5.44E+02	085	3.38E+02	070	9.13E+01	078
013	d04r02	1.12E+02	039	7.98E+02	066	9.54E+02	081
014	d04r03	5.89E+01	026	4.02E+02	010	9.77E+02	010
015	d04r04	8.89E+02	094	5.52E+02	055	6.57E+02	049
016	d04r05	2.99E+02	083	9.11E+02	038	7.75E+02	088
017	d04r06	4.42E+01	078	2.44E+01	079	6.69E+02	097
018	d04r07	2.40E+02	019	9.81E+02	100	8.68E+02	096
019	d04r08	1.80E+02	069	6.14E+02	087	7.95E+02	003
020	d04r10	3.08E+01	032	4.69E+02	068	8.02E+02	007
021	d05r03	1.02E+00	062	1.03E+02	071	2.53E+02	033
022	d05r07	3.41E+02	016	5.15E+02	004	8.66E+01	064
023	d06r02	3.09E+02	029	6.74E+02	065	5.93E+02	031
024	d06r03	7.21E+02	077	7.79E+02	002	7.25E+01	076
025	d06r04	1.49E+02	003	4.91E+01	050	5.58E+02	082
026	d06r05	9.38E+02	020	8.65E+01	013	4.61E+02	044
027	d06r06	1.54E+02	068	9.96E+02	057	8.29E+02	001
028	d06r07	5.52E+02	001	4.80E+02	014	9.03E+02	059
029	d06r10	4.35E+02	018	6.00E+02	022	5.05E+02	046
030	d07r01	7.74E+02	027	2.07E+02	093	4.92E+02	020

Table 3.19 Vector/T-field/mining factor/flow field mapping

Vector	T-field	Replicate R1		Replicate R2		Replicate R3	
		minp_fac	flow field	minp_fac	flow field	minp_fac	flow field
031	d07r02	5.30E+02	097	3.63E+01	018	6.16E+02	079
032	d07r05	2.04E+02	092	2.62E+02	061	3.64E+02	061
033	d07r06	7.66E+02	076	5.56E+00	056	6.49E+02	083
034	d07r07	4.25E+02	098	3.08E+02	045	6.79E+01	009
035	d07r08	8.11E+02	013	6.83E+02	043	4.34E+00	069
036	d07r09	2.48E+02	070	6.65E+02	096	1.78E+01	042
037	d07r10	7.52E+02	022	7.05E+02	060	5.75E+02	055
038	d08r01	3.63E+02	060	4.15E+02	052	6.99E+02	048
039	d08r02	1.71E+02	007	8.31E+02	020	7.07E+02	034
040	d08r03	4.85E+02	004	8.99E+02	023	7.57E+02	041
041	d08r04	8.70E+02	017	7.37E+02	092	7.88E+02	085
042	d08r05	6.03E+02	058	7.71E+01	059	5.88E+02	074
043	d08r06	9.77E+02	064	2.20E+02	085	3.77E+02	100
044	d08r07	8.57E+02	014	3.92E+02	015	2.99E+02	045
045	d09r02	7.97E+02	015	2.53E+02	076	2.66E+02	080
046	d09r03	6.16E+02	025	3.84E+02	048	4.39E+02	002
047	d09r04	9.56E+02	074	7.57E+02	021	4.30E+01	098
048	d09r05	2.73E+02	099	7.48E+02	051	1.92E+02	072
049	d09r06	1.96E+02	090	1.25E+02	003	9.19E+02	025
050	d09r07	3.99E+02	071	1.19E+02	037	2.81E+02	038
051	d09r08	2.59E+02	035	6.91E+02	007	4.44E+02	058
052	d09r09	8.32E+02	048	7.70E+02	044	8.38E+02	036
053	d09r10	2.61E+02	053	8.12E+02	049	3.02E+02	086
054	d10r02	9.18E+01	075	9.80E+02	019	9.92E+02	073
055	d10r03	6.97E+02	041	8.88E+02	029	2.81E+01	084
056	d10r04	5.06E+02	044	1.84E+02	081	3.91E+02	006
057	d10r06	2.18E+02	010	8.48E+02	028	1.72E+02	039
058	d10r07	2.90E+02	024	1.44E+02	027	6.27E+02	099
059	d10r08	6.82E+02	011	6.06E+02	063	7.67E+02	022
060	d10r09	4.55E+02	056	6.34E+02	042	6.02E+02	028
061	d10r10	5.14E+02	055	5.28E+02	039	4.02E+02	089
062	d11r01	3.21E+02	063	3.57E+02	012	4.71E+02	040
063	d11r02	3.37E+02	057	6.49E+02	098	3.26E+02	092
064	d11r06	1.86E+02	084	1.79E+02	099	3.55E+02	052
065	d11r07	4.67E+02	086	7.14E+02	025	1.43E+02	057
066	d11r08	8.98E+02	023	4.26E+02	016	7.38E+02	021
067	d11r09	6.37E+02	072	9.48E+02	011	8.75E+02	027
068	d11r10	9.47E+02	005	5.39E+02	030	9.83E+02	037
069	d12r01	9.21E+02	028	4.32E+02	031	8.86E+02	013
070	d12r02	3.57E+02	073	9.58E+02	094	5.35E+02	090
071	d12r03	1.36E+01	033	3.73E+02	017	9.37E+02	091
072	d12r05	5.93E+02	087	5.97E+01	058	1.39E+02	043
073	d12r06	9.69E+02	034	8.27E+02	040	5.62E+02	060

Table 3.19 Vector/T-field/mining factor/flow field mapping

Vector	T-field	Replicate R1		Replicate R2		Replicate R3	
		minp_fac	*flow field*	*minp_fac*	*flow field*	*minp_fac*	*flow field*
074	d12r07	3.25E+02	040	1.70E+02	008	2.09E+02	008
075	d12r08	8.47E+02	021	5.73E+02	062	2.21E+02	077
076	d12r09	6.26E+02	080	4.43E+02	053	6.76E+02	024
077	d13r01	4.79E+02	049	7.81E+02	074	5.30E+02	017
078	d13r02	9.13E+02	067	2.87E+02	047	9.60E+02	054
079	d13r03	1.25E+02	009	3.45E+02	064	3.87E+01	004
080	d13r05	8.01E+01	091	5.04E+02	009	3.11E+02	095
081	d13r06	4.14E+02	050	4.96E+02	032	2.50E+02	068
082	d13r07	1.04E+02	006	6.21E+02	054	4.16E+02	065
083	d13r08	6.63E+02	059	5.70E+02	082	7.17E+02	014
084	d13r09	6.60E+02	082	9.13E+01	089	8.91E+02	066
085	d21r01	4.99E+02	037	2.29E+02	006	3.84E+02	026
086	d21r02	8.73E+02	061	8.06E+02	035	4.53E+02	012
087	d21r03	8.45E+01	031	1.36E+02	097	1.63E+02	005
088	d21r04	3.94E+01	012	1.63E+01	083	8.52E+02	018
089	d21r05	5.66E+02	065	5.41E+02	067	1.89E+02	071
090	d21r06	2.31E+02	038	5.82E+02	046	5.99E+01	019
091	d21r07	8.22E+02	008	1.56E+02	078	4.88E+02	063
092	d21r10	6.48E+02	089	9.05E+02	084	4.23E+02	015
093	d22r02	4.44E+02	002	9.63E+02	033	2.37E+02	067
094	d22r03	7.18E+02	100	3.23E+02	034	1.13E+02	011
095	d22r04	9.95E+02	054	9.27E+02	095	2.75E+02	032
096	d22r06	6.71E+01	047	4.88E+02	088	8.13E+02	093
097	d22r07	6.72E+02	045	2.92E+02	072	1.08E+02	035
098	d22r08	7.32E+02	052	2.37E+02	005	9.47E+02	056
099	d22r09	4.05E+02	043	3.65E+02	090	8.43E+02	029
100	d22r10	1.37E+02	066	8.76E+02	026	7.48E+02	062

Table 3.20 Directories and files archived by ARCONS script

File/Module	CVS Repository	CVS Tag
Mining/Outputs/R1/	$CVSLIB/CRA1BC	AP-122
Mining/Outputs/R3/	$CVSLIB/CRA1BC	AP-122
Mining/Outputs/R2/	$CVSLIB/CRA1BC	AP-122
Mining/Outputs/secotp/	$CVSLIB/CRA1BC	AP-122
Mining/Outputs/mining_pabc.execute.log	$CVSLIB/CRA1BC	AP-122

3.2.3 Model Domain and Discretization

The model domain used in the CRA-2004 PABC analysis is the same as that used in the CRA-2004 calculations. A general description of the modeling domain and grid-layout is given in McKenna and Hart (2003a) and is reproduced here for completeness:

> The north-south and east-west extent of the model domain was specified by Richard Beauheim, Robert Holt, and Sean McKenna. This determination considered several factors including: 1) hydrogeological features in the vicinity of the WIPP site that could serve as groundwater flow boundaries (e.g. Nash Draw); 2) the areas to the north of the WIPP site that might create additional recharge to the Culebra due to water applied to potash tailings pile; and 3) the limits imposed on the domain size by the available computational resources and the desired fine scale discretization of the domain within the groundwater model. The final model domain is rectangular and aligned with the north-south and east-west directions. The coordinates of each corner of the domain are given in Table 1 [*not shown*] in UTM (*NAD27*) coordinates. A no-flow boundary corresponding roughly to the center of Nash Draw is shown in Figure 1 [*not shown*] as a purple line extending from the northern to southern boundaries in the western one-third of the model domain. Model cells falling to the west of this boundary are considered to be inactive in the groundwater flow calculations.

Table 3.21 Groundwater modeling domain (UTM NAD27 coordinates)

Domain Corner	X Coordinate (meters)	Y Coordinate (meters)
Ground Water Modeling Domain		
Northeast	624,100	3,597,200
Northwest	601,700	3,597,200
Southeast	624,100	3,566,500
Southwest	601,700	3,566,500
WIPP LWB		
Northeast	616,941	3,585,109
Northwest	610,495	3,585,068
Southeast	617,015	3,578,681
Southwest	610,567	3,578,623

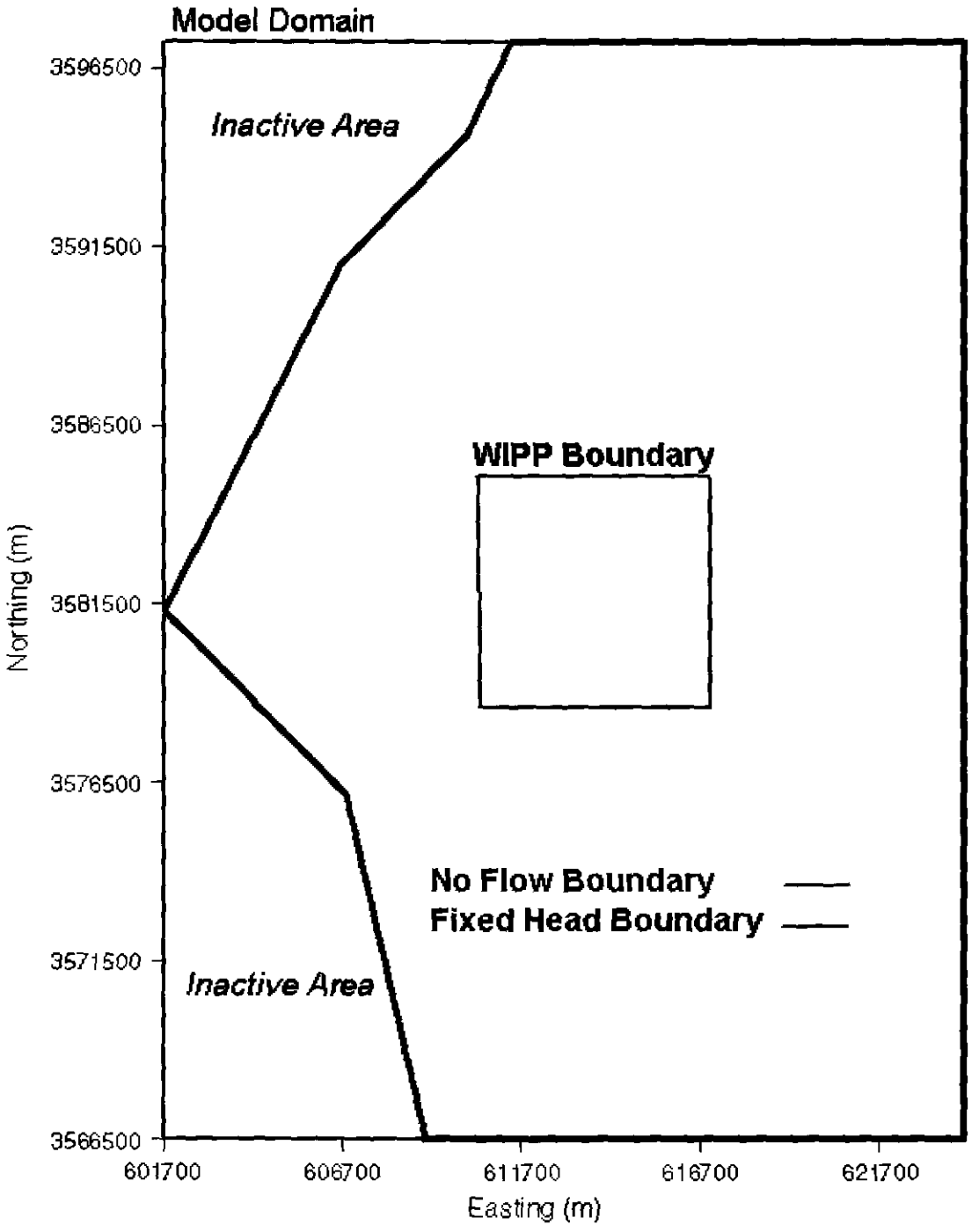

Figure 3.1 Groundwater modeling domain and boundary conditions

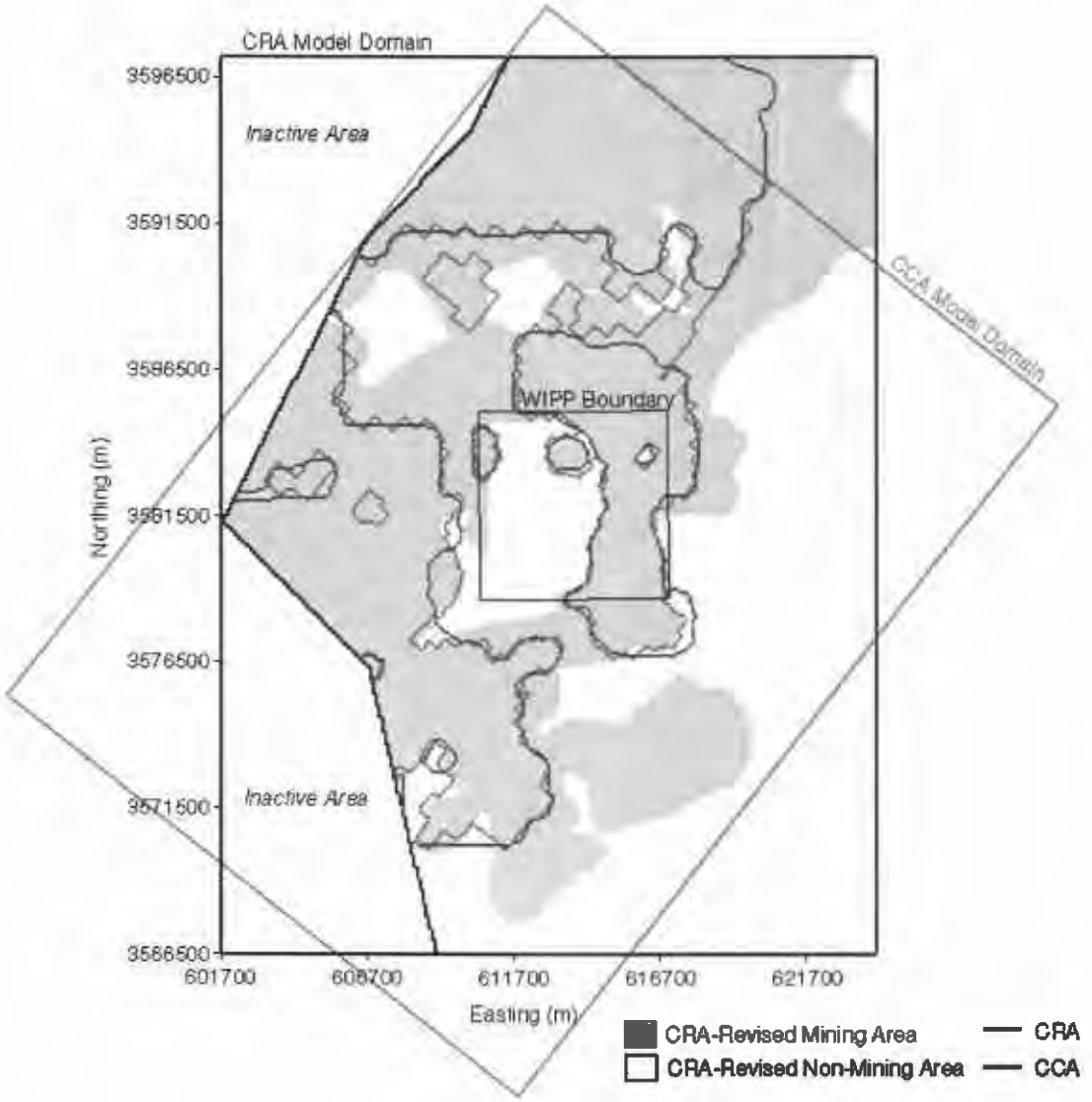

Figure 3.2 The CRA-2004 PABC full mining zones (shown as CRA-Revised in the legend) overlaid with the 1996 CCA (red) and the CRA-2004 (blue) delineations.

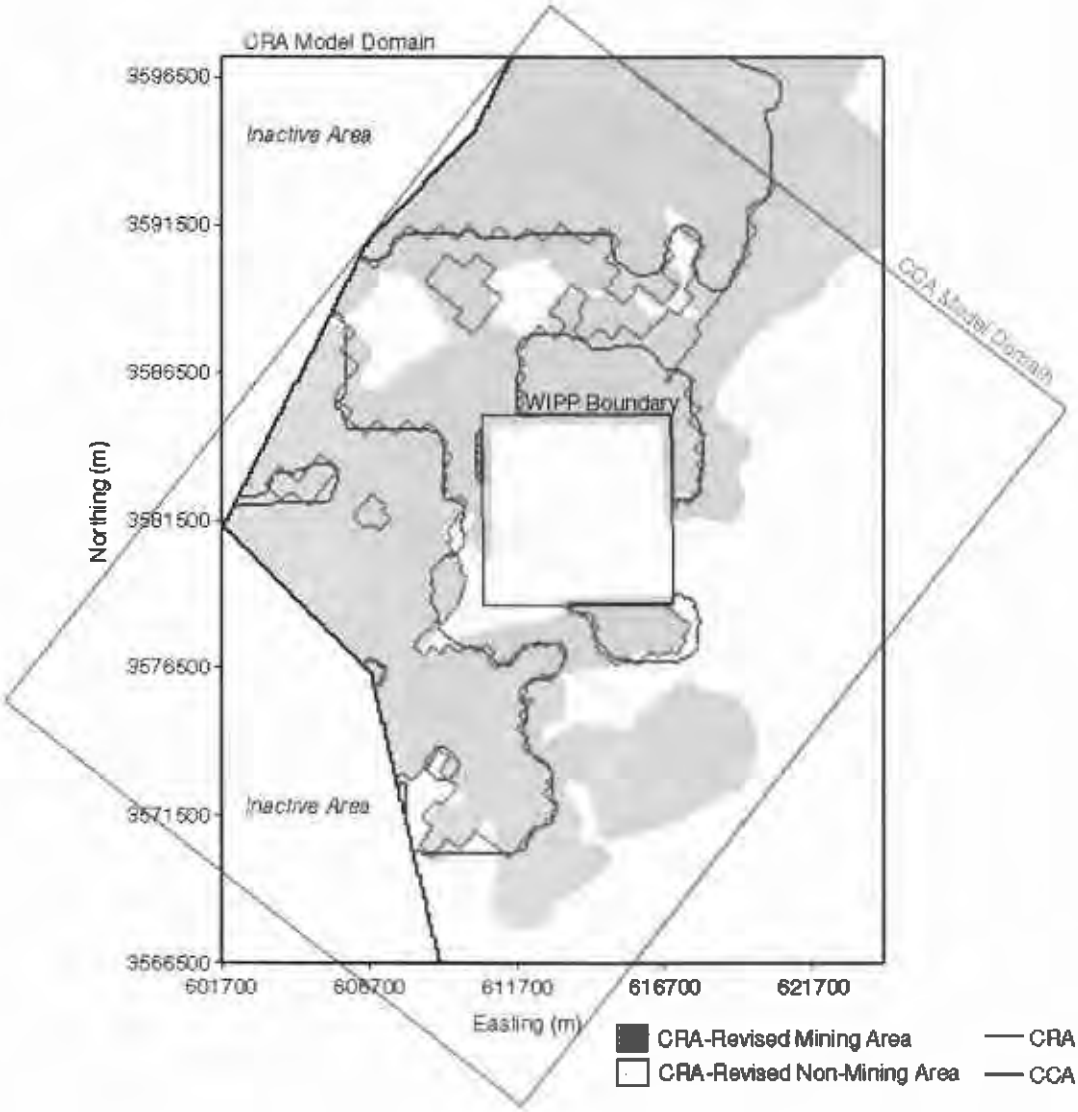

Figure 3.3 The CRA-2004 PABC partial mining zones (shown as CRA-Revised in the legend) overlaid with the 1996 CCA (red) and the CRA-2004 (blue) delineations.

3.2.4 Boundary and Initial Conditions

Like the model domain and discretization, the boundary and initial conditions used in the CRA-2004 PABC calculations are the same as those used in the CRA-2004 calculations (Lowry 2003b, a), and are described fully in McKenna and Hart (2003b). As a summary, field head data from the year 2000 consisting of 37 head measurements across the modeling domain are interpolated to the computational grid using kriging. A five-parameter Gaussian function is used to de-trend the head data at which point a Gaussian variogram model is used to describe the variability of the head residuals with distance. The variogram model is used to estimate the residuals at each node in the grid. The final step is to add the regional trend back to the estimated residuals using the five-parameter Gaussian function.

The model boundaries along the north, east, and south edges of the domain are considered fixed-head boundaries. The kriged head values determining the initial heads are assigned to each constant head cell and kept fixed throughout the simulation. Since all simulations for this Task are steady-state, determination of the initial heads is important only in relation to setting the fixed boundary conditions. The irregular western boundary is considered a no-flow boundary and falls roughly along the groundwater divide associated with Nash Draw. Nash Draw is interpreted as a regional groundwater divide, draining the Rustler units to the east and north (and also by implication via discharge symmetry, to the west). The initial head contours across the active modeling domain are shown in Figure 3.4.

Since the extent of possible potash mining extends well beyond the modeling domain, the effects of mining on the boundary conditions must be considered. Regional flow rates within the flow model are controlled by the boundary conditions and the hydraulic conductivity distribution. The regional gradient across the domain is approximately 0.0017, which is higher than the 0.001 quoted in Wallace (1996) for the CCA. It should be noted that the regional gradients are difficult to directly compare since the CCA grid is rotated approximately 38° clockwise from the CRA-2004 grid. Thus, for the CCA grid, the regional gradient is calculated by taking the difference of the highest constant head in the northern corner of the model and the lowest constant head in the southern end of the model, and dividing by the distance between these two points. For the current grid we average the constant heads along the northern boundary, subtract the average heads along the southern boundary, and then divide by the north-south model domain distance. Using only the cells with the highest and lowest constant heads and dividing by the distance between the two, as was done with the CCA grid, the regional gradient is calculated to be 0.0022, which overestimates the regional behavior. It is assumed that mining impacts would not significantly change this regional gradient and thus the boundary conditions for the mining scenarios are identical to those in Task 4 (McKenna and Hart 2003b). In addition, the CCA used the same conceptualization (keeping boundary conditions fixed between the mining and non-mining scenarios) and to allow for comparisons between the CCA and the CRA-2004, the same conceptualization is maintained.

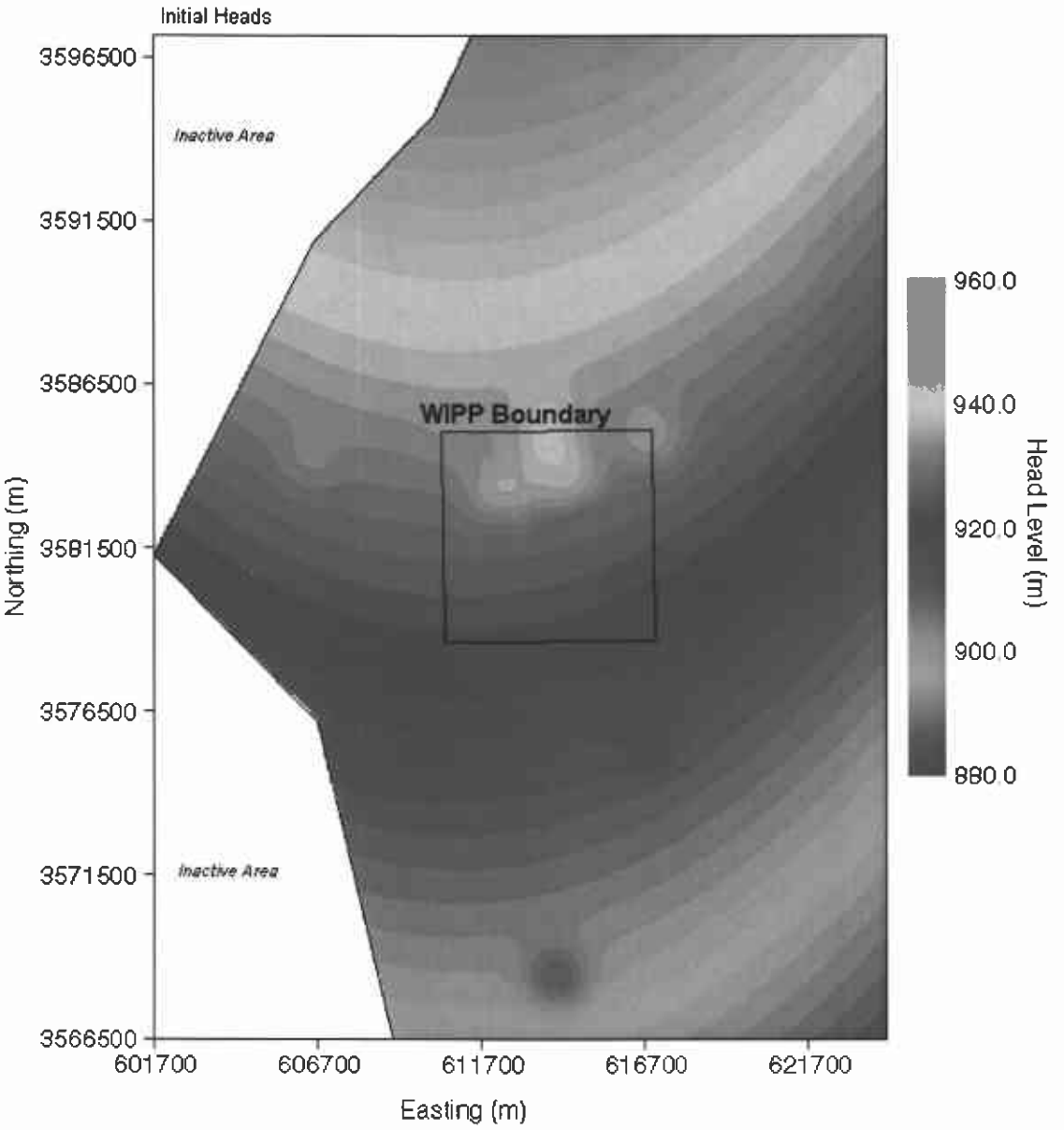

Figure 3.4 Initial heads across groundwater domain

3.2.5 Determination of Potential Mining Areas

The 2002 version of the original 1993 Bureau of Land Management (BLM) map, "Preliminary Map Showing Distribution of Potash Resources, Carlsbad Mining District, Eddy and Lea Counties, New Mexico" (BLM 1993), was obtained directly from David Hughes of Washington Regulatory Environmental Services (WRES) as an Autocad DXF file. This map was originally developed for the CCA and is periodically updated as part of the Delaware Basin Drilling Surveillance Program, which is performed by WRES.

The coordinates of the DXF file are in State Plane NAD 27, Region 3001 (New Mexico East), and thus required conversion to the UTM NAD 27 (zone 13) system used in this study. The coordinate conversion was done using the Department of Defense groundwater modeling software, GMS (GMS 2003). Two coverages were extracted from the DXF file, "Extent of Mining Outside the Controlled Area" and "Unmined Potash Resources" (see Figure 3.5). The first coverage, "Extent of Mining Outside the Controlled Area", delineates areas outside the LWB that have already been mined. This coverage was incomplete in that it did not include a previously mined area in the northern part of the modeling domain (bright blue area of Figure 3.5). These areas were manually added to the coverage. This combined area was then added to the second coverage, "Unmined Potash Resources" to provide the best estimate of areas with potential for existing resources to be developed, without substantial deference to whether the leases were currently viable for development (Cotsworth, 2004).

The difference between the CRA-revised (Lowry 2004), the CRA-2004 PABC delineation and the CRA-2004 delineation (Lowry 2003a) is the CRA-2004 eliminated a portion of the area from mining based on the coverage, "Mining Boundaries", which is a set of one-mile diameter circles around each well drilled for oil and gas exploration. These areas are under control of the oil and gas companies and have been deemed as off limits to potash mining. However, as stipulated in comment G-11, the CRA-revised analysis does not include the gas and oil well exclusion zones. In addition, the unmined potash resources coverage was included here to gain all areas of possible future potash mining, regardless of current economic viability. The addition of these zones significantly increases the potential potash mining area over that of the CRA-2004 reported in Lowry (2003a).

Since the potash mining area is located in the Salado Formation, below the Culebra, the areas disturbed by mining activities in the Culebra are larger than what is shown on the BLM map due to subsidence-induced angle-of-draw effects. The rationale for determining the extent of these effects is described in Wallace (1996) with the final conclusion stating that an additional 253 m wide collar was to be added to the mining-impacted areas. This is considered a conservative estimation of the angle-of-draw effects. To accommodate the angle of draw, the mining zone boundaries, as overlaid on the current model grid, were moved outward 3 cells in the x and y directions (300 m), and 2 cells in the diagonal direction (283 m). The CRA-2004 PABC modeling domain and mining zones for the full-mining case are shown in comparison to the 1996 CCA and the CRA-2004 delineations in Figure 3.2. The partial mining case is shown in Figure 3.3. A close-up of the WIPP site and the associated mining zones is shown in Figure 3.6.

The output of this delineation is a file that contains one value for each cell in the grid. A value of 0 is an inactive cell, a value of 1 means the cell lies within a potential mining zone, and a value of 2 means that it is outside a potential mining zone. One file for each scenario, full-mining and partial-mining, is generated, and used as input to the data conversion program min_fact (see Table 3.7 and execution flow discussion in section 3.2.2).

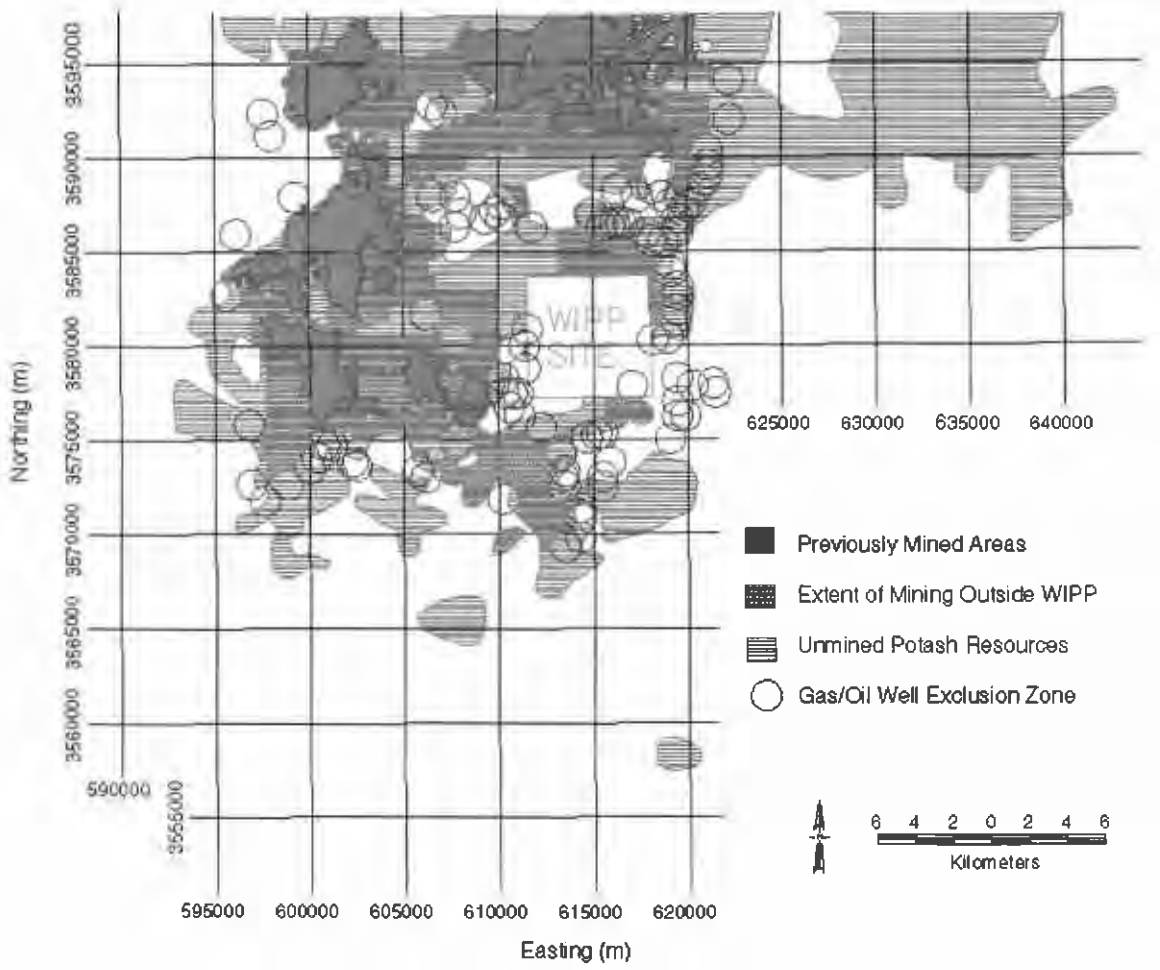

Figure 3.5 Distribution of potash resources in the vicinity of WIPP

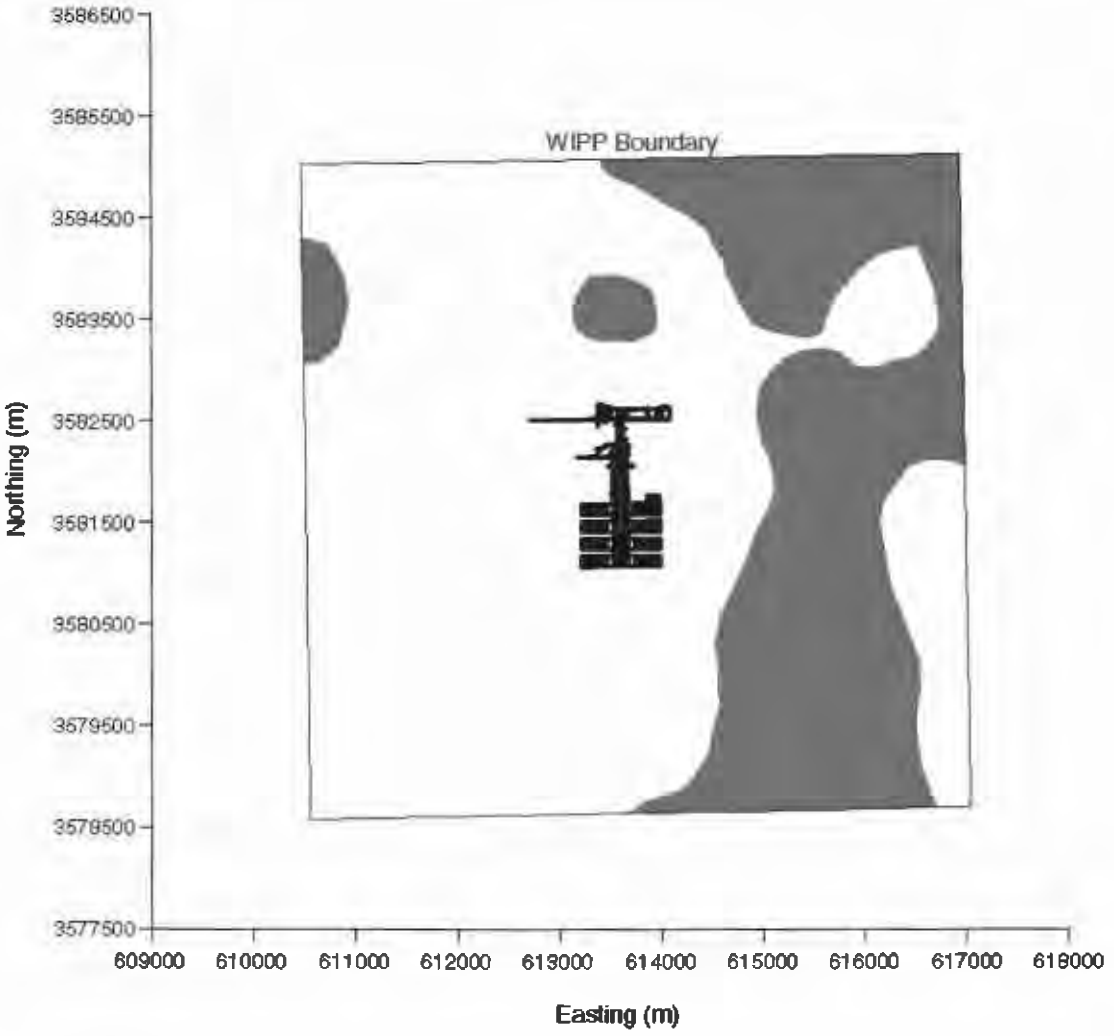

Figure 3.6 Potential potash distribution within WIPP LWB. (UTM NAD27 coordinates)

3.2.6 Use of Mining Zones in Forward Simulations

The calibration process in McKenna and Hart (2003b) produces a transmissivity field that minimizes the error between the steady-state and transient head distributions and the calculated distributions using the calibrated field. Since the calibration process does not produce a unique solution, i.e. given a different set of starting transmissivities a different final set of transmissivities may be reached, multiple T-fields are produced and 100 are selected based on the criteria set forth in Beauheim (2003). To simulate the effects of mining, each selected `T-field` is multiplied by its own unique mining scaling factor in areas of potential mining, and MF2K is run to produce the mining-affected head distribution and the cell-by-cell flow budget files. The cell-by-cell flow budget file is used for performing the particle tracking calculations as well as for the radionuclide transport calculations. To demonstrate stability in mean results, three different sets of mining factors are used, each set forming a replicate. Thus, for each mining scenario (full

and partial), 3 sets of 100 mining-altered T-fields are produced. The only difference between the CRA-revised Lowry (2004) calculations and the CRA-2004 PABC calculations is the updated set of random mining factors.

3.2.7 Particle Tracking Simulations

A single particle is tracked from the UTM NAD27 coordinate X = 6135975 m, Y = 35813852 m to the LWB for each `T-field` and replicate/scenario combination, using the DTRKMF code. Two outputs are generated from the suite of particle tracks. First are plots showing the individual tracks for all 100 T-fields in each scenario for each replicate (6 plots total). This allows for visual comparison of the prevailing flow directions for the full- and partial-mining scenarios and the qualitative comparison of the variability of the tracking direction. Secondly, cumulative distribution functions (CDF's) are constructed for each replicate and scenario. The CDF's describe the probability that a particle will cross the LWB in a given amount of time. The six plots and the CDF's are presented below in the results section.

3.3 Results

3.3.1 Particle Travel Times

Compared to the non-mining scenario, the travel times for both mining scenarios are longer; the median travel times across all 3 replicates for the full- and partial-mining scenarios are approximately 3.84 and 7.20 times greater than for the non-mining scenario, respectively (the CRA-revised travel times were 4.14 and 7.06 times greater). This is greater than either the CCA or CRA-2004 calculations (discussed more below). A plot of the cumulative distribution functions (CDF's) for the full-, partial-, and non-mining scenario's as compared to the CRA-revised Lowry (2004) is shown in Figure 3.7.

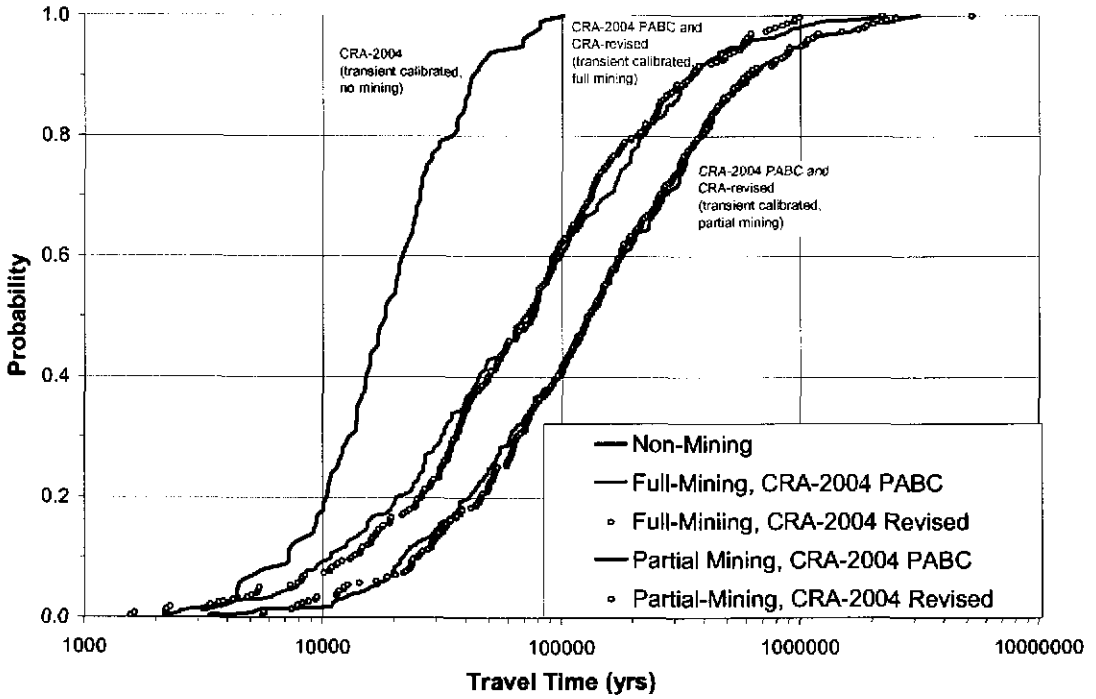

Figure 3.7 Cumulative distribution of travel times

Examination of the contours and flow patterns of the mining cases (see Lowry, 2004 for an example of this), reveals that the high transmissivity areas corresponding to the mining zones create preferential pathways through the system. These preferential pathways result in higher velocities and flow rates through the mining zone areas that translate to slower velocities in the non-mining zone areas. Since the starting point for the particle tracking is in a non-mining area, travel times are increased as compared to the non-mining scenario. A comparison of the median, maximum, and minimum values for each scenario travel times is presented in Table 3.22.

Table 3.22 Particle tracking travel time statisitics[1]

		CRA-2004 PABC		CRA-Revised		Non-Mining
Replicate	Stat.	Full	Partial	Full	Partial	
R 1	Med.	64,026	117,815	75,410	125,712	NA
	Max.	2,175,165	2,727,191	941,529	1,882,522	
	Min.	2,130	5,185	1,615	5,645	
R2	Med.	80,801	148,489	73,327	127,265	
	Max.	2,059,263	1,667,084	2,196,690	2,499,469	
	Min.	2,463	4,855	2,178	5,573	
R3	Med.	74,315	118,919	76,097	135,686	
	Max.	1,779,512	3,128,693	944,251	5,195,535	
	Min.	2,507	3,314	1,550	5,635	
Global	Med.	70,170	131,705	75,774	129,202	18,289
	Max.	2,175,165	3,128,693	2,196,690	5,195,535	101,205
	Min.	2,130	3,314	1,550	5,573	3,111

1. Median, maximum, and minimum travel time in years for the full and partial mining scenarios as compared to the CRA-revised (Lowry 2004) and non-mining scenarios

3.3.2 Flow Directions

The particle track directions for the full- and partial-mining scenarios for the CRA-2004 PABC are illustrated in Figure 3.8 to Figure 3.13. Like past mining scenario calculations, there is a strong similarity within each replicate for each scenario. With slight variations, individual tracks can be recognized from one replicate to the next. This indicates that particle track directions are determined more by the spatial variation of the calibrated T-field than by the random mining factors, although the random mining factors have a greater effect for the CRA-2004 PABC and the CRA-revised than in the CRA-2004 calculations Lowry (2003a).

The travel direction for the CRA-2004 PABC are similar to the CRA-revised full mining scenario, both of which are significantly different than the CRA-2004 (Lowry, 2003a). A wider mining zone to the west of the WIPP site in the CRA-revised delineation decreases the total flow through the mining area on the east boundary of the WIPP site, lowering the relative heads to the east and causing particles to move eastward towards the boundary between the mining and non-mining zone. Most particles tend to seek out this boundary and then move southward along that boundary. This is in contrast to the partial-mining scenario where the tracking directions for the CRA-2004 PABC and CRA-revised are similar to the CRA-2004 as well as to the non-mining scenario.

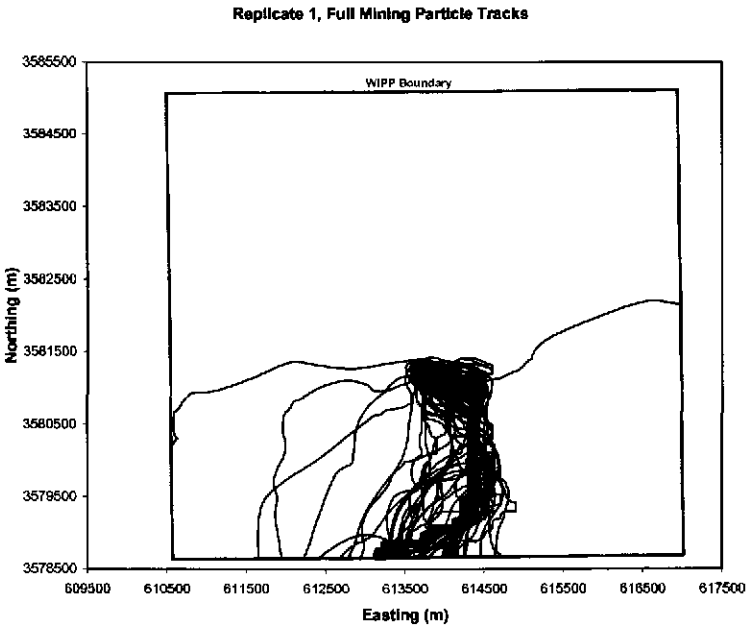

Figure 3.8 Particle tracks (CRA-2004 PABC, full-mining,replicate R1,)

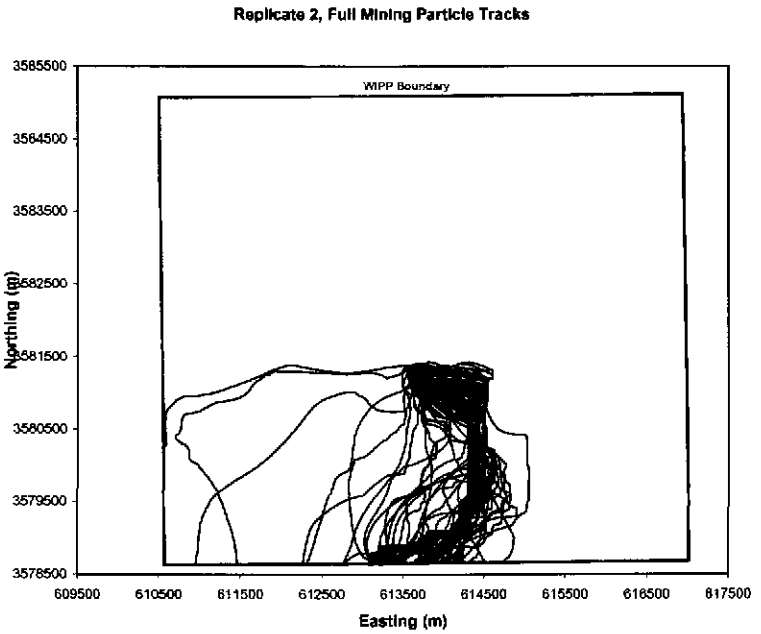

Figure 3.9 Particle tracks (CRA-2004 PABC, full-mining, replicate R2)

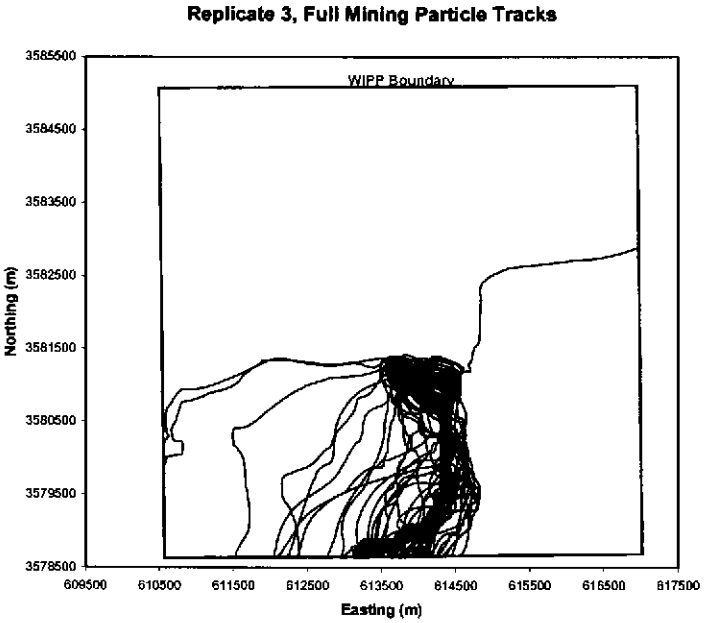

Figure 3.10 Particle tracks (CRA-2004 PABC, full-mining, replicate R3)

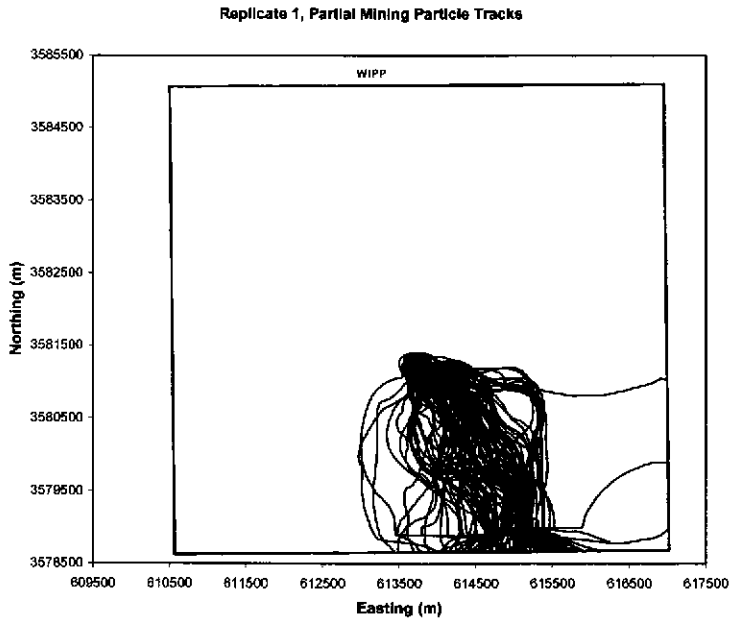

Figure 3.11 Particle tracks (CRA-2004 PABC, partial-mining, replicate R1)

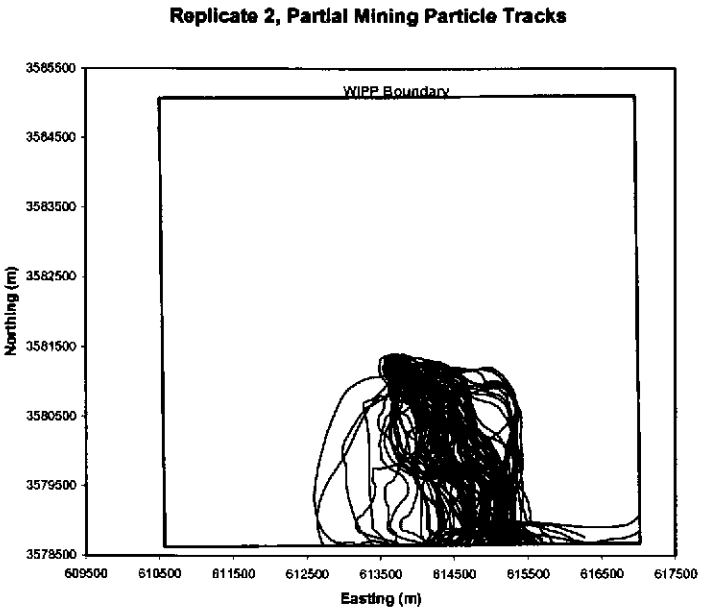

Figure 3.12 Particle tracks (CRA-2004 PABC, partial-mining, replicate R2)

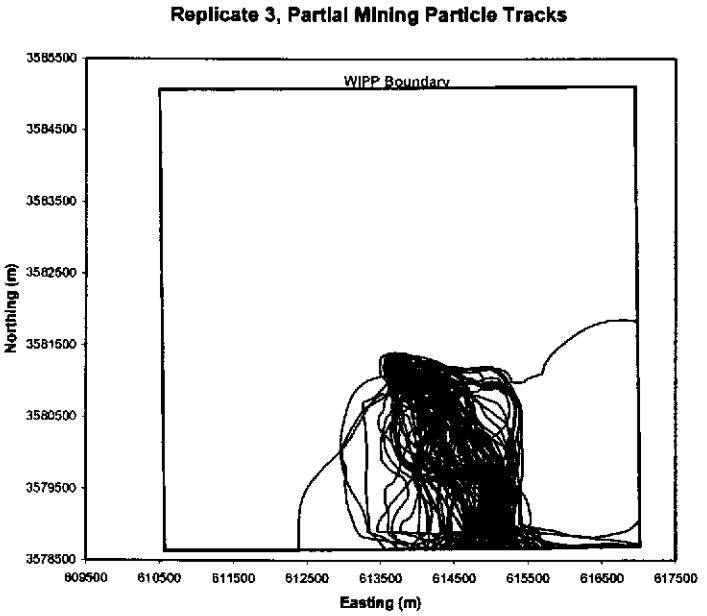

Figure 3.13 Particle tracks (CRA-2004 PABC, partial-mining, replicate R3)

3.4 Discussion

Correlation analysis for the CRA-2004 PABC calculations show correlations between travel time and the random mining factor for the full and partial-mining scenarios as 0.37 and 0.35, respectively. This compares to correlation factors of 0.32 (full-mining) and 0.30 (partial-mining) for the CRA-revised and 0.09 (full mining) and 0.15 (partial mining) for the CRA-2004 Lowry (2003a). Figure 3.14 and Figure 3.15 show the $\log_{10}$ travel times versus the random mining factor for the full- and partial-mining scenarios across all replicates for the CRA-2004 PABC. Like the particle travel directions, this increase in correlation between the random mining factor and the travel time can be explained by the increase in area of the mining zones. Like the CRA-revised, the flow fields in the CRA-2004 PABC analysis are highly influenced by the large area to the west of the WIPP site that is deemed as mining zone. Since this area is much larger in the CRA-2004 PABC than it was in the CRA-2004, a change in transmissivity to this area has a greater regional impact. An increase in transmissivity in the mining zone means higher flow rates through those areas, and correspondingly lower flow rates through the non-mining zone areas. The high scatter shown in Figure 3.14 and Figure 3.15 indicates that the transmissivity spatial distribution plays a significant role in determining the travel time. The standard deviation of the $\log_{10}$ travel time due only to differences in the T-field (i.e. standard deviation of the residual) is 0.5 for both the full- and partial-mining scenarios. With the assumption that the $\log_{10}$ travel times are normally distributed around the trendline, then the majority of values will fall within 3 standard deviations of the trendline. This means that the T-field spatial distribution accounts for the majority of the 3 orders of magnitude range of travel times.

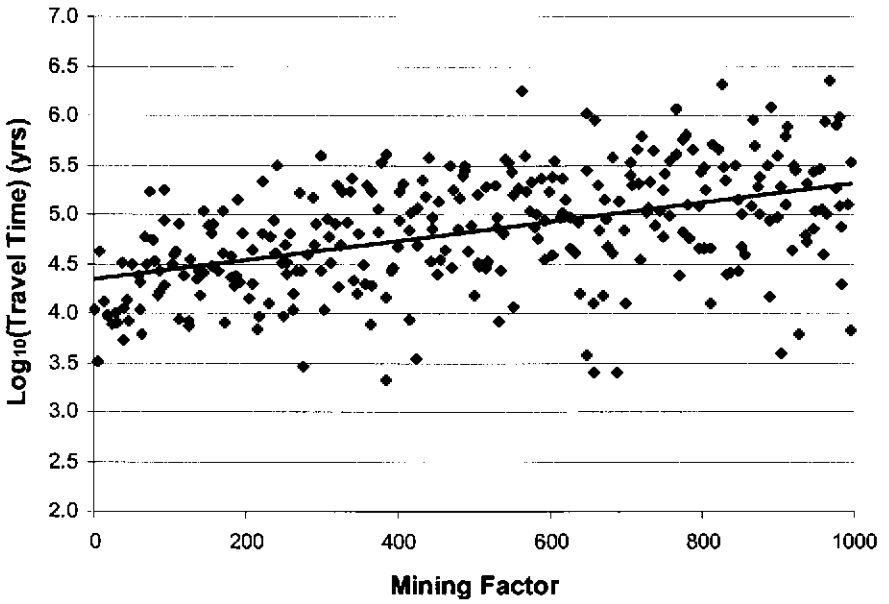

Figure 3.14 Correlation between the random mining factor and $\log_{10}$ travel time (full mining).

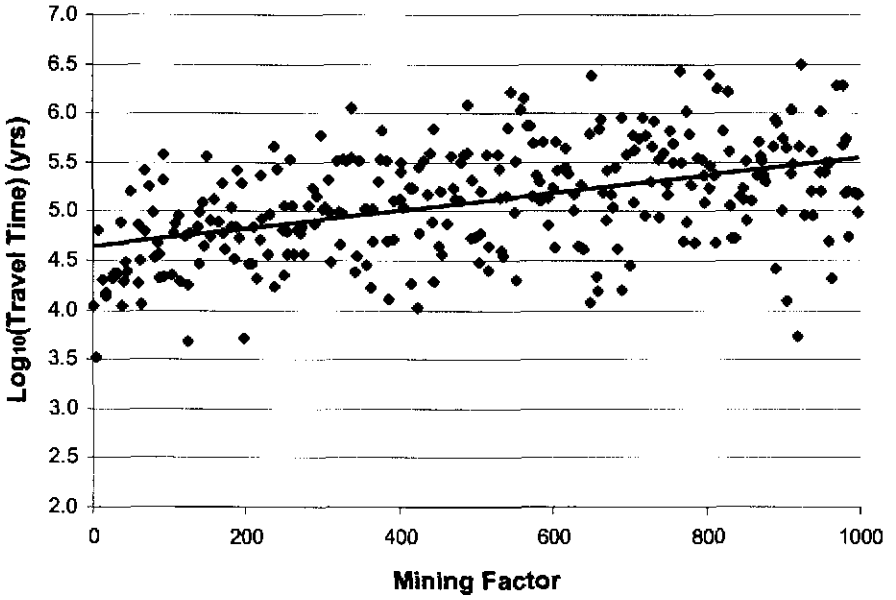

Figure 3.15 Correlation between the random mining factor and $\log_{10}$ travel time (partial mining).

4 Radionuclide Transport Calculations

4.1 Background and Theoretical Overview

The Culebra radionuclide transport calculations are performed using SECOTP2D, a two-dimensional, dual porosity solute transport code developed to simulate radionuclide transport through fractured porous media (Salari and Blaine 1996, Ramsey 1997). This section describes the process for incorporating the MODFLOW flow fields into the Culebra transport model, the theory underlying the SECOTP2D code, and the parameters used in the Culebra transport calculations.

4.1.1 Relationship between Flow and Transport Modeling Domains

The spatial domain used for the transport calculations, in relation to the groundwater modeling domain and the LWB, is shown in Figure 4.1. The UTM coordinates for the transport domain are given in Table 4.1.

The domain used in the transport calculations is a subregion of that used for the groundwater flow calculations. This subregion is approximately 7.5 km by 5.4 km, aligned with the principle directions of the groundwater flow domain. The transport domain extends beyond the boundaries of the WIPP in the east-west direction (approximately 250 m in the west and approximately 750 m in the east). Since the undisturbed groundwater flow direction is generally north to south, the transport domain is shifted so that it extends from a point midway between the waste panel and the northern LWB to approximately 1000 m beyond the LWB in the south. The transport calculations use a uniform computational grid composed of 50m by 50m cells.

Table 4.1 UTM Coordinates for Transport Domains

	UTM X (m)	UTM Y (m)
SW Corner	610250	3577600
SE Corner	617750	3577600
NE Corner	617750	3583000
NW Corner	610250	3583000

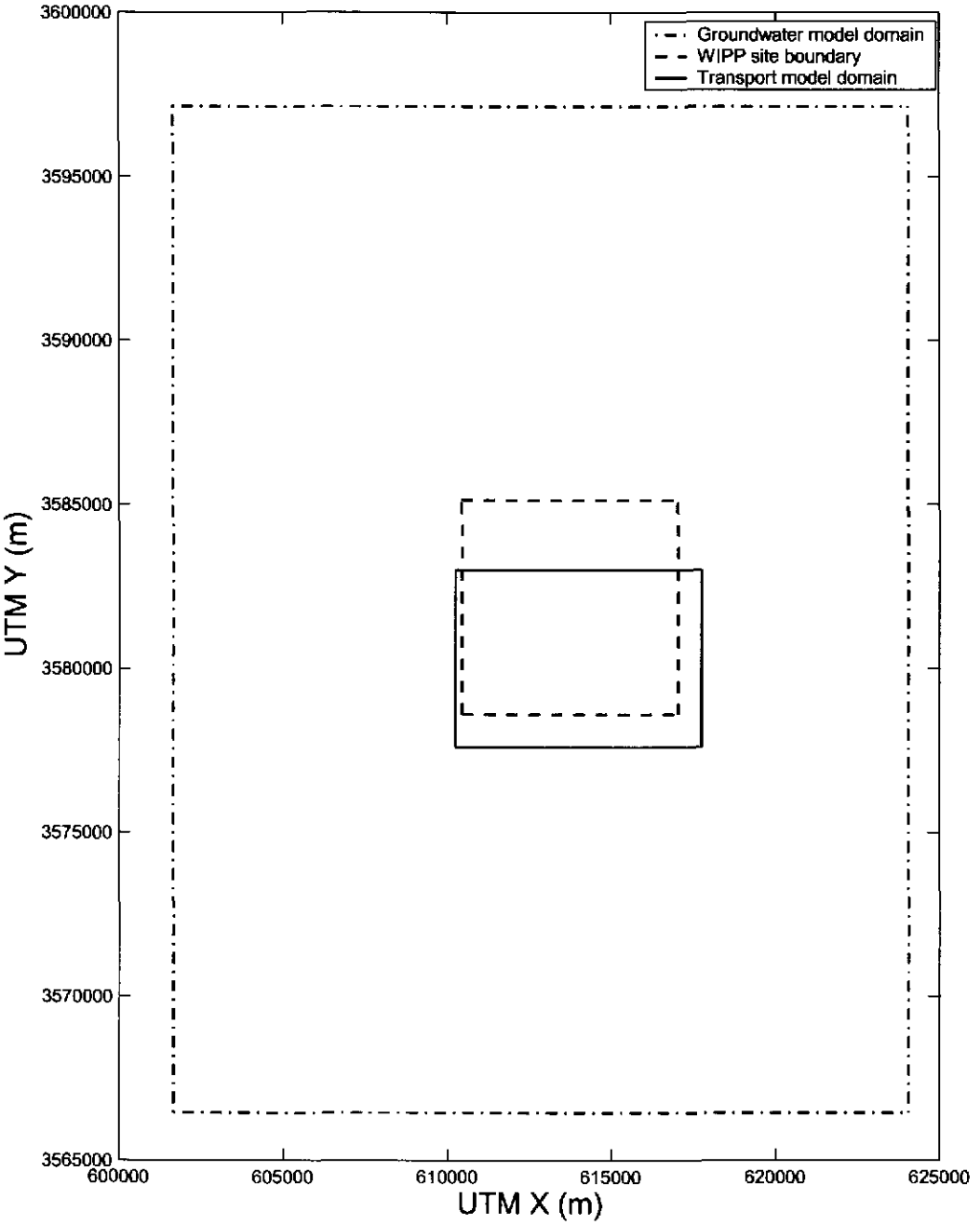

Figure 4.1 Culebra groundwater flow and radionuclide transport modeling domains.

4.1.2 Flow Field Extraction

Several issues need to be addressed when using the results of the groundwater flow calculations computed using MODFLOW as input to the Culebra transport calculations:

1. The MODFLOW code outputs the volumetric flux across the face of each cell in the computational mesh, while the SECOTP2D code suite expects the flow field in terms of the specific discharge at cell faces.
2. The computational domain used in the transport calculations is a sub-region of that used in the groundwater flow calculations.
3. The origin of the two-dimensional MODFLOW computational mesh corresponds to the northwest corner of the groundwater flow modeling domain while the SECOTP2D computational mesh locates its origin at the southwest corner of the transport model domain.
4. The coordinate system used by MODFLOW also differs from that used by SECOTP2D in that the positive y-direction in MODFLOW is opposite that of SECOTP2D and thus the flux in the y-direction has different sense in the two systems.
5. MODFLOW defines the x-direction flux for a given cell index as the flux through that cell's right face while SECOTP2D defines it as the flux through the left cell face.

The specific discharge or Darcy velocity across the cell face is computed by dividing the volumetric flux across the cell face by its area (see Figure 4.2).

$$u = \frac{Q_x}{A_x} = \frac{Q_x}{\Delta x \Delta y}$$

$$v = \frac{Q_y}{A_y} = \frac{Q_y}{\Delta x \Delta z}$$

where u,v are the specific discharge (Darcy velocity) across the cell face in the x- and y-direction, respectively; Q_x, Q_y are the volumetric flux across the cell faces; and A_x, A_y are areas of the cell face perpendicular to the x- and y-directions, respectively.

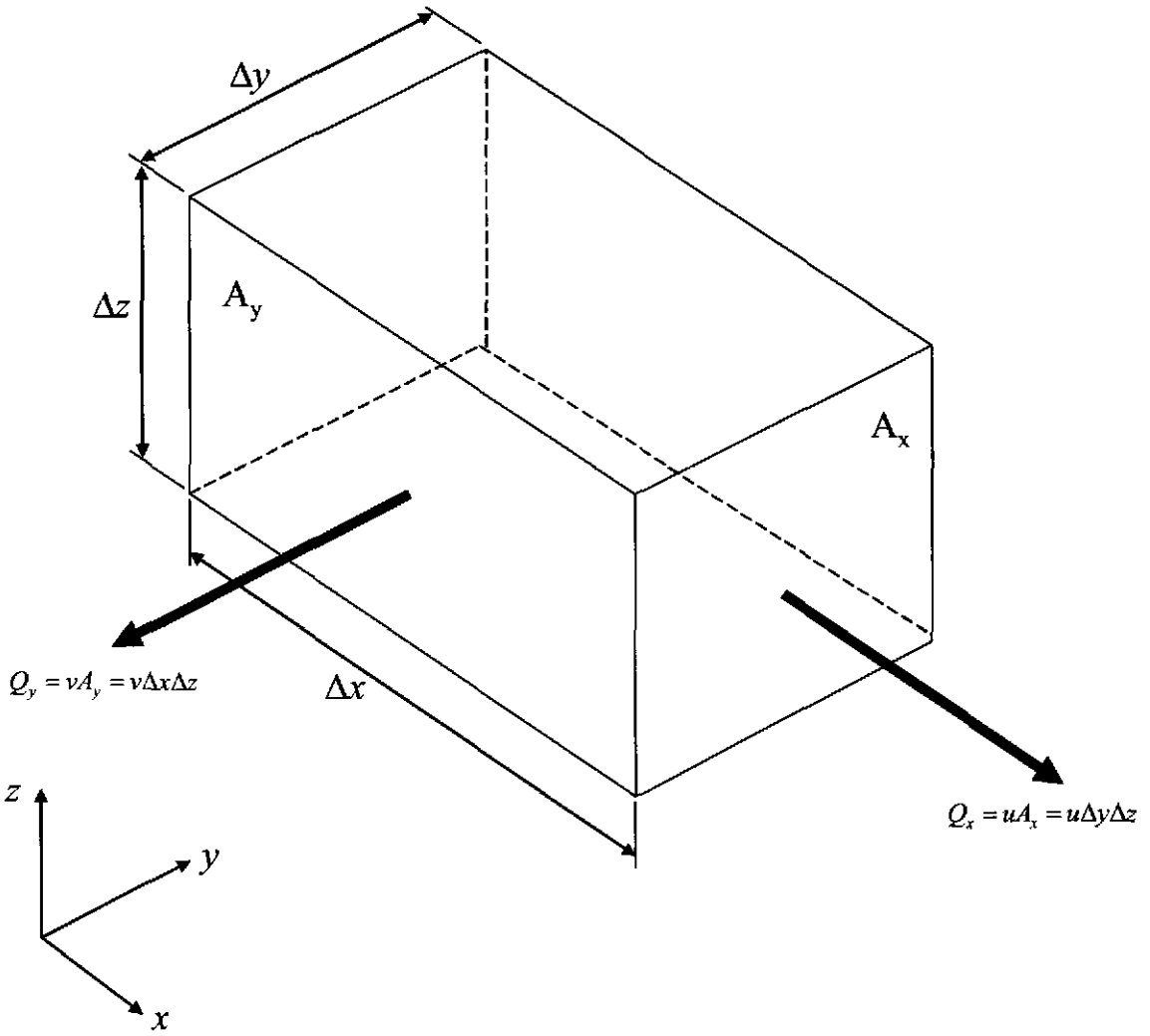

Figure 4.2 MODFLOW volumetric flux and Darcy velocity

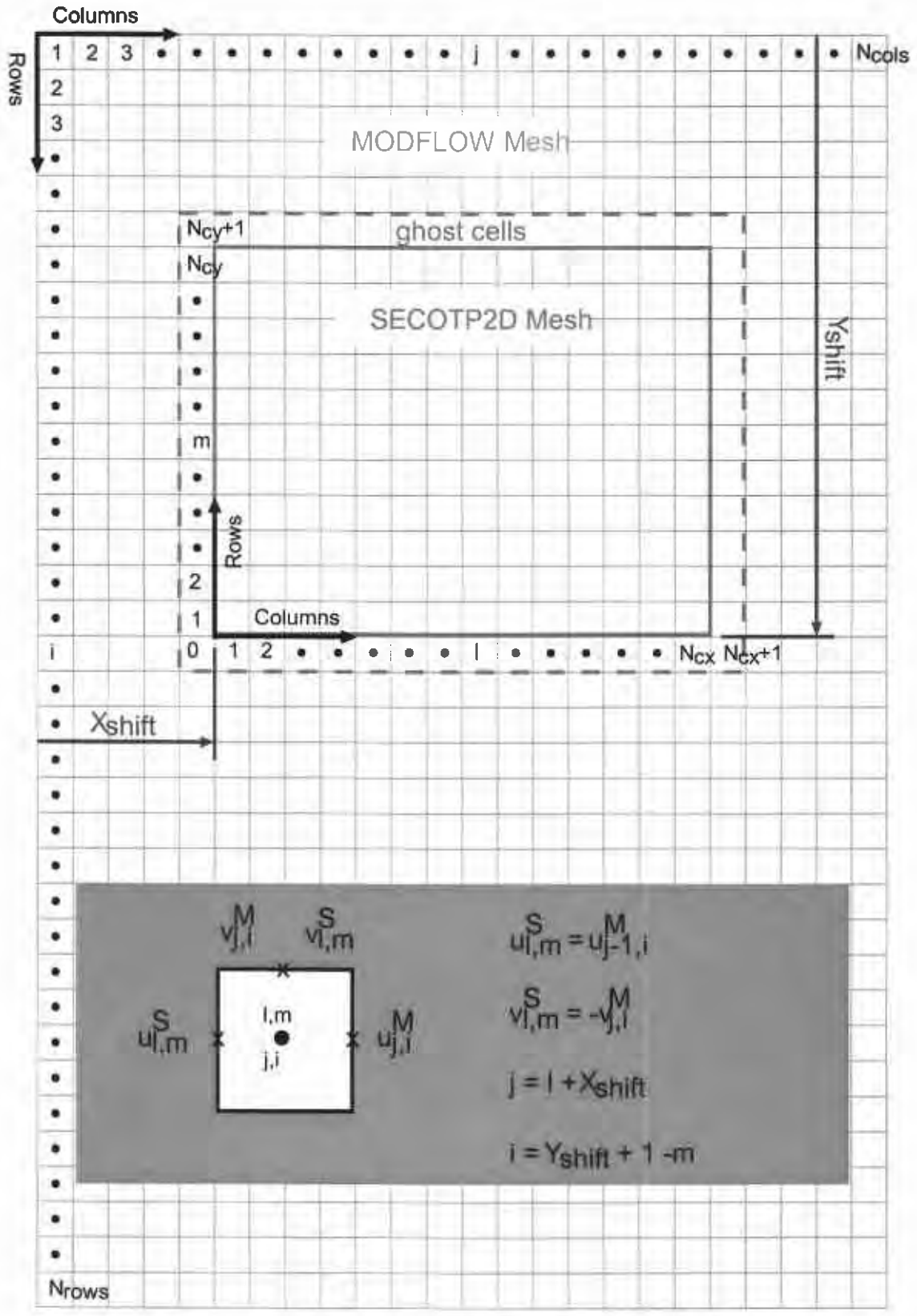

Figure 4.3 Velocity transfer between MODFLOW and SECOTP2D meshes

The remaining issues can be dealt with as outlined below and illustrated in Figure 4.3. Let (j,i) be the x-direction and y-direction indices of a cell in the MODFLOW mesh with $j \in [1, N_{cols}]$ and $i \in [1, N_{rows}]$. Let (l,m) be the indices of the *same cell* referenced to the SECOTP2D mesh with $l \in [0, N_{cx}+1]$ and $m \in [0, N_{cy}+1]$. Note that the SECOTP2D mesh uses a band of ghost cells which extend beyond the boundaries of the transport domain in order to implement boundary conditions.

Since the positive y-direction of the two meshes are opposite in sense, we must have

$$v^S_{l,m} = -v^M_{j,i}$$

where the S superscript denotes the SECOTP2D velocity and M denotes the MODFLOW velocity. The difference in conventions regarding which face to associate with a given cell can be written as

$$u^S_{l,m} = u^M_{j-1,i}$$

Let X_{shift} be the x-direction distance (in number of cells) between the origin of the MODFLOW mesh and the SECOTP2D. Let Y_{shift} represent the corresponding distance in the y-direction. Then the MODFLOW cell indices corresponding to the cell (l,m) in the SECOTP2D mesh are given by

$$j = l + X_{shift}$$
$$i = Y_{shift} + 1 - m$$

The preceding set of rules may be summarized by the following algorithm:

for $l = 0$ to N_{cx} do
  for $m = 0$ to N_{cy} do
    j $\leftarrow l + X_{shift}$
    $i \leftarrow Y_{shift} + 1 - m$
    $u^S_{l,m} \leftarrow u^M_{j-1,i}$
    $v^S_{l,m} \leftarrow -v^M_{j,i}$
  end for
end for

4.1.3 Solute Transport Modeling

The SECOTP2D code assumes a parallel plate type fracturing where fluid flow is restricted to the advective continuum (fractures) and mass is transferred between the advective and diffusive (matrix) continua via molecular diffusion. The dual porosity conceptualization is illustrated in Figure 4.4. Retardation is permitted in both the advective and diffusive domains assuming linear equilibrium isotherms. Radioactive decay is accounted for through the use of multiple straight decay chains.

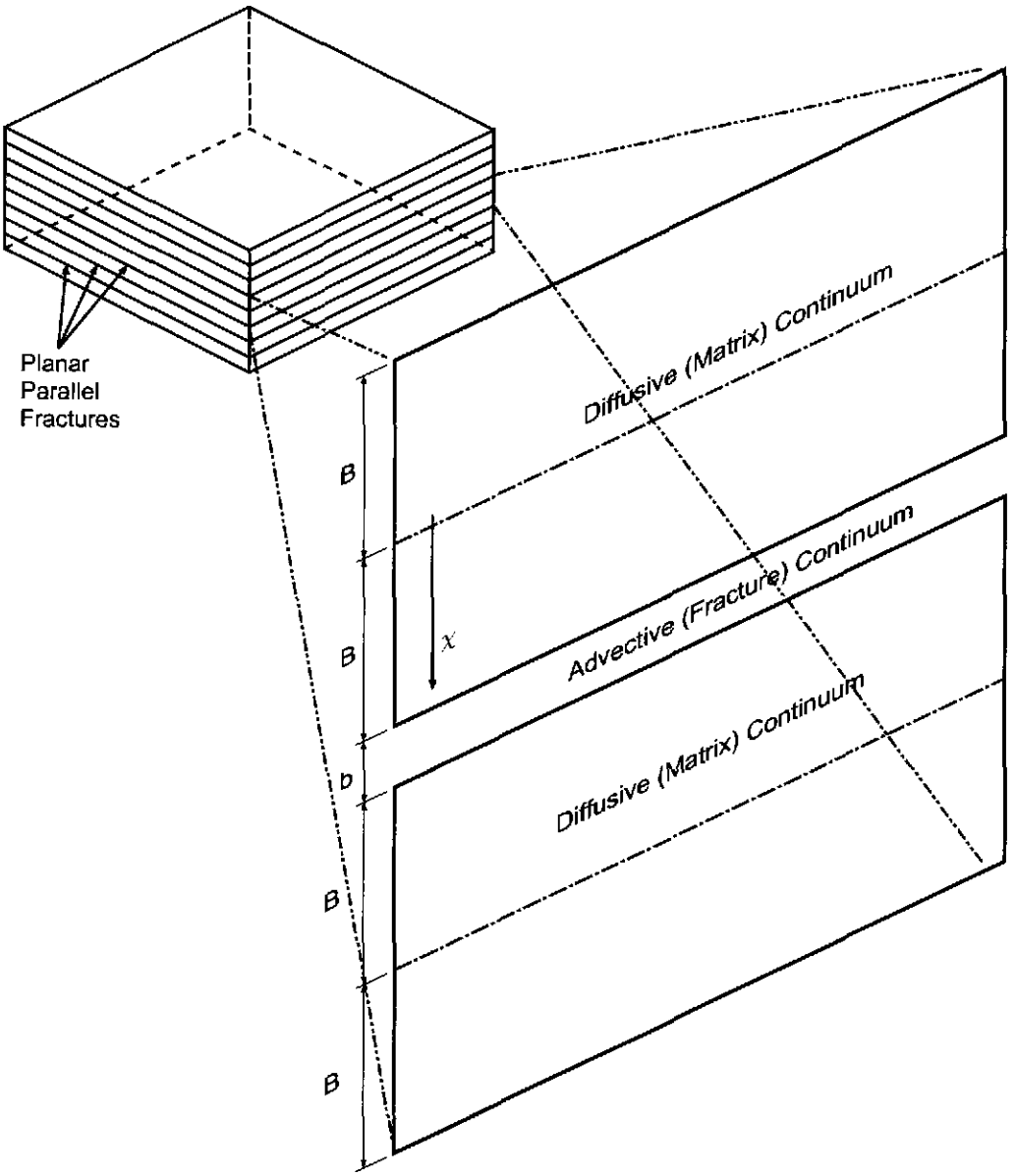

Figure 4.4 Dual Porosity Conceptual Model

SECOTP2D solves the following partial differential equation (PDE) for radionuclide transport in the advective continuum

$$\phi R_k \frac{\partial C_k}{\partial t} = -\nabla\bullet\left(\mathbf{v}C_k\right) + \nabla\bullet\left(\phi\mathbf{D}_k\nabla C_k\right) - \phi R_k\lambda_k C_k + \phi R_{k-1}\lambda_{k-1}C_{k-1} + Q_k + \Gamma_k$$

where k is a species index, C_k is the unknown concentration of the k^{th} radionuclide in the advective continuum (kg/m^3), $\mathbf{v}$ is the specific discharge vector (m/s), $\mathbf{D}_k$ is the hydrodynamic dispersion tensor (m^2/s), ϕ is the advective porosity (dimensionless), R_k is the retardation coefficient (dimensionless), λ_k is the radioactive decay rate constant (s^{-1}), Q_k is the specific injection rate (kg/m^3/s), and Γ_k denotes rate of mass transfer to the advective continuum from the diffusive continuum, per unit volume (kg/m^3/s).

The concentration C_k is defined as the mass of the k^{th} radionuclide per unit volume of pore fluid. The advective porosity, ϕ, is defined as the ratio of the advective pore volume to the total or bulk volume. Similarly, the specific injection rate is defined as the rate of mass injected per unit bulk volume. Terms involving $k-1$ are omitted for the parent of the decay chain ($k=1$). The advective transport equation is linear in C_k and is solved simultaneously for all species in a given decay chain ($k=1,2,...,N_s$), where N_s is the number of species in the decay chain.

The flow field, $\mathbf{v}$, is assumed to be independent of the solute concentration. In practice, the flow field is obtained from a groundwater flow code (MF2K in this analysis), and scaled by a random factor to account for the potential impact of climate change.

The product $\phi\mathbf{D}_k$ is defined as

$$\phi\mathbf{D}_k = \frac{1}{|\mathbf{v}|}\begin{bmatrix} u & -v \\ v & u \end{bmatrix}\begin{bmatrix} \alpha_L & 0 \\ 0 & \alpha_T \end{bmatrix}\begin{bmatrix} u & v \\ -v & u \end{bmatrix} + \phi\tau D_k^*$$

where α_L is the longitudinal dispersivity of the advective continuum (m), α_T is the transverse dispersivity (m), u and v are the x- and y-components of the specific discharge vector (m/s), D_k^* is the free water molecular diffusion coefficient (m^2/s), and τ is the advective tortuosity defined as the ratio of the fluid particle flow path length to the length of the porous medium (dimensionless). Note that WIPP PA takes no direct credit for hydrodynamic dispersion in Culebra transport calculations. It conservatively allows only mixing due to molecular diffusion (i.e., $\alpha_L = \alpha_T = 0$). Note also that WIPP PA treats the free liquid molecular diffusion coefficient as a function of both radionuclide species and oxidation state.

The retardation coefficient R_k is defined by

$$R_k = 1 + \frac{\rho_s (1-\phi)}{\phi} K_d^k$$

where ρ_s is the Culebra Dolomite grain density (kg/m^3) and K_d^k is the distribution coefficient of the k^{th} radionuclide (m^3/kg) which completely describes the linear isotherm for radionuclide sorption to the Culebra.

SECOTP2D solves the following one-dimensional PDE for radionuclide transport in the diffusive continuum

$$\phi' \frac{\partial C_k'}{\partial t} = \frac{\partial}{\partial \chi}\left(\phi' D_k' \frac{\partial C_k'}{\partial \chi} \right) - \phi' R_k' \lambda_k' C_k' + \phi' R_{k-1}' \lambda_{k-1}' C_{k-1}'$$

C_k' is the unknown concentration of the k^{th} radionuclide in the diffusive continuum (kg/m^3), χ is the spatial coordinate as shown in Figure 4.4, and D_k' is the matrix diffusion coefficient. The matrix diffusion coefficient is defined as

$$D_k' = \tau' D_k^*$$

where τ' is the matrix tortuosity.

All other symbols in the diffusive transport equation have the same meaning as those in the advective transport equation except that the prime denotes diffusive continuum properties.

The governing equations for the advective and diffusive continua are coupled through the mass transfer term, Γ_k. Applying Fick's law at the interface between the two continua results in the following equation for mass transfer:

$$\Gamma_k = -\frac{2\phi}{b}\left(\phi' D_k' \left. \frac{\partial C_k'}{\partial \chi} \right|_{\chi = B} \right)$$

where B is the matrix half-block length (m), b is the fracture aperture (m), and the terms in parentheses represent the mass flux per unit area of contact between the advective and diffusive continua. The term $2\phi / b$ represents the specific surface area (ratio of surface

area to bulk volume) of the coupled system. In the parallel plate formulation used in SECOTP2D, the fracture aperture b is defined by

$$b = \frac{\phi B}{1-\phi}$$

4.1.4 Model Parameters

The transport equations for the advective and diffusive continuums described in section 4.1.3 contain many parameters, which must be obtained from measurements, theoretical considerations, or expert judgment. In general, WIPP PA treats certain process model parameters as deterministic and others as uncertain. Uncertain parameters are represented by probability distributions, and sampled values of uncertain parameters are used in a probabilistic (Monte Carlo) modeling approach to predict repository performance.

The parameters can be divided into physical parameters and chemical parameters. The physical parameters are generally properties of the porous Culebra material. The chemical parameters are generally properties of the radionuclide species transported. Note that some chemical parameters are functions of the oxidation state as well as species.

WIPP PA treats the following Culebra physical transport parameters as deterministic: 1) advective continuum longitudinal dispersivity; 2) advective continuum transverse dispersivity; 3) fracture tortuosity; 4) matrix tortuosity; 5) skin resistance factor; and 6) Culebra material grain density. The WIPP PA Parameter Database (PAPDB) designations for these parameters, along with the values used in this analysis are shown in Table 4.2. Note that these parameter values have not changed since the CCA

Table 4.2 Deterministic physical transport parameters

Model Parameter	PAPDB MATERIAL:PROPERTY	Value	Units
Longitudinal dispersivity	CULEBRA:DISP_L	0	m
Transverse dispersivity	CULEBRA:DISP_T	0	m
Fracture tortuosity	CULEBRA:FTORT	1.0	-
Matrix tortuosity	CULEBRA:DTORT	0.11	-
Skin resistance	CULEBRA:SKIN_RES	0	-
Material grain density	CULEBRA:DNSGRAIN	2820	kg/m^3

WIPP PA treats the following Culebra physical transport parameters as subjectively uncertain: 1) advective (fracture) porosity; 2) diffusive (matrix) porosity; 3) matrix half-block length; 4) climate index. The PAPDB designations for these parameters, along with the probability distributions used in this analysis are shown in Table 4.3. Note that these parameter distributions have not changed since the CCA. The sampled values for any given analysis will depend upon the random seed used in the sampling algorithm.

Table 4.3 Uncertain Physical Parameters

Model Parameter	MATERIAL:PROPERTY	Units	Distribution	Range	Median
Advective porosity	CULEBRA:APOROS	-	loguniform	[1.00e-04, 1.00e-02]	1.00e-03
Diffusive porosity	CULEBRA:DPOROS	-	cumulative	[1.00e-01, 2.50e-01]	1.60e-01
Matrix half-block length	CULEBRA:HMBLKLT	m	uniform	[5.00e-02, 5.00e-01]	2.75e-01
Climate index	GLOBAL:CLIMTIDX	-	cumulative	[1.00e+00, 2.25e+00]	1.17e+00
Mining factor	CULEBRA:MINP_FAC	-	uniform	[1.00e+00, 1.00e+03]	5.005e+02
Flow field index	GLOBAL:TRANSIDX	-	uniform	[0.00e+00, 1.00e+00]	5.00e-01

WIPP PA treats the following radionuclide chemical parameters as deterministic: 1) radionuclide atomic weight; 2) radionuclide half-life; 3) radionuclide free liquid molecular diffusion coefficient. The PAPDB designations for these parameters, along with the values used in this analysis are shown in Table 4.4. Note that these parameter values have not changed since the CCA.

Table 4.4 Deterministic Chemical Parameters

Model Parameter	PAPDB MATERIAL:PROPERTY	Value	Units
Atomic Weight[1]			
^{241}Am	AM241:ATWEIGHT	2.4105700e-001	kg/mole
^{239}Pu	PU239:ATWEIGHT	2.3905200e-001	kg/mole
^{230}Th	TH230:ATWEIGHT	2.3003300e-001	kg/mole
^{234}U	U234:ATWEIGHT	2.3404100e-001	kg/mole
Half-life $(t_{1/2})$ [1,2]			
^{241}Am	AM241:HALFLIFE	1.3640000e+010	s
^{239}Pu	PU239:HALFLIFE	7.5940000e+011	s
^{230}Th	TH230:HALFLIFE	2.4300000e+012	s
^{234}U	U234:HALFLIFE	7.7160000e+012	s
Molecular diffusion coefficient[3]			
Am(III)	AM+3:MD0	3.0000000e-010	m^2/s
Pu(III)	PU+3:MD0	3.0000000e-010	m^2/s
Pu(IV)	PU+4:MD0	1.5300000e-010	m^2/s
Th(IV)	TH+4:MD0	1.5300000e-010	m^2/s
U(IV)	U+4:MD0	1.5300000e-010	m^2/s
U(VI)	U+6:MD0	4.2600000e-010	m^2/s

1. Atomic weight and half life used to calculate specific activity
2. $\lambda_k = \ln(2)/t_{1/2}$
3. Free liquid diffusion coefficient is a function of species and oxidation state

WIPP PA treats the following radionuclide chemical parameters as subjectively uncertain: 1) oxidation state; and 2) matrix distribution coefficient. The PAPDB designations for these parameters, along with the probability distributions used in this analysis are shown in Table 4.5. Note that these parameter distributions have not changed since the CCA. The sampled values for any given analysis will depend upon the random seed used in the sampling algorithm.

Table 4.5 Uncertain Chemical Parameters

Model Parameter	MATERIAL:PROPERTY	Units	Distribution	Range	Median
Oxidation state index	GLOBAL:OXSTAT	-	uniform	[1.00e-04, 1.00e-02]	1.00e-03
Matrix distribution coefficient					
Am(III)	AM+3:MKD_AM	m^3/kg	loguniform	[2.00e-02, 4.00e-01]	9.00e-02
Pu(III)	PU+3:MKD_PU	m^3/kg	loguniform	[2.00e-02, 4.00e-01]	9.00e-02
Pu(IV)	PU+4:MKD_PU	m^3/kg	loguniform	[7.00e-01, 1.00e+01]	2.60e+00
Th(IV)	TH+4:MKD_TH	m^3/kg	loguniform	[7.00e-01, 1.00e+01]	2.60e+00
U(IV)	U+4:MKD_U	m^3/kg	loguniform	[7.00e-01, 1.00e+01]	2.60e+00
U(VI)	U+6:MKD_U	m^3/kg	loguniform	[3.00e-05, 2.00e-002]	7.70e-04

4.2 Computational Approach

This section describes the methods used to organize and implement the radionuclide transport calculations, and the results of the calculations.

The SECOTP2D solute transport code is used in conjunction with a preprocessor (PRESECOTP2D) and a postprocessor (POSTSECOTP2D). In addition, several utility codes are used to sample from the probability distributions for subjectively uncertain parameters, define the mesh, set material properties and set model parameters. These codes and their use is described in the following sections. All of these codes are located in the WIPP Software Configuration Management System (SCMS, Long 2002) and are run on the WIPP PA Alpha Cluster. All codes used in the analysis, with the exception of the VTRAN2 utility code, are qualified per Nuclear Waste Management Procedure NP 19-1: Software Requirements (Chavez 2004). The VTRAN2 utility is qualified for use in this analysis per Nuclear Waste Management Procedure NP 9-1: Analyses (Chavez 2001). VTRAN2 code validation testing is presented in Appendix A.

The computations are divided into several steps according to the number of times a particular code is run, for efficiency, and to allow for inspection of intermediate results. Digital command language (DCL) run control scripts have been written to orchestrate the calculations in each step. Using these scripts, the calculations were performed under formal run control procedures by the WIPP PA Run Control Coordinator. See the CRA-2004 PABC Run Control Report (Long and Kanney 2005) for detailed information in the WIPP PA Run Control System.

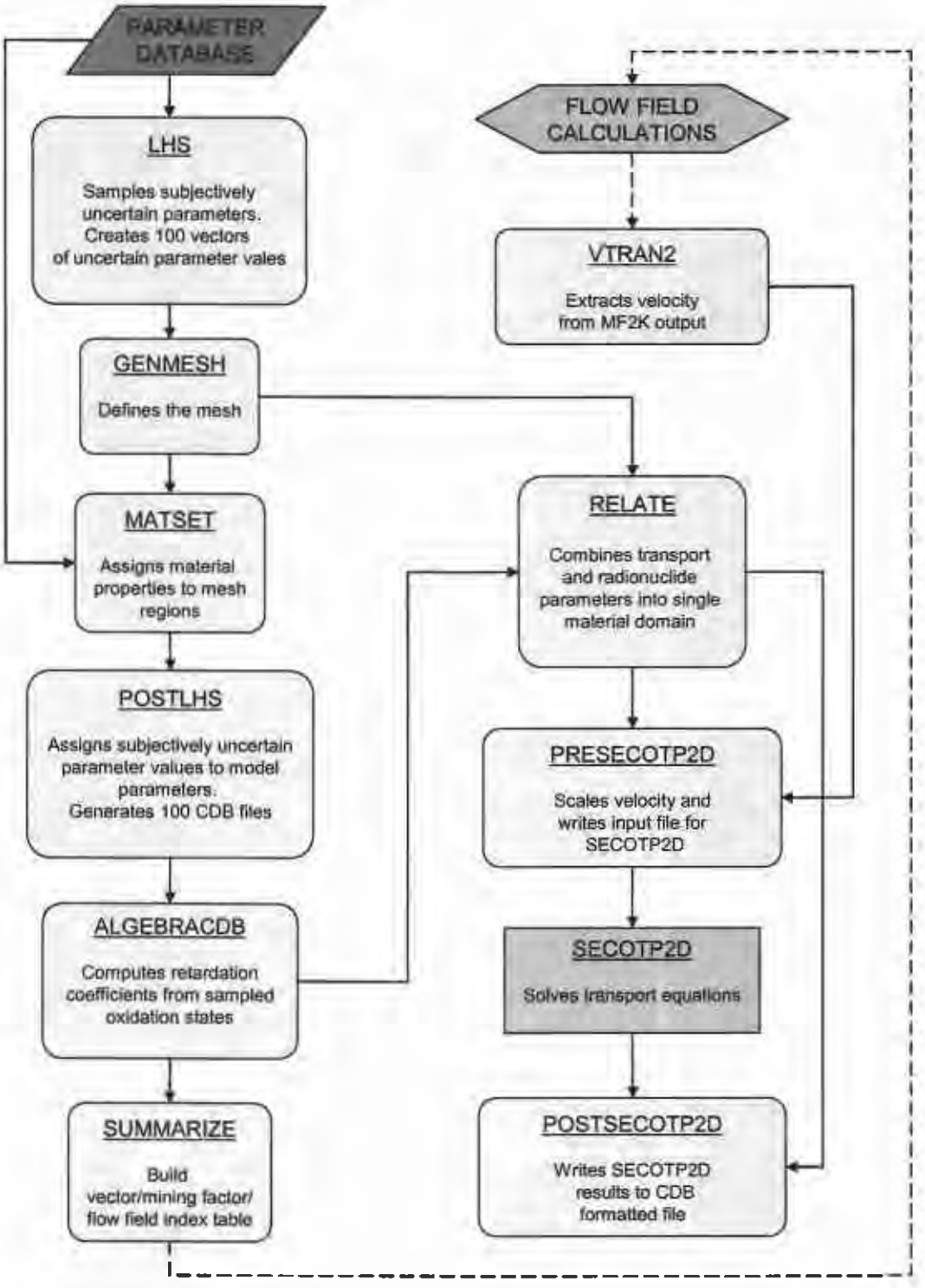

Figure 4.5 Culebra Transport Calculations Flow Chart

4.2.1.1 Step 0 - Sampling of Subjectively Uncertain Parameters

The subjectively uncertain Culebra transport parameters were not sampled in isolation. Instead, all subjectively uncertain parameters used in the CRA-2004 PABC were sampled at once at the beginning the of PA calculations in order to impose the appropriate correlations. The Latin hypercube sampling code LHS was used for this purpose. The LHS sampling is reported in (Kirchner 2005b).

4.2.1.2 Step 1 - Mesh Generation and Material Property Assignment

Step 1 is run once. The Step 1 script uses GENMESH version 6.08 to generate the computational grid and MATSET version 9.10 to assign material properties to element blocks. The Step 1 script, GENMESH and MATSET executables, script input and log files, as well as the input and output files for GENMESH and MATSET are shown in Table 4.6.

The GENMESH input file specifies a uniform computational mesh consisting of 50x50m cells, with 151 cells in the x-direction, and 109 cells in the y-direction. All cells are 4m thick.

The MATSET input file specifies 13 element blocks. Block 1 is for Culebra physical transport properties. Block 2 is for global properties. Block 3 is for reference constants. Blocks 4 through 7 are for the atomic weights and half-lives of radionuclide species ^{241}Am, ^{239}Pu, ^{230}Th, and ^{234}U, respectively. Blocks 8 through 13 are for the distribution coefficients and molecular diffusion coefficients for the species/oxidation state combinations Am(III), Pu(III), Pu(IV), Th(IV), U(IV), and U(IV), respectively.

MATSET assigns the values of deterministic model parameters to the appropriate element blocks. For uncertain model parameters, the median value is assigned to the appropriate element blocks.

Table 4.6 Step 1 input and output files

	File Names	CMS Library	CMS Class
SCRIPT	EVAL_GENERIC_STEP1.COM	LIBCRA1BC_EVAL	GENERIC_STEP1_V1.4
Input	EVAL_ST2D_CRA1BC_STEP1.INP	LIBCRA1BC_EVAL	CRA1BC-0
Log	EVAL_ST2D_CRA1BC_STEP1.LOG	LIBCRA1BC_ST2D	CRA1BC-0
GENMESH	GM_PA96.EXE	LIBGM	PA96
Input	GM_ST2D_CRA1BC.INP	LIBCRA1BC_ST2D	CRA1BC-0
Output	GM_ST2D_CRA1BC.CDB	LIBCRA1BC_ST2D	CRA1BC-0
Output	GM_ST2D_CRA1BC.DBG	NOT KEPT	NOT KEPT
MATSET	MATSET_QA0910.EXE	LIBMS	QA0910
Input	MS_ST2D_CRA1BC.INP	LIBCRA1BC_ST2D	CRA1BC-0
Input	GM_ST2D_CRA1BC.CDB	LIBCRA1BC_ST2D	CRA1BC-0
Output	MS_ST2D_CRA1BC.CDB	LIBCRA1BC_ST2D	CRA1BC-0
Output	MS_ST2D_CRA1BC.DBG	NOT KEPT	NOT KEPT

4.2.1.3 Step 2 - Uncertain Parameter Assignments (Step 2)

Step 2 is run once per replicate. The Step 2 script uses POSTLHS version 4.07A to assign the sampled parameter values to the appropriate element block properties. The Step 2 script, POSTLHS executable, script input and log files, as well as the input and output files for POSTLHS are shown in Table 4.7.

POSTLHS loops over all 100 vectors in the replicate. The result is 100 CAMDAT database (CDB) files per replicate, with each CDB file containing the sampled parameter values for that replicate/vector combination. Sampled values for physical parameters for replicates R1, R2, and R3 are shown in Table 4.8, Table 4.9, and Table 4.10, respectively. Sampled values for chemical parameters for replicates R1, R2, and R3 are shown in Table 4.11, Table 4.12, and Table 4.12, respectively.

Table 4.7 Step 2 input and output files

	File Names[1,2]	CMS Library	CMS Class
SCRIPT	EVAL_GENERIC_STEP2.COM	LIBCRA1BC_EVAL	GENERIC_STEP2_V1.2
Input	EVAL_ST2D_CRA1BC_STEP2_R*r*.INP	LIBCRA1BC_EVAL	CRA1BC-0
Log	EVAL_ST2D_CRA1BC_STEP2_R*r*.LOG	LIBCRA1BC_ST2D	CRA1BC-0
POSTLHS	POSTLHS_QA0407A.EXE	LIBLHS	QA0407A
Input	LHS3_DUMMY.INP	LIBCRA1BC_LHS	CRA1BC-0
Input	LHS2_CRA1BC_R*r*.TRN	LIBCRA1BC_LHS	CRA1BC-0
Input	MS_ST2D_CRA1BC.CDB	LIBCRA1BC_ST2D	CRA1BC-0
Output	LHS3_ST2D_CRA1BC_R*r*_V*vvv*.CDB	LIBCRA1BC_ST2D	CRA1BC-0
Output	LHS3_ST2D_CRA1BC_R*r*.DBG	LIBCRA1BC_ST2D	CRA1BC-0

1. $r \in \{1, 2, 3\}$
2. $vvv \in \{001, 002, ..., 100\}$ for each r

Table 4.8 Sampled Physical Parameter Values – Replicate R1

vector	APOROS	DPOROS	HMBLKLT	MINP_FAC	CLIMTIDX	TRANSIDX
1	3.47E-04	1.44E-01	2.73E-01	9.83E+02	1.09E+00	4.56E-01
2	1.17E-04	2.20E-01	1.73E-01	9.09E+02	1.17E+00	7.86E-01
3	3.08E-04	1.33E-01	4.27E-01	5.32E+02	1.20E+00	9.26E-01
4	2.76E-03	1.74E-01	2.10E-01	5.84E+02	1.01E+00	2.97E-01
5	7.70E-03	1.97E-01	4.37E-01	3.74E+02	1.04E+00	8.76E-01
6	1.51E-03	1.07E-01	2.50E-01	8.03E+02	1.59E+00	3.57E-01
7	2.13E-03	1.93E-01	3.47E-01	3.85E+02	1.19E+00	9.56E-01
8	9.46E-04	1.49E-01	3.67E-01	7.44E+02	1.12E+00	8.05E-01
9	8.13E-04	2.09E-01	5.26E-02	7.83E+02	1.17E+00	9.42E-01
10	4.18E-03	1.77E-01	3.98E-01	7.05E+02	1.13E+00	5.05E-01
11	5.22E-04	1.72E-01	2.34E-01	5.79E+02	1.15E+00	4.16E-01
12	2.58E-04	1.89E-01	3.38E-01	5.44E+02	1.24E+00	8.47E-01
13	1.65E-04	1.75E-01	2.99E-01	1.12E+02	1.07E+00	3.85E-01
14	8.58E-03	1.62E-01	4.21E-01	5.89E+01	1.24E+00	2.57E-01
15	1.82E-04	1.36E-01	1.07E-01	8.89E+02	1.21E+00	9.37E-01
16	4.95E-04	1.85E-01	4.66E-01	2.99E+02	1.03E+00	8.22E-01
17	1.46E-04	1.03E-01	1.97E-01	4.42E+01	1.16E+00	7.74E-01
18	4.46E-04	1.90E-01	4.64E-01	2.40E+02	1.75E+00	1.82E-01
19	7.08E-04	1.84E-01	4.99E-01	1.80E+02	1.16E+00	6.81E-01
20	6.27E-04	1.57E-01	3.63E-01	3.08E+01	1.62E+00	3.10E-01
21	1.66E-03	1.63E-01	3.20E-01	1.02E+00	1.07E+00	6.12E-01
22	2.26E-03	1.15E-01	2.86E-01	3.41E+02	1.01E+00	1.60E-01
23	1.20E-04	1.79E-01	4.16E-01	3.09E+02	1.14E+00	2.86E-01
24	1.61E-03	1.02E-01	4.90E-01	7.21E+02	1.71E+00	7.70E-01
25	8.64E-04	1.61E-01	4.08E-01	1.49E+02	1.24E+00	2.58E-02
26	5.27E-03	1.76E-01	2.65E-01	9.38E+02	1.13E+00	1.98E-01
27	1.26E-03	1.04E-01	3.73E-01	1.54E+02	1.18E+00	6.72E-01
28	6.98E-03	1.58E-01	4.86E-01	5.52E+02	2.07E+00	7.95E-03
29	9.67E-04	1.70E-01	2.93E-01	4.35E+02	1.13E+00	1.78E-01
30	1.13E-04	1.81E-01	1.52E-01	7.74E+02	1.88E+00	2.62E-01
31	2.10E-04	1.67E-01	2.40E-01	5.30E+02	1.11E+00	9.65E-01
32	1.09E-03	1.13E-01	8.01E-02	2.04E+02	1.17E+00	9.12E-01

Table 4.8 Sampled Physical Parameter Values – Replicate R1						
vector	APOROS	DPOROS	HMBLKLT	MINP_FAC	CLIMTIDX	TRANSIDX
33	1.83E-04	1.24E-01	3.21E-01	7.66E+02	1.24E+00	7.55E-01
34	5.73E-04	1.15E-01	3.03E-01	4.25E+02	1.10E+00	9.72E-01
35	2.30E-04	1.52E-01	2.16E-01	8.11E+02	1.19E+00	1.27E-01
36	4.80E-03	1.21E-01	1.14E-01	2.48E+02	1.54E+00	6.97E-01
37	2.84E-04	1.17E-01	4.05E-01	7.52E+02	1.10E+00	2.11E-01
38	2.65E-04	1.19E-01	2.05E-01	3.63E+02	2.15E+00	5.94E-01
39	5.27E-04	1.76E-01	6.35E-02	1.71E+02	1.22E+00	6.21E-02
40	1.28E-04	1.73E-01	2.47E-01	4.85E+02	1.03E+00	3.48E-02
41	2.28E-04	1.48E-01	4.44E-01	8.70E+02	1.03E+00	1.61E-01
42	8.95E-04	1.66E-01	3.82E-01	6.03E+02	1.16E+00	5.71E-01
43	4.14E-03	1.68E-01	3.56E-01	9.77E+02	1.05E+00	6.31E-01
44	4.67E-03	1.09E-01	1.02E-01	8.57E+02	1.04E+00	1.39E-01
45	5.92E-04	1.20E-01	2.60E-01	7.97E+02	1.02E+00	1.42E-01
46	1.01E-03	2.28E-01	2.56E-01	6.16E+02	1.05E+00	2.42E-01
47	7.56E-04	1.46E-01	1.13E-01	9.56E+02	1.15E+00	7.34E-01
48	5.64E-03	1.39E-01	3.09E-01	2.73E+02	1.08E+00	9.88E-01
49	3.64E-03	1.65E-01	2.83E-01	1.96E+02	1.06E+00	8.97E-01
50	3.49E-03	1.69E-01	1.42E-01	3.99E+02	1.06E+00	7.05E-01
51	3.35E-04	1.82E-01	3.12E-01	2.59E+02	1.11E+00	3.44E-01
52	9.82E-03	1.84E-01	3.84E-01	8.32E+02	1.21E+00	4.78E-01
53	2.04E-03	1.53E-01	2.30E-01	2.61E+02	1.02E+00	5.29E-01
54	1.44E-03	1.30E-01	2.37E-01	9.18E+01	1.05E+00	7.43E-01
55	7.61E-04	1.10E-01	2.78E-01	6.97E+02	1.09E+00	4.06E-01
56	4.39E-03	1.06E-01	2.68E-01	5.06E+02	1.00E+00	4.35E-01
57	2.90E-03	1.10E-01	3.77E-01	2.18E+02	1.94E+00	9.68E-02
58	3.28E-04	1.12E-01	1.35E-01	2.90E+02	1.23E+00	2.33E-01
59	1.24E-03	1.86E-01	4.48E-01	6.82E+02	1.19E+00	1.03E-01
60	6.83E-04	1.73E-01	8.39E-02	4.55E+02	1.11E+00	5.52E-01
61	1.91E-03	1.68E-01	3.31E-01	5.14E+02	1.23E+00	5.47E-01
62	1.01E-04	1.28E-01	4.38E-01	3.21E+02	1.00E+00	6.24E-01
63	8.75E-03	1.41E-01	1.57E-01	3.37E+02	1.22E+00	5.61E-01
64	9.38E-03	2.38E-01	1.78E-01	1.86E+02	1.81E+00	8.30E-01
65	2.37E-03	2.03E-01	3.93E-01	4.67E+02	1.07E+00	8.57E-01
66	5.85E-03	1.86E-01	3.28E-01	8.98E+02	1.04E+00	2.28E-01
67	5.22E-03	1.45E-01	1.28E-01	6.37E+02	1.25E+00	7.12E-01
68	2.64E-03	1.03E-01	4.56E-01	9.47E+02	2.01E+00	4.08E-02
69	2.56E-03	1.54E-01	1.46E-01	9.21E+02	1.21E+00	2.79E-01
70	1.10E-03	1.11E-01	4.72E-01	3.57E+02	1.57E+00	7.28E-01
71	4.26E-04	1.28E-01	2.19E-01	1.36E+01	1.98E+00	3.29E-01
72	1.98E-04	1.78E-01	4.74E-01	5.93E+02	2.02E+00	8.70E-01
73	1.07E-04	1.80E-01	7.48E-02	9.69E+02	1.66E+00	3.31E-01
74	4.01E-04	2.46E-01	4.91E-01	3.25E+02	2.18E+00	3.94E-01
75	3.68E-04	1.88E-01	8.65E-02	8.47E+02	2.08E+00	2.04E-01
76	1.34E-03	1.64E-01	4.82E-01	6.26E+02	1.15E+00	7.91E-01
77	8.20E-03	1.87E-01	1.62E-01	4.79E+02	1.22E+00	4.85E-01
78	6.13E-03	1.61E-01	1.26E-01	9.13E+02	1.07E+00	6.67E-01
79	3.81E-03	1.42E-01	3.57E-01	1.25E+02	1.02E+00	8.34E-02
80	1.77E-03	1.25E-01	5.64E-02	8.01E+01	1.50E+00	9.00E-01
81	3.04E-03	1.19E-01	1.65E-01	4.14E+02	1.18E+00	4.94E-01
82	2.00E-04	2.33E-01	1.72E-01	1.04E+02	1.04E+00	5.80E-02
83	3.19E-03	1.79E-01	2.89E-01	6.63E+02	1.91E+00	5.84E-01

Table 4.8 Sampled Physical Parameter Values – Replicate R1						
vector	APOROS	DPOROS	HMBLKLT	MINP_FAC	CLIMTIDX	TRANSIDX
84	2.50E-04	1.63E-01	4.11E-01	6.60E+02	2.11E+00	8.12E-01
85	1.37E-04	2.22E-01	9.59E-02	4.99E+02	1.12E+00	3.70E-01
86	4.68E-04	1.88E-01	1.84E-01	8.73E+02	1.10E+00	6.03E-01
87	1.44E-04	1.17E-01	4.54E-01	8.45E+01	1.08E+00	3.08E-01
88	1.53E-03	1.34E-01	7.10E-02	3.94E+01	1.08E+00	1.15E-01
89	2.45E-03	1.23E-01	1.93E-01	5.66E+02	1.84E+00	6.42E-01
90	3.39E-03	1.83E-01	6.59E-02	2.31E+02	1.12E+00	3.77E-01
91	1.18E-03	1.12E-01	1.85E-01	8.22E+02	2.20E+00	7.69E-02
92	3.93E-04	1.14E-01	9.39E-02	6.48E+02	1.23E+00	8.87E-01
93	6.39E-03	1.38E-01	1.21E-01	4.44E+02	1.19E+00	1.41E-02
94	1.84E-03	1.17E-01	3.36E-01	7.18E+02	1.14E+00	9.98E-01
95	7.32E-03	1.08E-01	3.47E-01	9.95E+02	1.10E+00	5.36E-01
96	6.64E-03	1.82E-01	1.38E-01	6.71E+01	2.24E+00	4.66E-01
97	6.56E-04	1.71E-01	4.31E-01	6.72E+02	1.78E+00	4.40E-01
98	1.56E-04	1.59E-01	3.88E-01	7.32E+02	1.70E+00	5.12E-01
99	2.98E-04	1.00E-01	2.23E-01	4.05E+02	1.17E+00	4.26E-01
100	1.72E-04	1.16E-01	2.03E-01	1.37E+02	1.20E+00	6.58E-01

Table 4.9 Sampled physical parameter values – Replicate R2

vector	APOROS	DPOROS	HMBLKLT	MINP_FAC	CLIMTIDX	TRANSIDX
1	4.47E-04	1.81E-01	2.37E-01	2.49E+02	1.01E+00	7.26E-01
2	3.59E-03	1.99E-01	7.37E-02	8.65E+02	1.05E+00	8.52E-01
3	6.14E-03	1.09E-01	3.13E-01	6.21E+01	1.90E+00	9.05E-01
4	2.71E-04	1.19E-01	2.70E-01	9.36E+02	1.06E+00	7.42E-01
5	7.17E-03	1.32E-01	1.14E-01	7.29E+02	2.14E+00	2.33E-01
6	2.40E-04	1.84E-01	4.91E-01	1.95E+02	1.23E+00	4.07E-01
7	1.91E-04	1.84E-01	1.64E-01	6.57E+02	1.07E+00	7.62E-01
8	2.85E-03	1.13E-01	4.82E-01	3.18E+02	2.00E+00	6.88E-01
9	7.52E-04	1.00E-01	2.31E-01	4.52E+02	1.14E+00	3.51E-01
10	2.47E-04	1.15E-01	1.70E-01	2.71E+02	1.11E+00	6.83E-03
11	9.99E-04	1.77E-01	4.40E-01	8.52E+02	1.25E+00	7.94E-01
12	9.51E-03	2.04E-01	2.82E-01	3.38E+02	1.08E+00	6.91E-01
13	9.58E-03	1.08E-01	4.96E-01	7.98E+02	1.04E+00	6.56E-01
14	1.09E-04	1.17E-01	1.84E-01	4.02E+02	1.23E+00	9.72E-02
15	3.59E-04	1.75E-01	3.86E-01	5.52E+02	1.21E+00	5.48E-01
16	1.58E-03	1.22E-01	1.52E-01	9.11E+02	1.18E+00	3.73E-01
17	8.29E-03	1.87E-01	3.35E-01	2.44E+01	1.13E+00	7.84E-01
18	4.98E-04	1.38E-01	8.94E-02	9.81E+02	1.14E+00	9.92E-01
19	3.35E-03	2.27E-01	3.05E-01	6.14E+02	1.12E+00	8.67E-01
20	4.69E-03	1.11E-01	3.69E-01	4.69E+02	1.58E+00	6.75E-01
21	7.10E-04	2.24E-01	3.25E-01	1.03E+02	1.20E+00	7.07E-01
22	1.26E-04	1.64E-01	3.92E-01	5.15E+02	1.21E+00	3.62E-02
23	1.32E-03	1.64E-01	9.21E-02	6.74E+02	1.17E+00	6.43E-01
24	5.63E-03	1.16E-01	2.59E-01	7.79E+02	2.08E+00	1.70E-02
25	1.89E-04	1.53E-01	5.39E-02	4.91E+01	1.85E+00	4.94E-01
26	2.12E-03	2.42E-01	2.73E-01	8.65E+01	1.08E+00	1.24E-01
27	5.26E-03	1.72E-01	1.32E-01	9.96E+02	1.93E+00	5.69E-01
28	8.89E-04	1.29E-01	2.02E-01	4.80E+02	1.03E+00	1.34E-01
29	5.07E-03	1.33E-01	6.58E-02	6.00E+02	1.20E+00	2.16E-01
30	2.05E-03	1.62E-01	2.05E-01	2.07E+02	1.10E+00	9.24E-01
31	2.46E-03	1.86E-01	4.02E-01	3.63E+01	1.15E+00	1.72E-01
32	7.63E-03	1.02E-01	1.74E-01	2.62E+02	1.05E+00	6.10E-01
33	6.20E-04	1.26E-01	1.88E-01	5.56E+00	1.06E+00	5.56E-01
34	1.80E-04	1.74E-01	4.11E-01	3.08E+02	1.15E+00	4.47E-01
35	2.25E-04	1.20E-01	1.24E-01	6.83E+02	1.19E+00	4.22E-01
36	1.80E-03	1.76E-01	4.82E-01	6.65E+02	1.08E+00	9.50E-01
37	1.73E-03	1.12E-01	4.60E-01	7.05E+02	1.20E+00	5.92E-01
38	1.48E-04	1.17E-01	4.16E-01	4.15E+02	1.74E+00	5.11E-01
39	9.44E-04	1.09E-01	4.58E-01	8.31E+02	1.09E+00	1.90E-01
40	3.40E-04	1.03E-01	4.06E-01	8.99E+02	1.18E+00	2.25E-01
41	3.27E-04	1.68E-01	1.93E-01	7.37E+02	1.12E+00	9.17E-01
42	6.40E-03	1.19E-01	1.76E-01	7.71E+01	2.05E+00	5.80E-01
43	2.76E-04	1.24E-01	3.76E-01	2.20E+02	1.15E+00	8.43E-01

Table 4.9 Sampled physical parameter values – Replicate R2

vector	APOROS	DPOROS	HMBLKLT	MINP_FAC	CLIMTIDX	TRANSIDX
44	1.65E-03	1.88E-01	4.31E-01	3.92E+02	2.02E+00	1.43E-01
45	1.10E-04	1.71E-01	3.17E-01	2.53E+02	1.67E+00	7.53E-01
46	1.40E-04	1.80E-01	1.31E-01	3.84E+02	1.00E+00	4.72E-01
47	3.87E-03	1.79E-01	8.44E-02	7.57E+02	1.12E+00	2.06E-01
48	8.81E-03	1.75E-01	2.88E-01	7.48E+02	1.20E+00	5.00E-01
49	2.36E-03	1.65E-01	1.55E-01	1.25E+02	1.53E+00	2.60E-02
50	2.01E-04	1.04E-01	4.36E-01	1.19E+02	1.61E+00	3.60E-01
51	8.22E-04	1.44E-01	1.40E-01	6.91E+02	1.16E+00	6.61E-02
52	4.34E-04	2.11E-01	1.21E-01	7.70E+02	1.97E+00	4.39E-01
53	5.63E-04	1.56E-01	3.97E-01	8.12E+02	1.10E+00	4.84E-01
54	1.11E-03	1.85E-01	1.39E-01	9.80E+02	1.22E+00	1.89E-01
55	4.22E-03	1.82E-01	2.09E-01	8.88E+02	1.02E+00	2.80E-01
56	5.10E-04	1.51E-01	1.48E-01	1.84E+02	1.16E+00	8.01E-01
57	5.35E-04	1.73E-01	4.25E-01	8.48E+02	1.81E+00	2.74E-01
58	2.21E-03	1.69E-01	5.97E-02	1.44E+02	1.25E+00	2.63E-01
59	4.14E-03	1.01E-01	9.79E-02	6.06E+02	1.24E+00	6.23E-01
60	3.63E-04	1.79E-01	2.79E-01	6.34E+02	1.09E+00	4.14E-01
61	4.50E-03	1.14E-01	3.51E-01	5.28E+02	1.16E+00	3.82E-01
62	4.01E-04	1.20E-01	3.42E-01	3.57E+02	1.64E+00	1.18E-01
63	1.39E-03	1.67E-01	2.97E-01	6.49E+02	1.22E+00	9.79E-01
64	5.82E-04	1.18E-01	4.71E-01	1.79E+02	1.02E+00	9.88E-01
65	1.70E-04	1.91E-01	4.74E-01	7.14E+02	1.01E+00	2.43E-01
66	2.59E-04	1.89E-01	2.64E-01	4.26E+02	1.14E+00	1.59E-01
67	1.83E-03	1.15E-01	4.22E-01	9.48E+02	1.02E+00	1.04E-01
68	8.61E-03	1.88E-01	2.53E-01	5.39E+02	1.17E+00	2.97E-01
69	1.16E-03	1.31E-01	3.56E-01	4.32E+02	1.09E+00	3.10E-01
70	6.89E-03	1.45E-01	4.49E-01	9.58E+02	1.19E+00	9.36E-01
71	1.93E-03	2.19E-01	3.58E-01	3.73E+02	1.05E+00	1.67E-01
72	3.03E-04	1.06E-01	1.03E-01	5.97E+01	1.01E+00	5.79E-01
73	1.48E-03	1.49E-01	2.43E-01	8.27E+02	1.79E+00	3.94E-01
74	7.55E-03	1.46E-01	3.31E-01	1.70E+02	1.19E+00	7.50E-02
75	3.16E-03	2.48E-01	6.96E-02	5.73E+02	1.74E+00	6.16E-01
76	1.10E-03	1.61E-01	2.28E-01	4.43E+02	1.11E+00	5.21E-01
77	1.05E-03	1.06E-01	1.07E-01	7.81E+02	1.70E+00	7.33E-01
78	1.27E-03	1.11E-01	1.96E-01	2.87E+02	1.10E+00	4.64E-01
79	4.77E-04	1.86E-01	4.52E-01	3.45E+02	2.19E+00	6.34E-01
80	7.69E-04	1.12E-01	2.18E-01	5.04E+02	1.03E+00	8.54E-02
81	1.20E-03	1.40E-01	1.61E-01	4.96E+02	1.11E+00	3.11E-01
82	1.65E-04	1.82E-01	2.45E-01	6.21E+02	1.24E+00	5.39E-01
83	2.57E-03	1.28E-01	3.07E-01	5.70E+02	1.13E+00	8.16E-01
84	2.93E-04	1.48E-01	5.86E-02	9.13E+01	1.07E+00	8.81E-01
85	6.72E-04	1.60E-01	3.01E-01	2.29E+02	1.15E+00	5.42E-02
86	1.24E-04	1.83E-01	4.87E-01	8.06E+02	2.12E+00	3.46E-01
87	1.19E-04	1.68E-01	3.20E-01	1.36E+02	1.07E+00	9.64E-01

Table 4.9 Sampled physical parameter values – Replicate R2

vector	APOROS	DPOROS	HMBLKLT	MINP_FAC	CLIMTIDX	TRANSIDX
88	3.29E-03	1.36E-01	2.51E-01	1.63E+01	2.19E+00	8.27E-01
89	4.94E-03	1.78E-01	3.70E-01	5.41E+02	1.22E+00	6.67E-01
90	2.94E-03	1.62E-01	2.23E-01	5.82E+02	1.18E+00	4.53E-01
91	3.76E-03	1.66E-01	3.45E-01	1.56E+02	1.55E+00	7.76E-01
92	1.02E-04	1.58E-01	8.14E-02	9.05E+02	1.12E+00	8.40E-01
93	6.35E-04	1.90E-01	3.63E-01	9.63E+02	1.05E+00	3.24E-01
94	8.34E-04	1.55E-01	3.96E-01	3.23E+02	1.02E+00	3.39E-01
95	1.32E-04	1.35E-01	2.14E-01	9.27E+02	2.25E+00	9.44E-01
96	2.16E-04	1.63E-01	1.11E-01	4.88E+02	1.23E+00	8.74E-01
97	5.80E-03	1.71E-01	3.80E-01	2.92E+02	1.03E+00	7.12E-01
98	3.89E-04	2.34E-01	2.89E-01	2.37E+02	1.86E+00	4.10E-02
99	1.54E-04	1.41E-01	4.43E-01	3.65E+02	1.24E+00	8.92E-01
100	2.70E-03	1.70E-01	4.68E-01	8.76E+02	1.04E+00	2.53E-01

Table 4.10 Sampled Physical Parameter Values – Replicate R3

vector	APOROS	DPOROS	HMBLKLT	MINP_FAC	CLIMTIDX	TRANSIDX
1	4.72E-04	1.57E-01	4.45E-01	6.39E+02	1.11E+00	4.67E-01
2	2.01E-03	1.81E-01	2.93E-01	7.28E+02	1.69E+00	7.50E-01
3	1.35E-04	1.89E-01	3.62E-01	2.14E+02	1.23E+00	6.99E-01
4	5.82E-03	1.53E-01	1.98E-01	1.26E+02	1.20E+00	2.25E-01
5	8.13E-03	1.76E-01	1.23E-01	3.47E+02	1.17E+00	8.64E-01
6	7.47E-03	1.48E-01	2.92E-01	9.22E+02	1.65E+00	5.06E-01
7	1.99E-03	1.75E-01	3.33E-01	6.89E+02	1.01E+00	4.97E-01
8	3.08E-04	1.73E-01	3.05E-01	3.32E+02	1.01E+00	5.22E-01
9	7.68E-04	1.18E-01	1.27E-01	5.17E+02	1.08E+00	9.32E-01
10	1.39E-03	2.22E-01	1.83E-01	5.49E+02	1.16E+00	1.57E-01
11	1.40E-04	1.68E-01	1.72E-01	1.54E+02	1.66E+00	2.95E-01
12	5.56E-03	1.78E-01	3.79E-01	9.13E+01	2.17E+00	7.71E-01
13	1.50E-04	1.74E-01	8.53E-02	9.54E+02	1.12E+00	8.06E-01
14	3.06E-03	1.30E-01	2.41E-01	9.77E+02	1.75E+00	9.42E-02
15	1.60E-03	1.88E-01	1.42E-01	6.57E+02	1.11E+00	4.87E-01
16	2.02E-04	2.14E-01	1.11E-01	7.75E+02	1.19E+00	8.73E-01
17	4.65E-03	1.20E-01	1.67E-01	6.69E+02	1.62E+00	9.64E-01
18	9.39E-03	2.04E-01	4.09E-01	8.68E+02	1.20E+00	9.54E-01
19	1.62E-04	1.81E-01	4.49E-01	7.95E+02	1.10E+00	2.04E-02
20	2.76E-04	1.02E-01	9.53E-02	8.02E+02	1.17E+00	6.30E-02
21	1.88E-04	1.71E-01	3.86E-01	2.53E+02	1.86E+00	3.28E-01
22	4.35E-03	1.00E-01	1.76E-01	8.66E+01	1.20E+00	6.40E-01
23	9.87E-04	2.28E-01	3.95E-01	5.93E+02	2.20E+00	3.05E-01
24	5.02E-03	1.82E-01	2.45E-01	7.25E+01	1.19E+00	7.56E-01
25	1.75E-03	1.28E-01	4.96E-01	5.58E+02	2.15E+00	8.14E-01
26	6.54E-03	1.51E-01	4.74E-01	4.61E+02	1.12E+00	4.40E-01
27	3.86E-03	1.91E-01	4.39E-01	8.29E+02	1.11E+00	6.61E-03

28	1.56E-04	1.24E-01	1.38E-01	9.03E+02	1.87E+00	5.82E-01
29	1.34E-03	1.83E-01	1.19E-01	5.05E+02	2.01E+00	4.50E-01
30	2.75E-04	1.31E-01	2.77E-01	4.92E+02	1.82E+00	1.97E-01
31	6.68E-04	1.07E-01	2.48E-01	6.16E+02	1.13E+00	7.87E-01
32	9.37E-04	1.17E-01	6.79E-02	3.64E+02	1.16E+00	6.06E-01
33	4.98E-04	1.85E-01	4.67E-01	6.49E+02	1.07E+00	8.26E-01
34	5.54E-04	1.12E-01	3.74E-01	6.79E+01	1.22E+00	8.10E-02
35	5.03E-04	1.66E-01	1.57E-01	4.34E+00	1.12E+00	6.80E-01
36	3.53E-04	1.35E-01	3.17E-01	1.78E+01	1.05E+00	4.12E-01
37	5.43E-04	2.00E-01	7.08E-02	5.75E+02	1.19E+00	5.47E-01
38	3.18E-03	1.77E-01	2.72E-01	6.99E+02	1.04E+00	4.77E-01
39	1.49E-03	1.02E-01	2.01E-01	7.07E+02	1.25E+00	3.31E-01
40	4.18E-04	1.23E-01	4.94E-01	7.57E+02	1.15E+00	4.06E-01
41	2.68E-03	1.15E-01	4.69E-01	7.88E+02	1.22E+00	8.48E-01
42	6.08E-03	1.16E-01	4.89E-01	5.88E+02	1.21E+00	7.38E-01
43	8.48E-03	1.79E-01	4.22E-01	3.77E+02	1.02E+00	9.92E-01
44	4.14E-04	1.71E-01	1.85E-01	2.99E+02	1.55E+00	4.49E-01
45	2.17E-03	1.09E-01	4.80E-01	2.66E+02	1.19E+00	7.93E-01
46	2.62E-04	1.33E-01	4.54E-01	4.39E+02	1.14E+00	1.81E-02
47	3.94E-04	1.62E-01	5.84E-02	4.30E+01	1.95E+00	9.78E-01
48	1.80E-04	1.03E-01	3.29E-01	1.92E+02	1.14E+00	7.18E-01
49	7.01E-04	1.82E-01	3.47E-01	9.19E+02	1.24E+00	2.42E-01
50	1.06E-03	1.72E-01	2.07E-01	2.81E+02	1.07E+00	3.77E-01
51	6.24E-04	1.58E-01	1.16E-01	4.44E+02	1.15E+00	5.73E-01
52	5.97E-04	1.11E-01	4.02E-01	8.38E+02	1.57E+00	3.52E-01
53	1.22E-04	1.54E-01	2.09E-01	3.02E+02	1.18E+00	8.59E-01
54	1.13E-04	1.60E-01	4.19E-01	9.92E+02	1.23E+00	7.27E-01
55	8.35E-04	2.13E-01	4.35E-01	2.81E+01	1.18E+00	8.39E-01
56	2.41E-03	1.19E-01	2.17E-01	3.91E+02	1.09E+00	5.40E-02
57	2.13E-04	1.49E-01	2.71E-01	1.72E+02	2.10E+00	3.89E-01
58	1.56E-03	1.20E-01	2.59E-01	6.27E+02	1.21E+00	9.86E-01
59	6.91E-03	1.13E-01	1.34E-01	7.67E+02	1.09E+00	2.13E-01
60	7.59E-03	1.64E-01	2.87E-01	6.02E+02	1.22E+00	2.75E-01
61	2.52E-03	1.05E-01	4.29E-01	4.02E+02	2.10E+00	8.80E-01
62	9.02E-04	1.86E-01	2.81E-01	4.71E+02	1.01E+00	3.97E-01
63	2.39E-04	1.09E-01	2.98E-01	3.26E+02	1.06E+00	9.18E-01
64	2.96E-03	1.30E-01	3.11E-01	3.55E+02	1.07E+00	5.20E-01
65	1.93E-04	1.65E-01	8.08E-02	1.43E+02	2.05E+00	5.62E-01
66	7.25E-04	1.08E-01	4.25E-01	7.38E+02	1.04E+00	2.07E-01
67	3.20E-04	1.70E-01	4.61E-01	8.75E+02	1.05E+00	2.67E-01
68	8.25E-04	1.37E-01	3.36E-01	9.83E+02	1.98E+00	3.63E-01
69	7.07E-03	1.17E-01	5.41E-02	8.86E+02	1.08E+00	1.24E-01
70	1.73E-04	1.77E-01	3.13E-01	5.35E+02	1.03E+00	8.92E-01
71	3.67E-04	2.36E-01	3.38E-01	9.37E+02	1.21E+00	9.03E-01
72	1.27E-04	1.61E-01	1.50E-01	1.39E+02	1.05E+00	4.25E-01
73	2.28E-03	1.43E-01	2.56E-01	5.62E+02	1.17E+00	5.91E-01

74	6.32E-04	1.58E-01	3.53E-01	2.09E+02	2.24E+00	7.73E-02
75	1.28E-03	1.39E-01	7.34E-02	2.21E+02	1.79E+00	7.70E-01
76	9.70E-03	1.64E-01	9.49E-02	6.76E+02	1.08E+00	2.35E-01
77	5.36E-03	1.14E-01	3.72E-01	5.30E+02	1.02E+00	1.69E-01
78	1.01E-04	1.69E-01	2.13E-01	9.60E+02	1.24E+00	5.37E-01
79	1.01E-03	1.83E-01	8.82E-02	3.87E+01	1.07E+00	3.52E-02
80	4.97E-03	1.14E-01	4.12E-01	3.11E+02	1.13E+00	9.49E-01
81	1.06E-04	1.25E-01	4.84E-01	2.50E+02	1.01E+00	6.70E-01
82	3.69E-03	1.19E-01	3.60E-01	4.16E+02	1.53E+00	6.41E-01
83	4.08E-03	1.62E-01	3.90E-01	7.17E+02	1.93E+00	1.36E-01
84	2.23E-04	1.45E-01	1.64E-01	8.91E+02	1.04E+00	6.58E-01
85	2.83E-03	1.10E-01	1.62E-01	3.84E+02	1.71E+00	2.56E-01
86	2.93E-04	1.86E-01	3.23E-01	4.53E+02	1.18E+00	1.14E-01
87	4.41E-03	1.41E-01	2.36E-01	1.63E+02	1.16E+00	4.26E-02
88	1.15E-03	1.87E-01	1.05E-01	8.52E+02	1.91E+00	1.72E-01
89	1.17E-04	1.12E-01	2.26E-01	1.89E+02	1.10E+00	7.08E-01
90	8.97E-03	1.89E-01	3.69E-01	5.99E+01	1.11E+00	1.88E-01
91	2.31E-03	1.80E-01	2.64E-01	4.88E+02	1.00E+00	6.25E-01
92	3.41E-04	1.06E-01	2.32E-01	4.23E+02	1.03E+00	1.46E-01
93	1.10E-03	1.42E-01	1.90E-01	2.37E+02	1.23E+00	6.60E-01
94	3.53E-03	2.49E-01	4.55E-01	1.13E+02	1.14E+00	1.03E-01
95	1.73E-03	1.84E-01	2.23E-01	2.75E+02	1.06E+00	3.13E-01
96	1.89E-03	2.44E-01	1.45E-01	8.13E+02	1.13E+00	9.28E-01
97	2.50E-04	1.90E-01	3.97E-01	1.08E+02	1.25E+00	3.49E-01
98	3.34E-03	1.46E-01	5.92E-02	9.47E+02	1.09E+00	5.58E-01
99	1.26E-03	1.68E-01	9.97E-02	8.43E+02	1.06E+00	2.86E-01
100	4.42E-04	1.66E-01	3.44E-01	7.48E+02	1.02E+00	6.11E-01

Table 4.11 Sampled Chemical parameter values – Replicate R1

vector	OXSTAT	MKD_AM	MKD_PU+3	MKD_PU+4	MKD_TH	MKD_U+4	MKD_U+6
1	7.30E-01	1.52E-01	1.24E-01	1.45E+00	8.58E+00	3.93E+00	3.33E-03
2	4.65E-01	8.80E-02	2.13E-01	1.39E+00	1.14E+00	3.67E+00	9.05E-05
3	2.29E-01	7.84E-02	1.16E-01	6.72E+00	8.77E-01	1.42E+00	6.68E-03
4	2.00E-01	1.97E-01	9.37E-02	1.01E+00	1.85E+00	4.93E+00	1.78E-04
5	8.67E-01	3.38E-02	1.28E-01	1.12E+00	9.30E-01	6.66E+00	3.69E-03
6	7.91E-01	4.41E-02	6.82E-02	3.82E+00	1.91E+00	1.01E+00	6.62E-05
7	4.75E-01	1.24E-01	3.07E-02	2.48E+00	1.22E+00	7.49E-01	2.96E-04
8	5.71E-01	2.25E-01	1.48E-01	4.59E+00	9.43E+00	5.93E+00	1.52E-03
9	7.14E-01	7.02E-02	6.28E-02	3.60E+00	1.66E+00	4.61E+00	1.31E-04
10	4.01E-01	2.73E-02	3.03E-01	9.11E+00	2.16E+00	7.53E+00	4.68E-04
11	4.31E-01	2.74E-01	2.05E-01	2.70E+00	2.32E+00	1.14E+00	2.62E-03
12	6.78E-01	5.19E-02	2.62E-02	4.07E+00	5.63E+00	1.81E+00	2.98E-03
13	6.48E-01	3.30E-02	3.15E-01	7.91E+00	8.83E+00	7.62E-01	4.95E-03
14	7.53E-01	4.07E-02	3.45E-01	3.48E+00	6.50E+00	6.89E+00	4.43E-04
15	1.24E-01	1.20E-01	2.25E-01	7.69E-01	3.78E+00	7.79E+00	4.60E-03
16	1.10E-01	6.81E-02	1.66E-01	2.83E+00	4.58E+00	7.84E-01	4.11E-04
17	3.41E-01	2.24E-02	4.38E-02	1.18E+00	6.31E+00	2.20E+00	8.51E-03
18	2.47E-01	2.32E-02	2.69E-02	6.27E+00	1.27E+00	1.62E+00	2.18E-03
19	3.90E-01	2.94E-02	1.04E-01	8.29E-01	9.94E-01	1.74E+00	3.64E-05
20	3.23E-01	1.29E-01	3.28E-02	2.51E+00	2.60E+00	9.08E-01	1.34E-03
21	1.63E-02	1.47E-01	6.00E-02	2.77E+00	9.88E-01	9.00E+00	4.95E-05
22	2.97E-01	1.34E-01	1.49E-01	7.31E+00	3.24E+00	1.18E+00	7.74E-04
23	8.17E-01	2.69E-02	2.13E-02	4.65E+00	8.64E-01	2.76E+00	4.10E-05
24	6.19E-01	3.71E-01	1.10E-01	7.25E+00	4.28E+00	3.13E+00	1.28E-03
25	3.36E-01	3.15E-01	3.36E-02	5.21E+00	3.14E+00	9.28E-01	6.35E-05
26	9.13E-01	4.24E-02	8.54E-02	2.61E+00	2.76E+00	8.71E-01	1.05E-04
27	7.67E-01	5.39E-02	5.26E-02	3.35E+00	5.41E+00	2.33E+00	1.61E-04
28	8.41E-02	2.99E-01	2.21E-02	1.55E+00	2.83E+00	3.59E+00	1.97E-02
29	2.75E-01	2.47E-01	2.54E-01	3.85E+00	6.07E+00	1.02E+00	1.04E-03
30	5.99E-01	3.90E-02	1.87E-01	8.72E-01	7.43E-01	9.33E+00	1.69E-02
31	4.21E-01	2.17E-01	8.23E-02	6.37E+00	1.61E+00	5.52E+00	1.97E-03
32	4.81E-01	6.28E-02	2.18E-01	9.92E+00	2.92E+00	1.29E+00	3.14E-05
33	3.80E-01	4.12E-02	1.60E-01	7.07E-01	7.02E+00	1.48E+00	8.31E-05
34	3.05E-01	1.69E-01	5.17E-02	3.13E+00	4.48E+00	4.27E+00	9.51E-05
35	3.20E-01	7.57E-02	6.86E-02	1.49E+00	4.05E+00	5.29E+00	2.56E-04
36	9.54E-01	7.20E-02	2.85E-01	6.02E+00	8.19E-01	2.10E+00	3.77E-03
37	4.11E-01	2.33E-02	2.74E-01	3.66E+00	1.45E+00	1.93E+00	8.64E-03
38	9.01E-02	3.50E-02	2.38E-01	1.86E+00	3.49E+00	9.44E-01	5.20E-05
39	1.75E-01	3.80E-02	3.74E-02	2.21E+00	5.93E+00	4.42E+00	2.82E-03
40	8.37E-01	1.16E-01	1.80E-01	6.62E+00	3.58E+00	3.07E+00	7.35E-03
41	7.05E-02	1.11E-01	4.88E-02	1.77E+00	1.53E+00	2.04E+00	2.32E-03
42	1.45E-01	2.14E-02	2.36E-02	1.21E+00	6.69E+00	1.24E+00	2.64E-04
43	2.87E-01	2.56E-01	1.77E-01	5.85E+00	8.36E-01	9.86E-01	1.99E-04

Table 4.11 Sampled Chemical parameter values – Replicate R1

vector	OXSTAT	MKD_AM	MKD_PU+3	MKD_PU+4	MKD_TH	MKD_U+4	MKD_U+6
44	5.82E-01	3.07E-02	4.25E-02	1.03E+00	8.00E+00	8.08E-01	8.66E-04
45	8.85E-01	1.83E-01	7.84E-02	7.42E-01	2.70E+00	1.71E+00	9.95E-04
46	8.10E-01	5.61E-02	3.85E-01	1.90E+00	5.48E+00	1.90E+00	3.20E-05
47	2.70E-01	1.26E-01	3.92E-02	3.01E+00	1.10E+00	2.60E+00	1.87E-04
48	9.05E-01	3.68E-02	2.86E-02	1.14E+00	1.50E+00	9.51E+00	5.19E-04
49	3.65E-01	2.28E-01	3.59E-02	5.35E+00	1.04E+00	4.04E+00	1.45E-02
50	3.57E-02	8.96E-02	1.43E-01	2.00E+00	1.79E+00	1.12E+00	6.02E-05
51	5.11E-01	1.85E-01	2.70E-02	3.99E+00	7.26E+00	7.27E+00	1.86E-02
52	8.99E-01	5.29E-02	7.37E-02	5.65E+00	5.87E+00	2.26E+00	7.82E-03
53	6.95E-01	7.30E-02	7.99E-02	2.38E+00	2.48E+00	1.09E+00	5.79E-03
54	9.27E-01	4.54E-02	2.01E-02	1.66E+00	3.99E+00	2.93E+00	1.85E-03
55	1.88E-01	2.01E-02	2.47E-02	9.26E+00	8.13E+00	6.05E+00	3.25E-04
56	9.88E-01	5.84E-02	4.57E-02	5.56E+00	1.70E+00	4.74E+00	4.28E-03
57	7.86E-01	2.98E-02	2.29E-01	4.19E+00	7.77E-01	1.22E+00	2.84E-04
58	1.53E-01	2.58E-02	3.97E-01	3.10E+00	2.42E+00	9.84E+00	7.06E-04
59	6.69E-02	4.78E-02	8.71E-02	8.15E-01	3.73E+00	4.17E+00	6.60E-04
60	5.29E-01	1.02E-01	5.52E-02	1.31E+00	1.40E+00	1.53E+00	1.55E-02
61	1.01E-01	8.51E-02	1.38E-01	7.77E+00	1.23E+00	5.75E+00	3.73E-04
62	4.57E-01	1.60E-01	4.71E-02	1.62E+00	5.19E+00	8.12E+00	8.91E-04
63	2.30E-01	4.76E-02	1.20E-01	3.25E+00	1.99E+00	5.26E+00	2.29E-04
64	3.87E-01	9.32E-02	5.73E-02	9.13E-01	9.52E+00	1.33E+00	1.11E-03
65	8.40E-01	5.93E-02	3.42E-01	9.60E-01	9.09E+00	7.16E-01	1.03E-02
66	5.06E-01	6.46E-02	1.70E-01	4.99E+00	1.06E+00	7.05E+00	1.29E-02
67	6.01E-01	2.05E-01	2.41E-02	1.43E+00	2.12E+00	1.46E+00	1.34E-04
68	8.51E-01	1.56E-01	2.08E-02	2.08E+00	1.32E+00	1.05E+00	1.19E-04
69	2.18E-01	2.13E-01	9.82E-02	1.27E+00	3.88E+00	6.28E+00	2.17E-04
70	7.47E-01	3.98E-01	9.54E-02	2.35E+00	9.92E+00	8.88E+00	1.50E-04
71	7.71E-01	1.08E-01	2.58E-01	9.23E-01	3.04E+00	6.50E+00	4.00E-04
72	4.42E-01	2.85E-02	3.80E-02	1.94E+00	2.22E+00	7.36E+00	6.18E-03
73	8.72E-01	2.55E-01	4.14E-02	4.87E+00	1.34E+00	1.65E+00	1.16E-03
74	6.61E-01	1.38E-01	6.46E-02	1.09E+00	2.99E+00	2.80E+00	9.83E-05
75	9.80E-01	4.94E-02	4.04E-02	8.36E+00	6.76E+00	3.44E+00	3.41E-04
76	5.30E-01	2.65E-01	1.54E-01	8.20E+00	1.56E+00	4.76E+00	1.21E-02
77	7.21E-01	2.50E-02	1.21E-01	1.81E+00	7.47E+00	8.58E+00	4.51E-05
78	1.66E-01	9.73E-02	6.12E-02	5.10E+00	9.01E-01	5.63E+00	5.61E-05
79	1.39E-01	1.78E-01	3.27E-01	8.55E-01	7.08E-01	2.70E+00	5.52E-04
80	4.38E-03	3.54E-01	2.44E-01	1.59E+00	4.64E+00	7.27E-01	1.40E-02
81	5.83E-02	2.45E-02	4.94E-02	2.10E+00	1.74E+00	1.85E+00	3.11E-03
82	3.55E-01	1.90E-01	1.33E-01	8.55E+00	2.35E+00	2.00E+00	7.87E-04
83	7.09E-01	1.43E-01	2.66E-01	8.79E+00	4.94E+00	2.40E+00	6.19E-04
84	6.40E-01	1.00E-01	3.61E-01	1.35E+00	3.34E+00	8.59E-01	1.11E-02
85	2.05E-01	2.81E-01	7.53E-02	9.68E+00	4.82E+00	2.55E+00	1.74E-04
86	5.59E-01	1.05E-01	2.27E-02	4.47E+00	1.95E+00	2.20E+00	9.18E-03
87	9.46E-01	3.15E-01	2.00E-01	6.11E+00	7.83E+00	8.51E+00	7.12E-05

Table 4.11 Sampled Chemical parameter values – Replicate R1

vector	OXSTAT	MKD_AM	MKD_PU+3	MKD_PU+4	MKD_TH	MKD_U+4	MKD_U+6
88	9.37E-01	8.38E-02	5.58E-02	2.30E+00	9.52E-01	1.30E+00	1.44E-03
89	2.12E-02	2.10E-02	2.89E-02	7.61E+00	8.49E+00	3.32E+00	1.12E-02
90	6.29E-01	2.37E-01	3.20E-02	7.32E-01	4.18E+00	5.12E+00	7.65E-05
91	4.88E-02	3.25E-01	1.90E-01	4.32E+00	5.05E+00	3.47E+00	5.61E-04
92	9.95E-01	3.58E-02	3.20E-01	2.14E+00	2.54E+00	1.58E+00	6.62E-03
93	6.59E-01	3.35E-01	7.21E-02	1.05E+00	7.41E+00	7.98E+00	1.62E-03
94	5.49E-01	3.81E-01	3.01E-02	3.45E+00	2.06E+00	2.49E+00	3.66E-05
95	2.56E-01	8.17E-02	3.72E-01	1.25E+00	1.17E+00	3.22E+00	2.39E-03
96	8.25E-01	2.90E-01	8.99E-02	7.01E+00	7.29E-01	3.80E+00	5.41E-03
97	4.98E-01	1.67E-01	2.94E-01	1.73E+00	3.39E+00	4.07E+00	1.14E-04
98	6.90E-01	3.14E-02	1.04E-01	9.86E-01	7.79E-01	1.39E+00	4.29E-05
99	5.63E-01	6.14E-02	3.52E-02	2.88E+00	1.39E+00	8.36E-01	1.79E-03
100	9.64E-01	3.58E-01	1.10E-01	7.85E-01	1.10E+00	2.98E+00	4.13E-03

Table 4.12 Sampled chemical parameter values – Replicate R2

vector	OXSTAT	MKD_AM	MKD_PU+3	MKD_PU+4	MKD_TH	MKD_U+4	MKD_U+6
1	6.80E-01	4.20E-02	2.78E-02	7.11E+00	1.02E+00	3.19E+00	6.33E-05
2	8.49E-01	2.39E-02	3.71E-01	8.85E-01	3.22E+00	2.90E+00	9.95E-03
3	7.80E-01	1.44E-01	4.10E-02	3.65E+00	1.26E+00	1.88E+00	1.60E-04
4	6.22E-01	2.58E-01	6.91E-02	2.49E+00	2.97E+00	1.43E+00	4.05E-05
5	2.83E-01	4.41E-02	3.77E-02	4.64E+00	2.73E+00	7.68E+00	8.69E-04
6	7.50E-01	8.47E-02	3.79E-01	7.38E+00	1.19E+00	1.37E+00	7.24E-03
7	9.06E-02	1.12E-01	1.32E-01	2.62E+00	2.02E+00	1.12E+00	4.39E-04
8	3.21E-01	3.06E-02	3.56E-01	4.38E+00	5.29E+00	7.37E-01	6.71E-04
9	2.42E-01	3.83E-02	5.58E-02	2.26E+00	2.86E+00	5.56E+00	8.75E-03
10	9.80E-01	2.69E-01	2.42E-02	9.18E-01	1.56E+00	1.84E+00	1.80E-03
11	5.97E-01	9.07E-02	1.18E-01	1.80E+00	2.66E+00	1.95E+00	1.82E-04
12	8.61E-01	1.14E-01	1.35E-01	6.02E+00	7.50E-01	5.40E+00	3.51E-04
13	8.15E-01	1.94E-01	5.23E-02	1.16E+00	4.97E+00	9.93E+00	2.57E-03
14	4.69E-01	5.19E-02	1.47E-01	1.43E+00	3.76E+00	3.44E+00	1.85E-04
15	4.84E-01	3.45E-02	4.85E-02	9.88E+00	8.13E-01	1.36E+00	3.27E-03
16	7.96E-01	5.42E-02	4.39E-02	1.65E+00	2.07E+00	6.72E+00	6.79E-03
17	8.53E-01	4.84E-02	1.69E-01	1.39E+00	4.31E+00	9.70E-01	2.62E-04
18	8.74E-01	2.26E-01	8.26E-02	9.05E+00	8.88E+00	1.10E+00	2.54E-04
19	2.50E-01	3.24E-01	1.04E-01	5.86E+00	1.61E+00	6.14E+00	5.07E-05
20	3.92E-01	2.79E-01	4.59E-02	6.47E+00	4.80E+00	1.05E+00	1.69E-04
21	2.23E-01	3.54E-02	9.97E-02	3.60E+00	5.65E+00	2.61E+00	6.87E-04
22	5.00E-01	6.43E-02	1.74E-01	1.91E+00	7.62E-01	4.21E+00	9.54E-05
23	1.69E-01	1.06E-01	2.50E-01	9.44E+00	3.32E+00	2.13E+00	1.05E-04
24	6.92E-01	2.99E-01	3.13E-01	5.06E+00	6.64E+00	9.65E+00	1.32E-02
25	5.27E-01	6.79E-02	2.53E-02	2.81E+00	1.80E+00	2.26E+00	1.33E-03
26	8.30E-01	2.86E-01	9.45E-02	7.88E-01	9.53E+00	1.98E+00	1.17E-03
27	9.92E-01	1.22E-01	2.79E-01	1.87E+00	9.68E-01	4.81E+00	2.26E-04

Table 4.12 Sampled chemical parameter values – Replicate R2

vector	OXSTAT	MKD_AM	MKD_PU+3	MKD_PU+4	MKD_TH	MKD_U+4	MKD_U+6
28	9.11E-01	2.31E-02	4.75E-02	2.69E+00	8.62E-01	8.09E+00	7.87E-04
29	5.80E-01	3.73E-01	3.53E-01	5.67E+00	6.81E+00	9.62E-01	1.75E-02
30	6.92E-02	6.56E-02	2.21E-02	6.29E+00	7.59E+00	3.11E+00	1.49E-03
31	3.88E-02	2.05E-02	6.49E-02	4.27E+00	8.43E-01	9.06E+00	1.06E-02
32	7.32E-01	9.86E-02	2.10E-02	2.54E+00	2.25E+00	8.07E+00	6.58E-05
33	6.87E-01	2.10E-01	3.95E-02	1.97E+00	1.32E+00	6.52E+00	5.60E-05
34	3.81E-01	1.67E-01	2.69E-02	3.85E+00	8.32E+00	5.98E+00	1.03E-03
35	1.58E-01	9.29E-02	1.63E-01	7.01E+00	4.40E+00	1.01E+00	1.32E-04
36	6.57E-01	1.80E-01	2.60E-01	8.00E-01	1.01E+00	2.66E+00	1.51E-02
37	2.40E-01	7.12E-02	8.96E-02	2.75E+00	2.45E+00	1.52E+00	3.69E-03
38	5.50E-01	2.60E-02	3.57E-02	1.62E+00	7.85E+00	1.76E+00	1.86E-02
39	8.06E-01	5.23E-02	6.82E-02	3.52E+00	7.80E-01	9.04E-01	3.78E-04
40	1.38E-01	7.79E-02	3.97E-01	3.82E+00	2.20E+00	2.38E+00	3.31E-04
41	4.36E-01	7.45E-02	3.22E-02	1.51E+00	1.67E+00	1.30E+00	3.64E-03
42	3.37E-01	8.88E-02	1.66E-01	4.90E+00	3.10E+00	4.30E+00	2.21E-03
43	4.78E-02	1.55E-01	3.67E-02	7.21E-01	8.64E+00	1.18E+00	1.69E-03
44	3.64E-01	1.03E-01	2.25E-01	8.36E+00	2.51E+00	8.81E+00	2.11E-03
45	9.89E-01	1.95E-01	8.89E-02	1.74E+00	8.86E-01	3.97E+00	4.22E-03
46	3.11E-01	3.92E-01	2.37E-01	2.10E+00	3.97E+00	1.49E+00	5.05E-03
47	8.81E-01	9.65E-02	4.98E-02	4.78E+00	2.44E+00	8.21E-01	1.11E-03
48	7.29E-01	1.61E-01	1.97E-01	1.22E+00	1.48E+00	7.52E-01	3.34E-05
49	5.40E-01	3.73E-02	1.84E-01	3.03E+00	5.94E+00	3.50E+00	1.38E-04
50	7.88E-01	1.25E-01	3.31E-01	8.47E-01	5.48E+00	2.25E+00	4.78E-04
51	7.89E-03	1.20E-01	2.69E-01	7.43E-01	7.30E-01	1.14E+00	2.19E-04
52	2.65E-01	3.15E-02	3.42E-02	1.72E+00	9.47E+00	3.31E+00	6.29E-04
53	6.36E-01	2.23E-02	1.82E-01	6.17E+00	5.23E+00	3.66E+00	5.05E-04
54	4.07E-01	1.38E-01	2.06E-01	8.99E-01	1.73E+00	1.78E+00	2.44E-03
55	7.40E-02	7.56E-02	5.86E-02	1.46E+00	7.23E+00	4.14E+00	9.36E-04
56	6.05E-01	3.79E-01	1.40E-01	9.92E-01	9.41E-01	8.70E+00	2.08E-04
57	5.11E-01	3.12E-01	2.93E-02	2.42E+00	6.90E+00	1.61E+00	3.76E-05
58	9.09E-01	1.76E-01	1.04E-01	3.01E+00	3.38E+00	2.19E+00	1.12E-02
59	2.04E-02	1.53E-01	7.86E-02	1.58E+00	2.09E+00	4.74E+00	9.71E-03
60	6.16E-01	4.93E-02	5.16E-02	1.05E+00	1.23E+00	1.45E+00	5.88E-05
61	2.97E-01	3.25E-01	4.13E-02	1.52E+00	1.14E+00	1.28E+00	4.17E-03
62	3.46E-01	2.64E-02	3.39E-01	6.89E+00	3.52E+00	4.92E+00	4.19E-05
63	5.42E-01	3.63E-01	2.92E-01	4.51E+00	1.39E+00	5.27E+00	1.41E-03
64	5.77E-01	8.31E-02	2.41E-01	9.44E-01	1.69E+00	7.12E+00	6.19E-03
65	9.48E-01	1.85E-01	1.89E-01	5.57E+00	9.94E+00	8.33E+00	8.39E-05
66	7.58E-01	1.48E-01	3.12E-02	9.70E+00	1.45E+00	9.35E-01	1.99E-03
67	5.65E-01	2.77E-02	2.99E-02	8.87E+00	1.92E+00	7.08E-01	4.60E-03
68	1.73E-02	4.72E-02	2.56E-02	1.18E+00	2.27E+00	7.85E-01	2.96E-03
69	1.05E-01	1.08E-01	2.16E-02	3.96E+00	2.38E+00	5.73E+00	1.85E-03
70	1.50E-01	5.96E-02	2.08E-01	5.22E+00	1.52E+00	7.51E+00	6.57E-03
71	2.06E-01	2.31E-01	2.33E-01	2.93E+00	1.96E+00	4.42E+00	3.51E-05

Table 4.12 Sampled chemical parameter values – Replicate R2

vector	OXSTAT	MKD_AM	MKD_PU+3	MKD_PU+4	MKD_TH	MKD_U+4	MKD_U+6
72	9.27E-01	5.85E-02	2.84E-01	7.63E+00	4.59E+00	1.71E+00	2.79E-04
73	5.10E-01	1.35E-01	9.65E-02	3.11E+00	6.50E+00	2.79E+00	1.22E-02
74	7.69E-01	3.39E-02	5.49E-02	9.65E-01	8.21E+00	1.57E+00	4.62E-05
75	4.74E-01	2.16E-02	1.41E-01	3.32E+00	4.14E+00	5.58E+00	1.00E-04
76	8.93E-01	2.51E-02	1.08E-01	7.70E-01	6.27E+00	8.85E-01	1.40E-02
77	2.78E-01	3.43E-01	7.06E-02	2.05E+00	2.90E+00	5.11E+00	3.11E-05
78	5.28E-02	5.59E-02	1.23E-01	3.25E+00	4.19E+00	2.51E+00	4.15E-04
79	2.18E-01	2.88E-01	2.31E-02	8.15E+00	7.09E-01	1.67E+00	5.38E-03
80	4.28E-01	3.31E-02	7.34E-02	7.76E+00	3.73E+00	6.29E+00	4.94E-05
81	7.07E-01	6.95E-02	1.26E-01	2.17E+00	6.10E+00	9.40E+00	1.99E-02
82	8.49E-02	2.79E-02	3.02E-01	1.22E+00	3.90E+00	3.80E+00	8.62E-05
83	3.75E-01	2.16E-01	1.56E-01	2.35E+00	4.71E+00	1.02E+00	7.31E-04
84	1.86E-01	4.52E-02	3.15E-01	1.10E+00	9.04E-01	2.04E+00	9.48E-04
85	3.59E-01	2.55E-01	2.17E-01	2.25E+00	1.11E+00	8.40E-01	3.07E-03
86	1.27E-01	2.34E-01	3.47E-02	8.26E-01	5.78E+00	7.00E+00	7.23E-05
87	4.20E-01	1.72E-01	6.23E-02	4.41E+00	2.60E+00	4.59E+00	5.77E-03
88	9.39E-01	8.05E-02	4.24E-02	1.29E+00	1.07E+00	8.46E-01	1.23E-04
89	3.05E-01	4.27E-02	6.25E-02	7.08E-01	9.29E-01	3.89E+00	7.93E-05
90	6.66E-01	6.07E-02	2.79E-02	8.68E+00	5.08E+00	6.67E+00	3.09E-04
91	4.52E-01	2.42E-02	1.50E-01	1.35E+00	7.33E+00	2.86E+00	5.27E-04
92	1.98E-01	3.92E-02	7.61E-02	1.09E+00	1.36E+00	7.34E+00	4.03E-04
93	6.50E-01	2.41E-01	2.02E-02	1.02E+00	1.41E+00	3.56E+00	1.56E-02
94	1.17E-01	1.30E-01	8.05E-02	6.66E+00	1.84E+00	7.69E-01	2.81E-03
95	8.22E-01	3.02E-02	2.38E-02	2.00E+00	3.12E+00	1.20E+00	5.97E-04
96	7.13E-01	2.92E-02	1.16E-01	7.89E+00	1.18E+00	3.01E+00	7.62E-03
97	1.74E-01	2.02E-01	8.50E-02	5.28E+00	7.96E+00	1.25E+00	1.26E-03
98	4.49E-01	3.51E-01	5.98E-02	4.12E+00	3.61E+00	3.05E+00	8.31E-03
99	9.67E-01	4.04E-02	1.11E-01	3.40E+00	9.22E+00	2.41E+00	1.50E-04
100	9.59E-01	2.11E-02	3.33E-02	1.31E+00	1.05E+00	2.50E+00	1.16E-04

Table 4.13. Sampled chemical parameters – Replicate R3

vector	OXSTAT	MKD_AM	MKD_PU+3	MKD_PU+4	MKD_TH	MKD_U+4	MKD_U+6
1	5.16E-01	5.04E-02	1.22E-01	7.03E+00	9.90E-01	1.06E+00	7.67E-04
2	2.01E-01	2.75E-02	4.94E-02	9.32E-01	8.14E-01	6.45E+00	1.05E-04
3	1.27E-01	2.89E-01	1.82E-01	5.27E+00	2.37E+00	2.66E+00	7.46E-05
4	5.88E-01	1.56E-01	7.18E-02	7.14E-01	1.16E+00	1.25E+00	5.22E-05
5	8.11E-04	2.43E-02	2.86E-01	3.75E+00	5.46E+00	7.04E+00	8.75E-05
6	9.67E-01	1.71E-01	8.35E-02	2.41E+00	3.09E+00	9.21E+00	9.94E-03
7	8.14E-01	3.59E-02	7.56E-02	7.26E+00	4.85E+00	3.45E+00	7.37E-05
8	2.60E-01	3.71E-02	6.66E-02	8.34E-01	2.81E+00	2.40E+00	4.17E-05
9	3.61E-01	3.47E-01	5.82E-02	6.51E+00	8.57E-01	6.55E+00	1.45E-03
10	3.26E-01	1.88E-01	2.57E-01	7.46E-01	7.21E+00	2.81E+00	7.99E-03
11	7.92E-01	9.66E-02	2.15E-01	7.41E+00	2.26E+00	9.43E+00	3.29E-04
12	6.94E-01	2.43E-01	1.49E-01	9.33E+00	3.69E+00	4.77E+00	8.22E-03
13	4.99E-01	2.06E-02	2.01E-01	4.88E+00	7.84E-01	8.94E-01	1.60E-02
14	1.63E-01	3.41E-01	1.52E-01	1.13E+00	3.41E+00	7.50E+00	9.79E-05
15	7.86E-02	8.90E-02	3.07E-02	1.45E+00	3.53E+00	5.40E+00	1.80E-04
16	5.52E-01	1.59E-01	2.93E-02	1.03E+00	1.35E+00	1.01E+00	1.12E-03
17	3.43E-01	2.66E-01	4.00E-01	7.66E-01	2.41E+00	9.31E-01	1.18E-04
18	6.15E-01	4.46E-02	5.38E-02	2.80E+00	9.20E-01	2.24E+00	3.16E-03
19	6.45E-01	2.13E-01	3.62E-02	1.47E+00	1.06E+00	1.75E+00	2.97E-04
20	5.28E-02	1.39E-01	4.78E-02	6.28E+00	2.15E+00	1.67E+00	1.89E-04
21	3.55E-01	1.05E-01	7.31E-02	8.76E-01	4.98E+00	7.21E-01	3.97E-03
22	7.63E-01	3.61E-01	6.16E-02	2.74E+00	1.41E+00	2.27E+00	5.72E-04
23	8.28E-01	2.27E-01	3.50E-02	5.85E+00	3.82E+00	9.97E+00	6.29E-04
24	1.72E-02	3.09E-01	3.01E-02	2.17E+00	1.80E+00	7.85E-01	1.86E-03
25	7.60E-01	8.33E-02	1.34E-01	1.72E+00	2.67E+00	1.16E+00	7.00E-03
26	6.41E-02	5.27E-02	2.78E-02	4.70E+00	2.96E+00	5.01E+00	3.40E-05
27	7.77E-01	3.85E-02	2.12E-01	1.88E+00	1.44E+00	1.02E+00	7.13E-04
28	1.97E-01	2.20E-02	7.77E-02	2.09E+00	7.55E+00	3.60E+00	1.10E-02
29	1.45E-01	2.82E-02	8.15E-02	1.65E+00	7.89E+00	2.98E+00	5.51E-05
30	3.89E-01	1.23E-01	2.51E-01	1.16E+00	7.25E-01	1.55E+00	1.65E-03
31	1.12E-01	6.65E-02	2.43E-01	2.01E+00	2.21E+00	1.39E+00	1.54E-03
32	9.26E-01	2.75E-01	2.66E-02	1.25E+00	9.52E-01	1.69E+00	6.51E-03
33	6.38E-01	3.14E-02	3.38E-02	3.27E+00	1.75E+00	5.86E+00	5.74E-03
34	6.62E-01	6.33E-02	2.10E-02	2.05E+00	6.70E+00	2.04E+00	9.60E-04
35	4.41E-01	2.50E-02	4.68E-02	1.56E+00	9.10E+00	6.33E+00	9.67E-05
36	9.11E-01	1.66E-01	3.32E-02	1.36E+00	2.46E+00	7.46E+00	6.48E-05
37	6.54E-01	2.05E-01	1.27E-01	4.37E+00	1.08E+00	8.79E+00	4.77E-04
38	2.66E-01	4.73E-02	9.68E-02	3.57E+00	1.55E+00	2.76E+00	2.25E-03
39	8.61E-01	1.28E-01	2.13E-02	4.17E+00	4.06E+00	2.49E+00	3.72E-05
40	8.09E-01	3.03E-02	1.42E-01	8.03E-01	3.22E+00	8.14E+00	1.81E-02
41	3.38E-01	2.58E-01	1.91E-01	1.52E+00	9.93E+00	1.12E+00	5.82E-03
42	7.14E-01	8.48E-02	1.02E-01	3.95E+00	1.91E+00	9.67E+00	1.16E-04

43	4.20E-01	8.12E-02	3.87E-02	2.49E+00	4.03E+00	9.78E-01	5.34E-04
44	8.94E-01	3.28E-01	5.88E-02	4.07E+00	8.79E+00	7.03E-01	1.30E-02
45	5.90E-01	1.27E-01	1.07E-01	8.93E+00	6.13E+00	8.38E-01	1.46E-04
46	9.03E-01	1.79E-01	6.51E-02	1.87E+00	3.28E+00	1.96E+00	2.04E-04
47	8.36E-01	4.61E-02	3.16E-02	8.99E-01	1.22E+00	2.36E+00	2.29E-04
48	4.66E-01	1.49E-01	3.09E-01	3.69E+00	5.19E+00	7.75E+00	9.33E-04
49	5.44E-01	2.36E-01	2.66E-01	5.99E+00	1.49E+00	1.36E+00	3.66E-04
50	6.74E-01	2.12E-02	6.98E-02	5.40E+00	1.63E+00	8.52E-01	1.39E-03
51	7.22E-01	2.15E-01	2.46E-02	2.23E+00	9.43E+00	7.42E-01	6.78E-05
52	9.56E-01	2.54E-02	1.05E-01	1.38E+00	8.74E-01	1.50E+00	3.47E-05
53	2.20E-01	1.77E-01	1.16E-01	1.43E+00	5.89E+00	1.08E+00	2.62E-03
54	2.39E-01	4.35E-02	2.51E-02	8.12E+00	2.52E+00	2.19E+00	1.17E-02
55	5.32E-01	5.20E-02	1.32E-01	3.34E+00	5.07E+00	8.80E-01	1.27E-03
56	4.04E-02	5.74E-02	2.35E-02	4.46E+00	7.56E-01	3.78E+00	3.38E-03
57	1.02E-01	5.99E-02	4.43E-02	1.16E+00	1.72E+00	3.47E+00	4.20E-04
58	7.38E-01	4.16E-02	2.30E-02	9.90E+00	5.32E+00	1.42E+00	2.86E-04
59	6.05E-01	2.79E-01	3.86E-01	1.08E+00	2.62E+00	1.62E+00	5.22E-04
60	2.18E-01	1.03E-01	3.80E-02	2.36E+00	1.97E+00	4.55E+00	1.72E-04
61	4.52E-01	1.44E-01	1.37E-01	1.27E+00	1.29E+00	1.56E+00	4.39E-04
62	3.78E-01	1.14E-01	2.20E-02	8.45E-01	4.25E+00	2.52E+00	1.88E-02
63	9.94E-01	5.40E-02	3.72E-01	2.51E+00	8.92E-01	1.90E+00	1.27E-04
64	3.50E-02	7.61E-02	2.01E-02	6.65E+00	2.02E+00	5.52E+00	2.86E-03
65	5.00E-01	2.35E-02	1.61E-01	5.11E+00	1.66E+00	6.15E+00	4.40E-03
66	2.73E-01	3.45E-02	8.96E-02	9.62E-01	3.88E+00	3.92E+00	4.90E-05
67	1.57E-01	1.93E-01	4.11E-02	3.40E+00	8.36E+00	3.17E+00	1.03E-03
68	5.64E-01	1.21E-01	2.03E-01	6.71E+00	9.59E+00	8.01E-01	8.29E-05
69	5.29E-01	4.90E-02	3.75E-02	7.64E+00	2.93E+00	1.45E+00	2.65E-04
70	1.76E-01	1.97E-01	3.26E-01	1.07E+00	4.68E+00	8.31E+00	8.80E-04
71	3.00E-01	2.97E-01	9.48E-02	4.62E+00	1.28E+00	6.73E+00	2.13E-04
72	2.85E-01	3.42E-02	2.98E-01	9.03E+00	3.13E+00	3.10E+00	6.09E-05
73	5.79E-01	2.48E-01	2.62E-02	8.08E+00	7.09E-01	1.22E+00	3.78E-03
74	2.26E-02	1.09E-01	8.47E-02	3.08E+00	1.23E+00	1.80E+00	1.39E-02
75	3.94E-01	4.01E-02	2.25E-01	7.81E-01	5.77E+00	5.25E+00	2.05E-03
76	3.17E-01	3.27E-02	3.60E-01	1.60E+00	1.19E+00	1.26E+00	2.36E-03
77	9.55E-02	1.13E-01	4.56E-02	1.80E+00	2.05E+00	5.88E+00	1.19E-02
78	1.82E-01	7.43E-02	8.84E-02	3.52E+00	8.17E+00	2.13E+00	3.43E-04
79	4.30E-01	9.37E-02	3.53E-01	9.58E+00	2.10E+00	7.75E-01	1.78E-03
80	1.32E-01	1.34E-01	1.63E-01	5.70E+00	1.12E+00	4.71E+00	1.52E-02
81	3.02E-01	9.87E-02	2.38E-01	1.29E+00	1.39E+00	1.86E+00	4.11E-05
82	2.46E-01	2.67E-02	1.71E-01	5.43E+00	4.62E+00	7.08E+00	3.85E-04
83	9.36E-01	2.13E-02	4.03E-02	2.58E+00	4.31E+00	3.32E+00	6.65E-04
84	6.25E-01	3.18E-01	1.74E-01	8.36E+00	1.02E+00	2.89E+00	1.36E-04
85	8.47E-01	7.76E-02	1.20E-01	1.75E+00	3.59E+00	4.11E+00	2.75E-03
86	8.96E-02	8.96E-02	3.40E-01	2.95E+00	2.76E+00	9.58E-01	1.62E-04
87	4.89E-01	3.04E-02	5.22E-02	7.82E+00	4.46E+00	3.19E+00	7.77E-04
88	9.77E-01	1.50E-01	1.11E-01	6.08E+00	6.41E+00	4.03E+00	4.53E-05

89	7.06E-01	3.95E-01	5.15E-02	3.92E+00	1.84E+00	3.71E+00	4.81E-03
90	4.38E-01	3.87E-01	1.86E-01	4.86E+00	6.33E+00	4.91E+00	4.78E-03
91	9.47E-01	7.16E-02	2.27E-01	8.61E+00	6.79E+00	2.02E+00	3.54E-03
92	7.85E-01	6.90E-02	1.55E-01	9.97E-01	8.32E-01	4.36E+00	7.49E-03
93	4.74E-01	2.28E-02	3.17E-01	2.87E+00	5.60E+00	8.04E+00	5.24E-03
94	7.45E-01	6.19E-02	2.73E-01	1.94E+00	9.69E-01	1.29E+00	2.41E-04
95	9.90E-01	2.95E-02	6.32E-02	2.28E+00	8.73E+00	2.64E+00	1.75E-02
96	8.83E-01	2.25E-01	4.32E-02	1.20E+00	1.59E+00	4.20E+00	3.07E-05
97	8.53E-01	6.50E-02	5.58E-02	3.14E+00	7.78E-01	4.49E+00	2.15E-03
98	8.79E-01	5.55E-02	9.99E-02	9.73E-01	7.36E+00	1.18E+00	1.21E-03
99	4.09E-01	3.70E-01	2.93E-01	2.68E+00	7.07E+00	8.61E+00	8.75E-03
100	6.85E-01	3.91E-02	2.84E-02	7.32E-01	7.71E+00	5.60E+00	9.68E-03

4.2.1.4 Step 3 – Evaluation of Oxidation-State-Dependant Parameters

Step 3 is run once per replicate. The Step 3 script loops over all 100 vectors in the replicate, invoking ALGEBRACDB version 2.35 and RELATE version 1.43 for each vector. The Step 3 script, ALGEBRACDB and RELATE executables, script input and log files, as well as the input and output files for ALGEBRACDB and RELATE are shown in Table 4.14.

The ALGEBRACDB code selects the sampled distribution coefficient and molecular diffusion coefficient based upon the value of the sampled oxidation state. The distribution coefficient is then used to calculate the retardation factor.

The RELATE code is used to remove all element blocks except for CULEBRA (all required non-CULEBRA block properties are transferred to the CULEBRA block).

Table 4.14 Step 3 Script, Executables, Input and Output Files

	File Names[1,2]	CMS Library	CMS Class
SCRIPT	EVAL_ST2D_STEP3.COM	LIBCRA1BC_EVAL	ST2D_STEP3_V1.0
Input	EVAL_ST2D_CRA1BC_STEP3_R*r*.INP	LIBCRA1BC_EVAL	CRA1BC-0
Log	EVAL_ST2D_CRA1BC_STEP3_R*r*.LOG	LIBCRA1BC_ST2D	CRA1BC-0
ALGEBRACDB	ALGEBRACDB_PA96.EXE	LIBALG	PA96
Input	ALG_ST2D_CRA1BC.INP	LIBCRA1BC_ST2D	CRA1BC-0
Input	LHS3_ST2D_CRA1BC_R*r*_V*vvv*.CDB	LIBCRA1BC_ST2D	CRA1BC-0
Output	ALG_ST2D_CRA1BC_R*r*_V*vvv*.CDB	LIBCRA1BC_ST2D	CRA1BC-0
Output	ALG_ST2D_CRA1BC_R*r*_V*vvv*.DBG	NOT KEPT	NOT KEPT
RELATE	RELATE_PA96.EXE	LIBREL	PA96
Input	REL_ST2D_CRA1BC.INP	LIBCRA1BC_ST2D	CRA1BC-0
Input	GM_ST2D_CRA1BC.CDB	LIBCRA1BC_ST2D	CRA1BC-0
Input	ALG_ST2D_CRA1BC_R*r*_V*vvv*.CDB	LIBCRA1BC_ST2D	CRA1BC-0
Output	REL_ST2D_CRA1BC_R*r*_V*vvv*.CDB	LIBCRA1BC_ST2D	CRA1BC-0
Output	REL_ST2D_CRA1BC_R*r*_V*vvv*.DBG	NOT KEPT	NOT KEPT

1. $r \in \{1, 2, 3\}$
2. $vvv \in \{001, 002, ..., 100\}$ for each r

4.2.1.5 Step 4 – Tabulation of Mining Factors and Flow Field Indices

Step 4 is run once per replicate. The Step 4 script fetches all 100 ALGEBRACDB output files produced in Step 3, then runs SUMMARIZE version 2.20 on them. The Step 4 script, SUMMARIZE executable, script input and log files as well as the input and output files for SUMMARIZE are shown in Table 4.15.

The SUMMARIZE code is used to construct tables of the uncertain mining factor parameter CULEBRA:MINP_FAC and the flow field index parameter CULEBRA:TRANSIDX (flow field index = INT[CULEBRA:TRANSIDX]. These tables are transferred to the WIPP PA Pentium Cluster for use in the Culebra flow calculations. Each table contains four columns: the vector number, time (not used), MINP_FAC, and TRANSIDX.

Table 4.15 Step 4 Script, Executables, Input and Output Files

	File Names[1,2]	CMS Library	CMS Class
SCRIPT	EVAL_ST2D_STEP4.COM	LIBCRA1BC_EVAL	ST2D_STEP4_V1.0
Input	EVAL_ST2D_CRA1BC_STEP4_R*r*.INP	LIBCRA1BC_EVAL	CRA1BC-0
Output	SUM1_ST2D_CRA1BC_R*r*.INP	LIBCRA1BC_ST2D	CRA1BC-0
Log	EVAL_ST2D_CRA1BC_STEP4_R*r*.LOG	LIBCRA1BC_ST2D	CRA1BC-0
SUMMARIZE	SUMMARIZE_QA_0220.EXE	LIBSUM	QA0220
Input	SUM1_ST2D_CRA1BC_R*r*.INP	LIBCRA1BC_ST2D	CRA1BC-0
Input	ALG_ST2D_CRA1BC_R*r*_V*vvv*.CDB	LIBCRA1BC_ST2D	CRA1BC-0
Output	SUM1_ST2D_CRA1BC_R*r*.TBL	LIBCRA1BC_ST2D	CRA1BC-0
Output	SUM1_ST2D_CRA1BC_R*r*.LOG	NOT KEPT	NOT KEPT
Output	SUM1_ST2D_CRA1BC_R*r*_ERROR.LOG	NOT KEPT	NOT KEPT

1. $r \in \{1, 2, 3\}$
2. $vvv \in \{001, 002, ..., 100\}$ for each r

4.2.1.6 Step 5 – Flow Field Extraction

The rules for converting the MODFLOW output data (volumetric flux) to SECOTP2D input data (Darcy velocity) described in section 4.1.2 above were implemented in the Fortran code VTRAN2. VTRAN2 neither models physical phenomena nor solves differential equations that model physical phenomena. Rather, it is a utility code that processes the output data produced by a modeling code and formats that data for use in another modeling code. VTRAN2 has been qualified for this analysis per Nuclear Waste Management Procedure NP 9-1: Analysis (Chavez 2001). The source code listing, build information, and verification testing for VTRAN2 are provided in Appendix A.

The VTRAN2 code takes five command line arguments, four required and one optional. All arguments are the names of input or output files, descriptions of which follow:

- **File 1 (cmd_file)** is an input ASCII format command file. The command file describes the MODFLOW mesh, the SECOTP2D mesh, the x- and y-direction offsets between the two meshes and the format that was used to write the MODFLOW velocities into the ASCII budget file (see below).

- **File 2 (bud_file)** is an input ASCII format MODFLOW budget file containing the volumetric flux values for each cell in the groundwater flow modeling mesh.

- **File 3 (trn_file)** is a binary format output file containing the groundwater flow velocities for the transport domain (including the ghost cells) in the format required by the SECOTP2D transport code.

- **File 4 (dbg file)** is an output ASCII format diagnostic/debug file containing information about the VTRAN2 run.

- **File 5 (txt file)** is an optional output ASCII format file containing the same data as the trn_file.

A sample command line that executes VTRAN2 is shown below:

$ VTRAN2 TEST.CMD TEST.BUD TEST.TRN TEST.DBG TEST.TXT

The flow fields obtained from the Culebra flow calculations introduce the concept of mining scenarios in to the transport calculations. The Step 5 script is run once per replicate/mining scenario combination. The script loops over all 100 flow field indices in the replicate/scenario combination, using the VTRAN2 utility code to extract the mining-modified Culebra flow fields (corresponding to the sub-domain used in the Culebra transport calculations) from the MODFLOW output files. The script, executable, script input and log files, along with the input and output files for the VTRAN2 utility are shown in Table 4.16.

Table 4.16 Step5 Script, Executable, Input and Output Files

	File Names[1,2,3]	CMS Library	CMS Class
SCRIPT	EVAL_ST2D_STEP5.COM	LIBCRA1BC_EVAL	ST2D_STEP5_V1.0
Script Input	EVAL_ST2D_CRA1BC_STEP5_R*r*_*Mm*.INP	LIBCRA1BC_EVAL	CRA1BC-0
Log	EVAL_ST2D_CRA1BC_STEP5_R*r*_*Mm*.LOG	LIBCRA1BC_MF2K	CRA1BC-0
VTRAN2	VTRAN2.EXE	LIBCRA1BC_MF2K	VTRAN2_V1.1
Input	VTRAN2_CRA1BC.INP	LIBCRA1BC_MF2K	CRA1BC-0
Input	MF2K_CRA1BC_R*r*_M*m*_F*fff*.OUT	LIBCRA1BC_MF2K	CRA1BC-0
Output	MF2K_CRA1BC_R*r*_M*m*_F*fff*.TRN	LIBCRA1BC_MF2K	CRA1BC-0
Output	VTRAN2_ST2D_CRA1BC_R*r*_M*m*_F*fff*.DBG	NOT KEPT	NOT KEPT

1. $r \in \{1, 2, 3\}$
2. $m \in \{F, P\}$ for each r
3. $fff \in \{001, 002, ..., 100\}$ for each m

4.2.1.7 Step 6 – Transport Calculations

The Step 6 script runs the SECOTP2D suite of codes (PRESECOTP2D version 1.22, SECOTP2D version 1.41A, and POSTSECOTP2D version 1.04) to calculate radionuclide transport through the Culebra. Two DCL run control scripts are used in Step 6. The master script is invoked once for each replicate/scenario combination. The master script loops over all 100 vectors for each replicate/scenario combination. For each vector, the master script performs the following steps:

- Use GROPECDB version 2.12 to extract the value of the CULEBRA:TRANSIDX parameter from the ALGEBRACDB output file generated in Step 3. The value of this parameter indicates the flow field index to use with the vector.
- Write input file for slave script
- Run the slave script

The slave script then runs PRESECOTP2D, SECOTP2D, and POSTSECOTP2D for that vector. Both the master and the slave scripts produce log files to record their actions.

In the paragraphs that follow, the input and output files for the generic case are described, then the procedure followed to re-run certain replicate/scenario/vector combinations with a modified PRESECOTP2D input file to overcome numerical stability problems.

Table 4.17 Step 6 Scripts, Executables, Input and Output Files (General Case)

	File Names[1,2,3,4,5]	CMS Library	CMS Class
MASTER SCRIPT	EVAL_ST2D_STEP6_MASTER.COM	LIBCRA1BC_EVAL	ST2D_STEP6_V1.0
Input	EVAL_ST2D_CRA1BC_STEP6_R*r*_M*m*.INP	LIBCRA1BC_EVAL	CRA1BC-0
Log	EVAL_ST2D_CRA1BC_STEP6_R*r*_M*m*.LOG	LIBCRA1BC_ST2D	CRA1BC-0
SLAVE SCRIPT	EVAL_ST2D_STEP6_MASTER.COM	LIBCRA1BC_EVAL	ST2D_STEP6_V1.0
Log	EVAL_ST2D_CRA1BC_STEP6_R*r*_M*m*_V*vvv*.LOG	LIBCRA1BC_ST2D	CRA1BC-0
GROPECDB	GROPECDB_PA96.EXE	LIBGR	PA96
Input	GROPE_ST2D_CRA1BC.INP	LIBCRA1BC_ST2D	CRA1BC-0
Input	ALG_ST2D_CRA1BC_R*r*_V*vvv*.CDB	LIBCRA1BC_ST2D	CRA1BC-0
Output	GROPE_ST2D_CRA1BC_R*r*_M*m*_V*vvv*.TXT	NOT KEPT	NOT KEPT
PRESECOTP2D	PRESECOTP2D_QA0122.EXE	LIBST2D	QA0122
Input	ST2D1_CRA1BC.INP	LIBCRA1BC_ST2D	CRA1BC-0
Input	REL_ST2D_CRA1BC_R*r*_V*vvv*.CDB	LIBCRA1BC_ST2D	CRA1BC-0
Input	MF2K_CRA1BC_R*r*_M*m*_F*fff*.TRN	LIBCRA1BC_MF2K	CRA1BC-0
Output	ST2D2_CRA1BC_R*r*_M*m*_V*vvv*.INP	NOT KEPT	NOT KEPT
Output	ST2D1_CRA1BC_R*r*_M*m*_V*vvv*.PRP	NOT KEPT	NOT KEPT
Output	ST2D1_CRA1BC_R*r*_M*m*_V*vvv*.VEL	NOT KEPT	NOT KEPT
Output	ST2D1_CRA1BC_R*r*_M*m*_V*vvv*.DBG	NOT KEPT	NOT KEPT
SECOTP2D	SECOTP2D_QA0141A.EXE	LIBST2D	QA0141A
Input	ST2D2_CRA1BC_R*r*_M*m*_V*vvv*.INP	NOT KEPT	NOT KEPT
Input	ST2D1_CRA1BC_R*r*_M*m*_V*vvv*.PRP	NOT KEPT	NOT KEPT
Input	ST2D1_CRA1BC_R*r*_M*m*_V*vvv*.VEL	NOT KEPT	NOT KEPT
Output	ST2D2_CRA1BC_R*r*_M*m*_V*vvv*.BIN	NOT KEPT	NOT KEPT
Output	ST2D2_CRA1BC_R*r*_M*m*_V*vvv*.DBG	NOT KEPT	NOT KEPT
POSTSECOTP2D	POSTSECOTP2D_QA0104.EXE	LIBST2D	QA0104
Input	ST2D2_CRA1BC_R*r*_M*m*_V*vvv*.BIN	NOT KEPT	NOT KEPT
Input	REL_ST2D_CRA1BC_R*r*_V*vvv*.CDB	LIBCRA1BC_ST2D	CRA1BC-0
Output	ST2D3_CRA1BC_R*r*_M*m*_V*vvv*.CDB	LIBCRA1BC_ST2D	CRA1BC-0
Output	ST2D3_CRA1BC_R*r*_M*m*_V*vvv*.DBG	LIBCRA1BC_ST2D	CRA1BC-0

1. $r \in \{1, 2, 3\}$
2. $m \in \{F, P\}$ for each r
3. $fff \in \{001, 002, ..., 100\}$ for each m
4. $vvv \in \{001, 002, ..., 100\}$ for each m
5. flow field index matched with vector number through the TRANSIDX parameter for each vector

In the few instances where SECOTP2D failed due to numerical instability using the generic numerical control parameters, a new PRESECOTP2D input file was submitted by the analyst and the case was re-run in a manner similar to that described above. In order

to track these cases a special tag ("MOD") was inserted into the PRESECOTP2D input file name, as well as the master script input file and log file names

The replicate/scenario/vectors requiring modified PRESECOTP2D input files are shown in Table 4.18. The modified file names are shown in Table 4.19. Other files have the same names as for the generic case. Files in the libraries from the previous runs were replaced with files from the re-run.

Table 4.18 Culebra Transport Step 6 Modified Input Runs

Replicate	Mining Scenario	Vector
1	Full	81
1	Partial	81
2	Full	81
2	Partial	81
3	Full	42, 81
3	Partial	42, 81

Table 4.19 Culebra Transport Step 6 Modified Input Run File Names

	File Names[1,2,3]	CMS Library	CMS Class
MASTER SCRIPT			
Input	EVAL_ST2D_CRA1BC_STEP6_R*r*_M*m*_V*vvv*_MOD.INP	LIBCRA1BC_EVAL	CRA1BC-0
Log	EVAL_ST2D_CRA1BC_STEP6_R*r*_M*m*_V*vvv*_MOD.LOG	LIBCRA1BC_ST2D	CRA1BC-0
PRESECOTP2D			
Input	ST2D1_CRA1BC_R*r*_V*vvv*.INP	LIBCRA1BC_ST2D	CRA1BC-0

1. $r \in \{1, 2, 3\}$
2. $m \in \{F, P\}$ for each r
3. *vvv* as shown in Table 4.18.

4.3 Results

Radionuclide transport calculations for the Culebra were performed with the SECOTP2D code suite as described in the preceding sections. All calculations were performed on the WIPP Alpha Cluster under formal run control procedures as described in Long and Kanney (2005).

The specific quantity of interest in the Culebra transport calculations is the cumulative release of radionuclides at the LWB during the 10,000-year regulatory period, in response to unit releases (1 kg) from a point source located at the center of the waste panel area during the first 50 years after repository closure. The radionuclides transported in the Culebra are ^{241}Am, ^{234}U, ^{230}Th and ^{239}Pu. Pu may be present in ether the Pu(III) or Pu(IV) oxidation state. U may be present as U(IV) or U(VI).

Transport calculations were performed for both full mining and partial mining scenarios. The partial mining scenario assumes the extraction of all potash reserves outside the LWB while full mining assumes that all reserves both inside and outside the LWB are exploited. The effect of mining enters the transport calculations through the Culebra flow field computed using the code MODFLOW2000 (see section 3).

Since the CRA-2004 PABC used a total of 300 sample elements (three replicates of 100 vectors each) and calculations were required for both full and partial mining conditions, 600 Culebra transport simulations were performed. Along with the input files referenced above, the output (CAMDAT database) files from these simulations are stored in CMS library LIBCRA1BC_ST2D, class CRA1BC-0 on the WIPP PA Alpha Cluster. The naming convention for the CAMDAT database files is: ST2D3_CRA1BC_R*r*_M*m*_V*vvv*.CDB, where $r \in \{1, 2, 3\}$, $m \in \{\mathrm{F}, \mathrm{P}\}$, and $vvv \in \{001, 002, ..., 100\}$. See Long and Kanney (2005) for a complete description of the run control procedures used to perform the Culebra transport calculations.

In each transport simulation, 1 kg of each of four radionuclides (^{241}Am, ^{234}U, ^{230}Th, and ^{239}Pu) are released at the center of the waste panel area. Transport of the ^{230}Th daughter product of ^{234}U decay is calculated and tracked as a separate species. In the following discussion, ^{230}Th will refer to the ^{234}U daughter product and ^{230}ThA will refer to that released at the waste panel area.

4.3.1 Radionuclide Transport under Partial Mining Conditions

Under partial-mining conditions, only the ^{234}U species and its ^{230}Th decay product were transported to the LWB in any significant amount during the course of the 10,000-year simulation. Table 4.20 shows that no releases greater than one billionth of the 1 kg source were calculated for Replicates R1 and R3. For replicate R2, three vectors produced ^{234}U releases greater than 10^{-9} kg. One of these vectors also resulted in a ^{230}Th release greater 10^{-9} kg.

Table 4.20 Radionuclide Transport to the LWB under Partial Mining Conditions[1,2]

Replicate	^{241}Am	^{239}Pu	^{234}U	^{230}Th	^{230}ThA
1	0	0	0	0	0
2	0	0	3	1	0
3	0	0	0	0	0

1. Number of vectors that have releases (transport to LWB) greater than one billionth of the 1 kg source released at center of waste panel.
2. ^{230}ThA refers to thorium released at the waste panel area. ^{230}Th refers to thorium resulting from ^{234}U decay.

4.3.2 Radionuclide Transport under Full Mining Conditions

Under full-mining conditions, only the ^{234}U species and its ^{230}Th decay product were transported to the LWB in any significant amount during the course of the 10,000-year simulation. More vectors resulted in releases greater than 10^{-9} kg for the full-mining scenario than were seen under partial mining conditions. In addition, releases greater than 10^{-9} kg were calculated for all three replicates. Table 4.21 shows that three vectors in replicate R1, 6 vectors in replicate R2, and 3 vectors in replicate R3 had ^{234}U releases greater than 10^{-9} kg. None of the three vectors in replicate R1 that showed a ^{234}U release grater than 10^{-9} kg showed a release of ^{230}Th daughter product greater than 10^{-9} kg. In replicate R2, three vectors of the six vectors that showed a ^{234}U release grater than 10^{-9} kg showed a release of ^{230}Th daughter greater than 10^{-9} kg. In replicate R2, three vectors of the six vectors that showed a ^{234}U release grater than 10^{-9} kg showed a release of ^{230}Th daughter greater than 10^{-9} kg.

Table 4.21 Radionuclide Transport to the LWB under Full Mining Conditions[1,2]

Replicate	^{241}Am	^{239}Pu	^{234}U	^{230}Th	^{230}ThA
1	0	0	3	0	0
2	0	0	6	3	0
3	0	0	3	1	0

1. Number of vectors that have releases (transport to LWB) greater than one billionth of the 1 kg source released at center of waste panel.
2. ^{230}ThA refers to thorium released at the waste panel area. ^{230}Th refers to thorium resulting from ^{234}U decay.

4.4 Discussion

In summary, very few vectors showed significant transport of radionuclides to the LWB during the 10,000-year simulation under partial or full mining conditions. Only ^{234}U and its ^{230}Th daughter product were transported in any significant amount.

Comparing these results to those for the CRA-2004 PA, one observes the same general trends: 1) the ^{234}U species dominates the releases; and 2) there are more releases under full-mining conditions than under partial-mining conditions. There are also some noticeable differences: 1) there are generally fewer vectors that show transport of radionuclides to the LWB in the CRA-2004 PABC results; and 2) no releases of ^{239}Pu are calculated in the CRA-2004 PABC PA while two such vectors were observed in the CRA-2004 results.

Sensitivity analysis indicates that releases of ^{234}U in both the full and partial mining conditions is associated with the U(VI) oxidation state. This result is reasonable because the matrix distribution coefficients for uranium in the (IV) state are much lower than for the (VI) state. This sensitivity was also observed and reported in the CRA-2004 PA.

5 Summary and Conclusions

Results show that for both the full- and partial-mining scenarios, the median particle travel times of 70,170 and 131,705 years are 3.84 and 7.20 times greater than for the non-mining scenario (18,289 years), respectively (the CRA-revised travel times were 4.14 and 7.06 times greater). The increase in transmissivity due to mining increases the relative flow rate through the mining zones, with a corresponding decrease in flow through the non-mining zones. This decrease in flow through the non-mining zones produces longer travel times for the mining scenarios.

Like the CRA-revised calculations, a negative correlation was found in the CRA-2004 PABC analysis between the travel times and the random mining factor (the higher the random mining factor, the longer the particle travel time). This again is due to a higher percentage of mining zone area in the CRA-revised analysis as compared to the CRA-2004. With a higher percentage of mining area, the random mining factor has a larger influence on the regional flow regime. As the mining factor is increased, the flow through the non-mining areas is decreased, producing longer travel times and the negative correlation. However, additional analysis shows that most of the travel time variability is due to differences in the base T-fields and not the random mining factor.

Very few vectors showed significant transport of radionuclides to the LWB during the 10,000-year transport simulations under partial or full mining conditions. Only ^{234}U and its ^{230}Th daughter product were transported in any significant amount.

Comparing these results to those for the CRA-2004 PA, one observes the same general trends: 1) the ^{234}U species dominates the releases; and 2) there are more releases under full-mining conditions than under partial-mining conditions. There are also some noticeable differences: 1) there are generally fewer vectors that show transport of radionuclides to the LWB in the CRA-2004 PABC results; and 2) no releases of ^{239}Pu are calculated in the CRA-2004 PABC PA while two such vectors were observed in the CRA-2004 results.

Sensitivity analysis indicates that releases of ^{234}U in both the full and partial mining conditions is associated with the U(VI) oxidation state. This result is reasonable because the matrix distribution coefficients for uranium in the (IV) state are much lower than for the (VI) state. This sensitivity was also observed and reported in the CRA-2004 PA.

6 References

Beauheim, R. L. 2003. AP-100 Task 1: Development and Application of Acceptance Criteria for Culebra Transmissivity (T) Fields. Analysis Report ERMS 531136, Carlsbad, NM.

BLM. 1993. Preliminary Map Showing Distribution of Potash Resources, Carlsbad Mining District, Eddy and Lea Counties, New Mexico. U.S. Bureau of Land Management (BLM), Roswell, NM.

Chavez, M. J. 2001. Nuclear Waste Management Procedure NP 9-1: Analyses, Revision 4. ERMS 519375, Sandia National Laboratories, Carlsbad, NM.

Chavez, M. J. 2004. Nuclear Waste Management Procedure NP 19-1: Software Requirements, Revision 11. Sandia National Laboratories, Carlsbad, NM.

Corbet, T. 1996. FEP NS-9, Two-dimensional Assumption for Culebra Calculations Technical Memorandum ERMS 230802, pp 19-26. Sandia National Laboratories, Carlsbad, NM.

Cotsworth, E. 2004. Third Set of CRA Comments (September 2, 2004 Letter to R. Paul Detwiler, Acting Manger, Carlsbad Field Office, U.S. Department of Energy). U.S. Environmental Protection Agency.

Cotsworth, E. 2005. Sixth Set of EPA Comments (March 4, 2005 Letter to Ines Triay). U.S. Environmental Protection Agency.

GMS. 2003. Groundwater Modeling System: Developed by Brigham Young University Environmental Modeling Research Laboratory in partnership with the U.S. Army Corps of Engineers Waterways Experiment Station. Viscksburg, MS http://chl.wes.army.mil/software/gms/default.htp.

Harbough, A. W., E. Banta, M. C. Hill, and M. McDonald. 2000. MODFLOW 2000: The U.S. Geological Survey Modular Ground-Water Model - User Guide to Modularization Concepts and the Ground-Water Flow Process. Open File Report 00-92, U.S. Geological Survey, Reston, VA.

Hart, D. B. 2005. Installation and Checkout for Linux MODFLOW and Utilities and Regression testing for the Intel Xeon/Linux 2.6 Platform. ERMS 540423, Sandia National Laboratories, Carlsbad, NM.

Holt, R. M. 1997. Conceptual Model for Transport Processes in the Culebra Dolomite Member of the Rustler Formation Contractor Report SAND97-0194. Sandia National Laboratories, Albuquerque, NM.

Holt, R. M., and D. W. Powers. 1988. Facies Variability and Post-Depositional Alteration Within the Rustler Formation in the Vicinity of the Waste Isolation Pilot Plat, Southeastern New Mexico. WIPP-DOE-88-004, Department of Energy, Carlsbad, NM.

Kanney, J. F. 2005. Analysis Plan for Culebra Transport Calculations: Post CRA Baseline Calculation. ERMS 539540, Sandia National Laboratories, Carlsbad, NM.

Kanney, J. F., and C. Leigh. 2005. Analysis Plan for Post CRA PA Baseline Calculation (AP-122). ERMS 539624, Sandia National Laboratories, Carlsbad, NM.

Kirchner, T. B. 2005a. Analysis Report for Migration of CVS CRA WIPP PA Repositories from the Linux AMD Cluster to the Intel Pentium 4 Xeon Cluster. ERMS 539823, Sandia National Laboratories, Carlsbad, NM.

Kirchner, T. B. 2005b. Generation of the LHS Samples for the CRA-2004 PA Baseline Calculations. ERMS 540279, Sandia National Laboratories, Carlsbad, NM.

Long, J. J. 2002. WIPP Performance Assessment Software Configuration Management System (SCMS) Plan, Version 2.0. ERMS 524707, Sandia National Laboratories, Carlsbad, NM.

Long, J. J., and J. F. Kanney. 2005. Execution of Performance Assessment Codes for the CRA-2004 Performance Assessment Baseline Calculation. ERMS 541394, Sandia National Laboratories, Carlsbad, NM.

Lowry, T. L. 2003a. Analysis Report, Task 5 of AP-088: Evaluation of Mining Scenarios. Sandia National Laboratories, Carlsbad, NM.

Lowry, T. L. 2003b. Analysis Report, Tasks 2 & 3 of AP-100: Grid Size Conversion and Generation of SECOTP2D Input. ERMS 531137, Sandia National Laboratories, Carlsbad, NM.

Lowry, T. S. 2004. Analysis Report for Inclusion of Omitted Areas in Mining Transmissivity Calculations in Response to EPA Comment G-11. ERMS 538218, Sandia National Laboratories, Carlsbad, NM.

MacKinnon, R., and G. Freeze. 1997a. Summary of EPA-Mandated Performance Assessment Verification Test (Replicate 1) and Comparison With the Compliance Certification Application Calculations, Revision 1. ERMS 422595, Sandia National Laboratories, Carlsbad, NM.

MacKinnon, R. J., and G. Freeze. 1997b. Summary of Uncertainty and Sensitivity Analysis Results for the EPA-Mandated Performance Assessment Verification Test. ERMS 420669, Sandia National Laboratories, Carlsbad, NM.

MacKinnon, R. J., and G. Freeze. 1997c. Supplimental Summary of EPA-Mandated Performance Assessment Verification Test (All Replicates) and Comparison With the Compliance Certification Application Calculations, Revision 1. ERMS 414880, Sandia National Laboratories, Carlsbad, NM.

McKenna, S. A., and D. B. Hart. 2003a. Task 3 of AP-088: Conditioning of Base T Fields to Steady-State Heads. Analysis Report ERMS 529633, Sandia National Laboratories, Carlsbad, NM.

McKenna, S. A., and D. B. Hart. 2003b. Task 4 of AP-088: Conditioning of Base T Fields to Transient Heads. Analysis Report ERMS 521124, Sandia National Laboratories, Carlsbad, NM.

Meigs, L. C., R. L. Beauheim, and T. L. Jones. 2000. Interpretations of Tracer Tests Performed in the Culebra Dolomite at the Waste Isolation Pilot Plant Site
Sandia Report SAND97-3109. Sandia National Laboratories, Albuquerque, NM.

Powers, D. W., S. J. Lambert, S. E. Shaffer, L. R. Hill, and W. D. Weart. 1978. Geological Characterization Report, Waste Isolation Pilot Plant (WIPP) Site, Southeastern New Mexico
Sandia Report SAND 78-1596. Sandia National Laboratories, Albuquerque, NM.

Ramsey, J. L. 1997. WIPP PA User's Manual for SECOTP2D, Version 1.41. Sandia National Laboratories, Carlsbad, NM.

Ramsey, J. L., and M. Wallace. 1996. Analysis Package for the Culebra Flow and Transport Calculations (Task 3) of the Performance Assessment Analyses Supporting the Compliance Certification Application. ERMS 240516, Sandia National Laboratories, Carlsbad, NM.

Salari, K., and R. Blaine. 1996. WIPP PA User's Manual for SECOTP2D, Version 1.30. Sandia National Laboratories, Carlsbad, NM.

U.S. DOE. 1996. Title 40 CFR Part 191 Compliance Certification Application for the Waste Isolation Pilot. DOE/CAO-1996-2184, U.S. Department of Energy Waste Isolation Pilot Plant, Carlsbad Area Office, Carlsbad, NM.

U.S. DOE. 2004. Title 40 CFR Part 191 Compliance Recertification Application for the Waste Isolation Pilot. DOE/WIPP 2004-3231, U.S. Department of Energy Waste Isolation Pilot Plant, Carlsbad Field Office, Carlsbad, NM.

Vine, J. D. 1963. Surface Geology of the Nash Draw Quadrangle, Eddy County, New Mexico

USGS Bulletin 1141-B. U.S. Geolgical Survey.

Wallace, M. G. 1996. Record of FEP Screening Work, FEP ID# NS-11: Subsidence Associated with Mining Inside or Outside the Controlled Area. ERMS 240816, Sandia National Laboratories, Carlsbad, NM.

WIPP PA. 2002. User's Manual for DTRKMF Version 1.00. ERMS 523246, Sandia National Laboratories, Carlsbad, NM.

Appendix A VTRAN2 Utility

This appendix provides the source listing, build information, and a summary of testing for the Fortran utility code VTRAN2. VTRAN2 was used to extract the groundwater flow velocity data from MODFLOW200 output budget files (see sections 4.1.1 and 4.2.1.6).

A.1 VTRAN2 Source Code

The Fortran source code file for the VTRAN2 utility (VTRAN2.F) is shown below. This file is archived in CMS library LIBCRA1BC_MF2K, class VTRAN2_V1.1 on the WIPP PA Alpha Cluster.

```
C-----------------------------------------------------------------------
      PROGRAM VTRAN2
C-----------------------------------------------------------------------
C     Version 1.1
C     2005 July 20
C
C     Joseph Kanney
C     Sandia National Laboratories
C     Org 6821
C-----------------------------------------------------------------------
C
C     This utility code is used to extract fluxes from a specified
C     subdomain of a modflow budget file, convert them to velocities,
C     then write them to an output file in a format that can be read
C     by PRESECOTP2D.
C
C     nrowmf - number of rows cells in the mf2k grid
C     ncolmf - number of columns in the mf2k grid
C
C     ncx - number of cells in x-direction in the st2d grid
C     ncy - number of cells in y-direction in the st2d grid
C
C     jshftx - x offset of transport domain (# of cells in col
direction)
C     ishfty - y offset of transport domain (# of cells in row
direction)
C-----------------------------------------------------------------------
---
C
      PARAMETER (nfmat = 2, mxfile=5)

      CHARACTER*80 author, date, title
      CHARACTER*80 filenm(mxfile)
      CHARACTER*80 fmat(nfmat),rdfmat
      CHARACTER*80 fnmcmd, fnmbud, fnmtrn, fnmdbg, fnmvel

      INTEGER ierr
      INTEGER iunscr, iuncmd, iunbud, iuntrn, iundbg, iunvel
      INTEGER nfiles, nfiler
```

```
      INTEGER nrowmf, ncolmf, ncx, ncy
      INTEGER istart, ishift, jstart, jshift
      INTEGER match, irdfmt
      DOUBLE PRECISION time
      DOUBLE PRECISION ayz_inv, axz_inv, dx, dy, dz
      DOUBLE PRECISION, ALLOCATABLE :: qxin(:,:), qyin(:,:)
      DOUBLE PRECISION, ALLOCATABLE :: qxout(:,:), qyout(:,:)

      LOGICAL wrtvel


C---------------------
C.....Setup
C---------------------


C.....Assign file unit numbers

      nfiles = 5

      iunscr = 6
      iuncmd = 11
      iunbud = 12
      iuntrn = 13
      iundbg = 14
      iunvel = 15

C.....Valid budget file input formats

      fmat(1) = '(448e16.8)'
      fmat(2) = '(448(e23.16,1x))'


C-----------------------------------------
C.....Process command line (get file names)
C-----------------------------------------

C      WRITE(iunscr,*) 'VTRAN >> Processing command line'


C.....Required args  (1-4) are fnmcmd, fnmbud, fnmtrn, fnmdbg
C.....Optional arg (5) is fnmvel

      CALL filcmdlin( nfiles, nfiler, filenm )

C      write(iunscr,*) 'nfiler = ', nfiler

      IF ( nfiler .GT. nfiles ) THEN
         CALL QAABORT( 'VTRAN>> Too many command line arguments')
      ELSE
         IF ( nfiler .LT. nfiles-1 ) THEN
            CALL QAABORT( 'VTRAN>> Too few command line arguments')
         ENDIF
      ENDIF
```

```
      fnmcmd = filenm(1)
      fnmbud = filenm(2)
      fnmtrn = filenm(3)
      fnmdbg = filenm(4)

      IF (nfiler .eq. nfiles ) THEN
         wrtvel = .true.
         fnmvel = filenm(5)
      ELSE
         wrtvel = .false.
         fnmvel = 'None'
      ENDIF

C          write(iunscr,*) 'fnmcmd is ', fnmcmd
C          write(iunscr,*) 'fnmbud is ', fnmbud
C          write(iunscr,*) 'fnmtrn is ', fnmtrn
C          write(iunscr,*) 'fnmdbg is ', fnmdbg
C          write(iunscr,*) 'fnmvel is ', fnmvel



C.....Open Diagnostics/Debug file

      OPEN (UNIT=iundbg, FILE=fnmdbg, STATUS='UNKNOWN',IOSTAT=ierr)
      IF ( ierr .NE. 0 ) THEN
         CALL QAABORT ('Error opening command file')
      ENDIF


C-------------------------
C.....Process command file
C-------------------------

C      WRITE(iunscr,*) 'VTRAN >> Processing command file'

C.....Open command file

      OPEN (UNIT=iuncmd, FILE=fnmcmd, STATUS='OLD',
     +      READONLY, IOSTAT=ierr)
      IF ( ierr .NE. 0 ) THEN
         WRITE(iundbg,*) 'Error opening command file'
         CALL QAABORT ('Error opening command file')
      ENDIF

C.....Read from command file

      READ (iuncmd,*)
      READ (iuncmd,10) author
      READ (iuncmd,*)
      READ (iuncmd,10) date
      READ (iuncmd,*)
      READ (iuncmd,10) title
      READ (iuncmd,*)
      READ (iuncmd,10) rdfmat
      READ (iuncmd,*)
      READ (iuncmd,*) iscrn
      READ (iuncmd,*)
```

```
      READ (iuncmd,*) ncolmf, nrowmf
      READ (iuncmd,*)
      READ (iuncmd,*) jshftx, ishfty, ncx, ncy
      READ (iuncmd,*)
      READ (iuncmd,*) dx, dy, dz

 10   FORMAT(A80)
 11   FORMAT(3e01.3)
C.....Close command file

      CLOSE (UNIT=iuncmd,STATUS='KEEP')

C.....Send diagnostic ouput to screen or to debug file

      IF (iscrn .EQ. 0 ) THEN
        iunscr = iundbg
      ENDIF

C.....Echo input

      WRITE(iunscr,20) fnmcmd, fnmbud, fnmtrn, fnmdbg, fnmvel

 20   FORMAT (1X, 'command file                    = ',A80/
     +        1X, 'budget file                     = ',A80/
     +        1X, '(binary) velocity transfer file = ',A80/
     +        1X, 'diagnostic/debug file           = ',A80/
     +        1X, '(ascii) velocity output file    = ',A80
     +       )


      WRITE(iunscr,50) author, date, title, rdfmat
      WRITE(iunscr,100) iscrn, ncolmf, nrowmf,
     +                  jshftx, ishfty, ncx, ncy,
     +                  dx, dy, dz

 50   FORMAT(1X,' author   = ' A80/
     +       1X,' date     = ',A80/
     +       1X,' title    = ',A80/
     +       1X,' format   = ',A80
     +       )
 100  FORMAT(1X,' iscrn    = ',i5 /
     +       1X,' ncolmf   = ',i5 /
     +       1X,' nrowmf   = ',i5 /
     +       1X,' jshftx   = ',i5 /
     +       1X,' ishfty   = ',i5 /
     +       1X,' ncx      = ',i5 /
     +       1X,' ncy      = ',i5 /
     +       1X,' dx       = ',e10.4 /
     +       1X,' dy       = ',e10.4 /
     +       1X,' dz       = ',e10.4
     +      )


C.....Assign correct format number

      irdfmt = 0
      match  = 0
```

```
      DO i=1,nfmat
         IF( LLE(rdfmat,fmat(i)) .AND. LLE(fmat(i),rdfmat)) THEN
         irdfmt = i
         match = 1
         ENDIF
      ENDDO


      IF ( match .ne.1 ) THEN
         WRITE(iunscr,*) 'Invalid input format'
         CALL QAABORT ('Invalid input format')
      ENDIF

      WRITE(iunscr,150) irdfmt, rdfmat
 150  FORMAT(1X,'Using input format (',i2, ') = ',A80)


C.....Sanity check. Since ghost cells are added, we must have:
C.....jshftx >= 1 and ishifty >= ncy+1

      IF ( jshftx .LT. 1 ) THEN
         WRITE(iunscr,*) 'Invalid jshftx value'
         CALL QAABORT ('Invalid jshftx value')
      ENDIF

      IF ( ishfty .LT. (ncy+1) ) THEN
         WRITE(iunscr,*) 'Invalid ishfty value'
         CALL QAABORT ('Invalid ishfty value')
      ENDIF


C--------------------
C.....Allocate memory
C--------------------

C.....Mf2k grid is (1:ncolmf,1:nrowmf).
C.....Ghost cells placed around transport domain, so ST2D grid is
C.....(0:ncx,0:ncy). Thus qxout and qyout are padded to account for
C.....required ghost cells

      ALLOCATE( qxin(1:ncolmf,1:nrowmf),
     +          qyin(1:ncolmf,1:nrowmf),
     +          qxout(0:ncx+1,0:ncy+1),
     +          qyout(0:ncx+1,0:ncy+1),
     +          STAT=ierr )

      IF ( ierr .NE. 0 ) THEN
         WRITE(iunscr,*) 'Error allocating memory'
         CALL QAABORT ('Error allocating memory')
      ENDIF


C---------------------
C.....Read budget file
C---------------------

      WRITE(iunscr,*) 'VTRAN >> Reading budget file'
```

```
      OPEN (UNIT=iunbud, FILE=fnmbud, FORM='FORMATTED',
     +                   STATUS='OLD', IOSTAT=ierr)
      IF ( ierr .NE. 0 ) THEN
         WRITE(iunscr,*) 'Error opening budget file'
         CALL QAABORT ('Error opening budget file')
      ENDIF

      DO i=1,nrowmf
         READ(iunbud,rdfmat) (qxin(j,i),j=1,ncolmf)
      END DO
      READ(iunbud,*)
      DO i=1,nrowmf
         READ(iunbud,rdfmat) (qyin(j,i),j=1,ncolmf)
      END DO

C.....Close budget file

      CLOSE (UNIT=iunbud,STATUS='KEEP')

C.....Budget file contains volume fluxes, so must divide
C.....by area of cell face perpendicular to flow direction
C.....to get specific discharge (darcy velocity)

C.....X direction

      ayz_inv = 1.d0/(dy*dz)
      DO i=1,nrowmf
         DO j=1,ncolmf
           qxin(j,i) = qxin(j,i) * ayz_inv
         END DO
      END DO

C.....Y direction

      axz_inv = 1.d0/(dx*dz)
      DO i=1,nrowmf
         DO j=1,ncolmf
           qyin(j,i) = qyin(j,i) * axz_inv
         END DO
       END DO


C-----------------------
C.....Process velocities
C-----------------------

      WRITE(iunscr,*) 'VTRAN >> Processing velocities'

C.....Now grab velocities for internal cells and ghost cells.
C.....Let (l,m) be indices of the ST2D grid cells, ranging from 0:ncx+1
C.....and 0:ncy+1, repsectively. We must compute the corresponding
C.....MF2K indices. The computed mf2k indices must account for:
C.....  1) The offset of the ST2D grid origin
C.....  2) The oppossite sense of the y-coord in the two meshes
C.....  3) ST2D face-centered velocities of a given cell are defined
```

```
C.....     at the trailing edges of cells (defined according to sense
of
C.....     the ST2D axes) while the MF2K face-centered velocities are
C.....     defined at the "right" and "front"  faces of the cell.


      DO m=0,ncy+1
         DO l=0,ncx+1
            j = jshftx + l
            i = ishfty + 1 - m
            qxout(l,m) = qxin(j-1,i)
            qyout(l,m) = qyin(j,i)
         END DO
      END DO

C.... For ST2D, face centered velocities defined at trailing edges
C     of cells. Ghost cells are placed around the computational domain,
C     but cells on left and bottom do not have defined velocities
associated
C     with them. Consider the x-dimension with limits [0,x1], with ncx
C     regular cells and a ghost cell on each side of the domain. Then
C       u(0,m) is not defined,
C       u(1,m) = u at x=0, and
C       u(ncx+1,m) = u at x1
C     Similarly, Consider the y-dimension with limits [0,y1], with ncx
C     regular cells and a ghost cell on each side of the domain. Then
C       v(l,0) is not defined,
C       v(l,1) = v at y=0, and
C       v(l,ncy+1) = v at y1

C.....Zero out the undefined components

      DO m=0,ncy+1
         qxout(0,m) = 0.D0
      END DO

      DO l=0,ncx+1
         qyout(l,0) = 0.D0
      END DO

C.....Change sign of y-velocities. MODFLOW convention is that
C.....flow is positive in direction of increasing row numbers.
C.....But row numbers increase in negative y-direction.

      DO m=0,ncy+1
         DO l=0,ncx+1
            qyout(l,m) = -qyout(l,m)
         END DO
      END DO


C---------------------------------
C.....Write velocity transfer file
C---------------------------------

      WRITE(iunscr,*) 'VTRAN >> Writing velocity transfer file'
```

```
C.....Open the file

      OPEN (UNIT=iuntrn, FILE=fnmtrn, FORM='UNFORMATTED',
     +      STATUS='UNKNOWN',IOSTAT=ierr)
      IF ( ierr .NE. 0 ) THEN
         WRITE(iunscr,*) 'Error opening velocity transfer file'
         CALL QAABORT ('Error opening velocity transfer file')
      ENDIF


C.....Write the following line because sf2d wrote it and
C.....st2d1 expects it (but does not use them)

      time = 0.d0
      WRITE(iuntrn) ncx, ncy, time


C.....Write velocities to output file. Include the undefined
C.....components, since ST2D1 expects them. (ST2D1 reads
C.....them in, but does not write them to the velocity file
C.....it passes to ST2D2)

      WRITE(iuntrn) ( ( qxout(l,m), l=0,ncx+1),m=0,ncy+1 )
      WRITE(iuntrn) ( ( qyout(l,m), l=0,ncx+1),m=0,ncy+1 )


C.....Close output file

      CLOSE (UNIT=iuntrn,STATUS='KEEP')


C-------------------------------------
C.....Write ascii velocity output file
C-------------------------------------

      IF ( wrtvel ) THEN

      WRITE(iunscr,*) 'VTRAN >> Writing ascii velocity output file'


C.....Open the file


C      OPEN (UNIT=iunvel, FILE=fnmvel, FORM='FORMATTED',
C     +      STATUS='UNKNOWN',IOSTAT=ierr)

      irecl = 448*(23+1)
      OPEN (UNIT=iunvel, FILE=fnmvel, FORM='FORMATTED',
     +      STATUS='UNKNOWN',RECL=irecl,IOSTAT=ierr)

      IF ( ierr .NE. 0 ) THEN
         WRITE(iunscr,*) 'Error opening ascii velocity output file'
         CALL QAABORT ('Error opening ascii velocity outpuit file')
      ENDIF
```

```
C.....Write the following line because sf2d wrote it and
C.....st2d1 expects it (but does not use them)

      time = 0.d0
      WRITE(iunvel,200) ncx, ncy, time
 200  FORMAT(1x,2(i5,2x),e16.8)

C.....Write velocities to output file

C      WRITE(iunvel,rdfmat) ( ( qxout(l,m), l=0,ncx+1),m=0,ncy+1 )
C      WRITE(iunvel,rdfmat) ( ( qyout(l,m), l=0,ncx+1),m=0,ncy+1 )

      DO m=0,ncy+1
         WRITE(iunvel,rdfmat) (qxout(l,m), l=0,ncx+1)
      END DO

      DO m=0,ncy+1
         WRITE(iunvel,rdfmat) (qyout(l,m), l=0,ncx+1)
      END DO

C.....Close output file

      CLOSE (UNIT=iunvel,STATUS='KEEP')

      ENDIF

C-------------
C.....Clean up
C-------------

      WRITE(iunscr,*) 'VTRAN >> Cleaning up'

      DEALLOCATE(qxin,qxout,qyin,qyout)


      WRITE(iunscr,*) 'VTRAN >> Normal Completion'
      CLOSE (UNIT=iundbg,STATUS='KEEP')

C     Signal normal completion

      STOP 'VTRAN >> Normal Completion'
      END
```

A.2 VTRAN2 Build Info

The VTRAN2 utility build was performed by the WIPP PA Run Control Coordinator, using the Digital Command Language (DCL) script VTRAN2_BUILD.COM. This script extracted the source code from the appropriate access-controlled CMS library, built the executable, and archived the executable in CMS. The build script also generated a log file and archived it in CMS. The files and storage locations associated with building the VTRAN2 utility are given in Table A.1.

Table A.1 VTRAN2 build information

Description	File	CMS Library	CMS Class
Build script	VTRAN2_BUILD.COM	LIBCRA1BC_MF2K	VTRAN2_V1.1
Builds script log file	VTRAN2_BUILD.LOG	LIBCRA1BC_MF2K	VTRAN2_V1.1
Source code	VTRAN2.F	LIBCRA1BC_MF2K	VTRAN2_V1.1
VTRAN2 Executable	VTRAN2.EXE	LIBCRA1BC_MF2K	VTRAN2_V1.1

A.3 VTRAN2 Verification

Test cases for the VTRAN2 utility were developed by the analysts and executed by the Run Control Coordinator. The DCL script VTRAN2_TEST.COM was used to automate and control execution of the test cases. This script extracted the VTRAN2 executable and VTRAN2 input files from an access-controlled CMS library, ran the tests, and archived the VTRAN2 output files in CMS. The test script also generated a log file and archived it in CMS. The script, log file, executable, and input/output files are shown in Table A.2.

Table A.2 VTRAN2 test files

Description	File	CMS Library	CMS Class
Test script	VTRAN2_TEST.COM	LIBCRA1BC_MF2K	VTRAN2_V1.1
Test log file	VTRAN2_TEST.LOG	LIBCRA1BC_MF2K	VTRAN2_V1.1
VTRAN2 executable	VTRAN2.EXE	LIBCRA1BC_MF2K	VTRAN2_V1.1
Test 1			
Input command file	VTRAN_TEST1.CMD	LIBCRA1BC_MF2K	VTRAN2_V1.1
Input budget file	VTRAN_TEST1.BUD	LIBCRA1BC_MF2K	VTRAN2_V1.1
Output binary velocity file	VTRAN_TEST1.TRN	LIBCRA1BC_MF2K	VTRAN2_V1.1
Output ASCII velocity file	VTRAN_TEST1.VEL	LIBCRA1BC_MF2K	VTRAN2_V1.1
Output debug file	VTRAN_TEST1.DBG	LIBCRA1BC_MF2K	VTRAN2_V1.1
Test 2			
Input command file	VTRAN_TEST2.CMD	LIBCRA1BC_MF2K	VTRAN2_V1.1
Input budget file	VTRAN_TEST2.BUD	LIBCRA1BC_MF2K	VTRAN2_V1.1
Output binary velocity file	VTRAN_TEST2.TRN	LIBCRA1BC_MF2K	VTRAN2_V1.1
Output ASCII velocity file	VTRAN_TEST2.VEL	LIBCRA1BC_MF2K	VTRAN2_V1.1
Output debug file	VTRAN_TEST2.DBG	LIBCRA1BC_MF2K	VTRAN2_V1.1

The VTRAN2 utility code was verified using two test cases. Case 1 demonstrates the conversion of volumetric flux to Darcy velocities, the sign change of the y-direction velocities and the inclusion of ghost nodes. Case 2 demonstrates that the indexing selects the correct subregion.

Both test cases use the mesh layout shown in Figure A.1. The volume fluxes are specified on the 10x15 cell mesh. The 4x3 cell sub-region outlined in red represents the transport domain. The dashed lines indicate the ghost nodes. We run VTRAN2 such that

it writes the output in both ASCII and binary format, so we can visually inspect the ASCII file to verify the results.

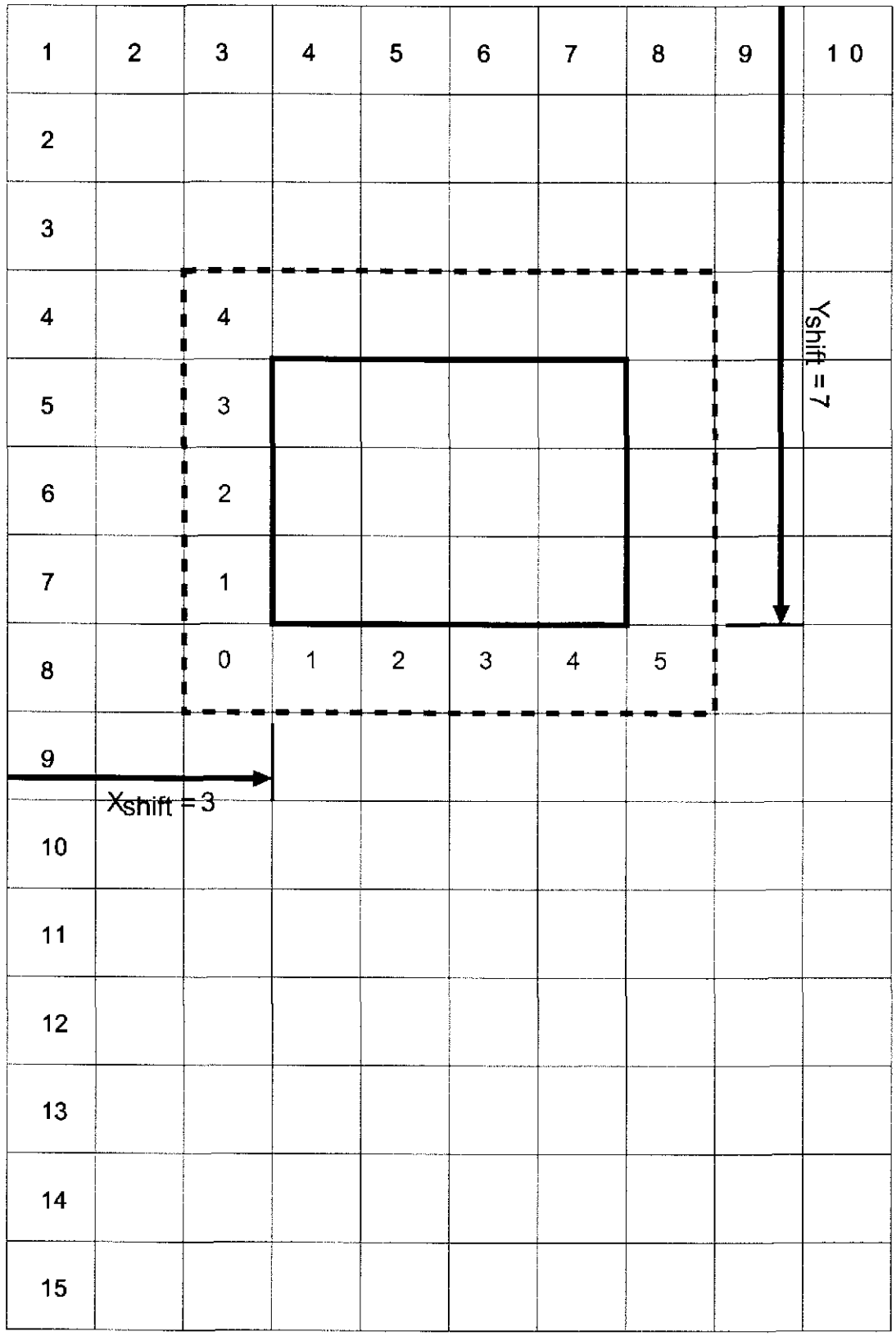

Figure A.1 Mesh for VTRAN2 verification

A.3.1 VTRAN2 Verification Test Case 1

In this test we use a uniform volume flux ($Q_x = Q_y = 1$), and choose $dx = 1$, and $dy = dz = 2$ in the VTRAN2 command file such that $A_x = 4$ and $A_y = 2$. Thus, for the transport mesh, we will have $u = 0.25$ and $v = 0.5$ for all cell faces except for the left and bottom boundaries. $u = 0$ at the left boundary and $v = 0$ at the bottom because the respective velocity at these faces is undefined in the SECOTP2D convention.

The command file (VTRAN2_TEST_1.CMD), and the budget file (VTRAN2_TEST_1.BUD) are shown in Figure A.2, and Figure A.3, respectively. Running VTRAN2 with these input files produces the ASCII velocity file (VTRAN2_TEST_1.VEL) and the diagnostic file (VTRAN2_TEST_1.DBG) show in Figure A.4, and Figure A.5, respectively. We note that u and v are 0.25 and -0.5, as expected. We also note that the 4x3 cell transport domain has been appropriately padded with ghost cells to make a 6x5 array for each velocity component.

```
* author
Joseph F. Kanney
* date
2003.09.24
* title
vtran2 test 1
* input format type
(4d8e16.8)
* iscrn > 0 will print to screen, otherwise to dbg file
0
* ncol nrow
10 15
* jshftx ishfty ncx ncy
3 7 4 3
* dx dy dz (3e10.3)
 1.000E+00 2.000E+00 2.000E+00
```

Figure A.2 VTRAN2_TEST_1.CMD

```
0.10000000E+01 0.10000000E+01 0.10000000E+01 0.10000000E+01 0.10000000E+01 0.10000000E+01 0.10000000E+01 0.10000000E+01 0.10000000E+01 0.10000000E+01
0.10000000E+01 0.10000000E+01 0.10000000E+01 0.10000000E+01 0.10000000E+01 0.10000000E+01 0.10000000E+01 0.10000000E+01 0.10000000E+01 0.10000000E+01
0.10000000E+01 0.10000000E+01 0.10000000E+01 0.10000000E+01 0.10000000E+01 0.10000000E+01 0.10000000E+01 0.10000000E+01 0.10000000E+01 0.10000000E+01
0.10000000E+01 0.10000000E+01 0.10000000E+01 0.10000000E+01 0.10000000E+01 0.10000000E+01 0.10000000E+01 0.10000000E+01 0.10000000E+01 0.10000000E+01
0.10000000E+01 0.10000000E+01 0.10000000E+01 0.10000000E+01 0.10000000E+01 0.10000000E+01 0.10000000E+01 0.10000000E+01 0.10000000E+01 0.10000000E+01
0.10000000E+01 0.10000000E+01 0.10000000E+01 0.10000000E+01 0.10000000E+01 0.10000000E+01 0.10000000E+01 0.10000000E+01 0.10000000E+01 0.10000000E+01
0.10000000E+01 0.10000000E+01 0.10000000E+01 0.10000000E+01 0.10000000E+01 0.10000000E+01 0.10000000E+01 0.10000000E+01 0.10000000E+01 0.10000000E+01
0.10000000E+01 0.10000000E+01 0.10000000E+01 0.10000000E+01 0.10000000E+01 0.10000000E+01 0.10000000E+01 0.10000000E+01 0.10000000E+01 0.10000000E+01
0.10000000E+01 0.10000000E+01 0.10000000E+01 0.10000000E+01 0.10000000E+01 0.10000000E+01 0.10000000E+01 0.10000000E+01 0.10000000E+01 0.10000000E+01
0.10000000E+01 0.10000000E+01 0.10000000E+01 0.10000000E+01 0.10000000E+01 0.10000000E+01 0.10000000E+01 0.10000000E+01 0.10000000E+01 0.10000000E+01
0.10000000E+01 0.10000000E+01 0.10000000E+01 0.10000000E+01 0.10000000E+01 0.10000000E+01 0.10000000E+01 0.10000000E+01 0.10000000E+01 0.10000000E+01
0.10000000E+01 0.10000000E+01 0.10000000E+01 0.10000000E+01 0.10000000E+01 0.10000000E+01 0.10000000E+01 0.10000000E+01 0.10000000E+01 0.10000000E+01
0.10000000E+01 0.10000000E+01 0.10000000E+01 0.10000000E+01 0.10000000E+01 0.10000000E+01 0.10000000E+01 0.10000000E+01 0.10000000E+01 0.10000000E+01
0.10000000E+01 0.10000000E+01 0.10000000E+01 0.10000000E+01 0.10000000E+01 0.10000000E+01 0.10000000E+01 0.10000000E+01 0.10000000E+01 0.10000000E+01
0.10000000E+01 0.10000000E+01 0.10000000E+01 0.10000000E+01 0.10000000E+01 0.10000000E+01 0.10000000E+01 0.10000000E+01 0.10000000E+01 0.10000000E+01

0.10000000E+01 0.10000000E+01 0.10000000E+01 0.10000000E+01 0.10000000E+01 0.10000000E+01 0.10000000E+01 0.10000000E+01 0.10000000E+01 0.10000000E+01
0.10000000E+01 0.10000000E+01 0.10000000E+01 0.10000000E+01 0.10000000E+01 0.10000000E+01 0.10000000E+01 0.10000000E+01 0.10000000E+01 0.10000000E+01
0.10000000E+01 0.10000000E+01 0.10000000E+01 0.10000000E+01 0.10000000E+01 0.10000000E+01 0.10000000E+01 0.10000000E+01 0.10000000E+01 0.10000000E+01
0.10000000E+01 0.10000000E+01 0.10000000E+01 0.10000000E+01 0.10000000E+01 0.10000000E+01 0.10000000E+01 0.10000000E+01 0.10000000E+01 0.10000000E+01
0.10000000E+01 0.10000000E+01 0.10000000E+01 0.10000000E+01 0.10000000E+01 0.10000000E+01 0.10000000E+01 0.10000000E+01 0.10000000E+01 0.10000000E+01
0.10000000E+01 0.10000000E+01 0.10000000E+01 0.10000000E+01 0.10000000E+01 0.10000000E+01 0.10000000E+01 0.10000000E+01 0.10000000E+01 0.10000000E+01
0.10000000E+01 0.10000000E+01 0.10000000E+01 0.10000000E+01 0.10000000E+01 0.10000000E+01 0.10000000E+01 0.10000000E+01 0.10000000E+01 0.10000000E+01
0.10000000E+01 0.10000000E+01 0.10000000E+01 0.10000000E+01 0.10000000E+01 0.10000000E+01 0.10000000E+01 0.10000000E+01 0.10000000E+01 0.10000000E+01
0.10000000E+01 0.10000000E+01 0.10000000E+01 0.10000000E+01 0.10000000E+01 0.10000000E+01 0.10000000E+01 0.10000000E+01 0.10000000E+01 0.10000000E+01
0.10000000E+01 0.10000000E+01 0.10000000E+01 0.10000000E+01 0.10000000E+01 0.10000000E+01 0.10000000E+01 0.10000000E+01 0.10000000E+01 0.10000000E+01
0.10000000E+01 0.10000000E+01 0.10000000E+01 0.10000000E+01 0.10000000E+01 0.10000000E+01 0.10000000E+01 0.10000000E+01 0.10000000E+01 0.10000000E+01
0.10000000E+01 0.10000000E+01 0.10000000E+01 0.10000000E+01 0.10000000E+01 0.10000000E+01 0.10000000E+01 0.10000000E+01 0.10000000E+01 0.10000000E+01
0.10000000E+01 0.10000000E+01 0.10000000E+01 0.10000000E+01 0.10000000E+01 0.10000000E+01 0.10000000E+01 0.10000000E+01 0.10000000E+01 0.10000000E+01
0.10000000E+01 0.10000000E+01 0.10000000E+01 0.10000000E+01 0.10000000E+01 0.10000000E+01 0.10000000E+01 0.10000000E+01 0.10000000E+01 0.10000000E+01
0.10000000E+01 0.10000000E+01 0.10000000E+01 0.10000000E+01 0.10000000E+01 0.10000000E+01 0.10000000E+01 0.10000000E+01 0.10000000E+01 0.10000000E+01
```

Figure A.3 VTRAN2_TEST_1.BUD

```
   4    3  0.00000000E+00
 0.00000000E+00  0.25000000E+00  0.25000000E+00  0.25000000E+00  0.25000000E+00  0.25000000E+00
 0.00000000E+00  0.25000000E+00  0.25000000E+00  0.25000000E+00  0.25000000E+00  0.25000000E+00
 0.00000000E+00  0.25000000E+00  0.25000000E+00  0.25000000E+00  0.25000000E+00  0.25000000E+00
 0.00000000E+00  0.25000000E+00  0.25000000E+00  0.25000000E+00  0.25000000E+00  0.25000000E+00
 0.00000000E+00  0.25000000E+00  0.25000000E+00  0.25000000E+00  0.25000000E+00  0.25000000E+00
 0.00000000E+00  0.00000000E+00  0.00000000E+00  0.00000000E+00  0.00000000E+00  0.00000000E+00
-0.50000000E+00 -0.50000000E+00 -0.50000000E+00 -0.50000000E+00 -0.50000000E+00 -0.50000000E+00
-0.50000000E+00 -0.50000000E+00 -0.50000000E+00 -0.50000000E+00 -0.50000000E+00 -0.50000000E+00
-0.50000000E+00 -0.50000000E+00 -0.50000000E+00 -0.50000000E+00 -0.50000000E+00 -0.50000000E+00
-0.50000000E+00 -0.50000000E+00 -0.50000000E+00 -0.50000000E+00 -0.50000000E+00 -0.50000000E+00
```

Figure A.4 VTRAN2_TEST_1.VEL

```
command file                 = VTRAN2_TEST_1.CMD
budget file                  = VTRAN2_TEST_1.BUD
(binary) velocity transfer file = VTRAN2_TEST_1.TRN
diagnostic/debug file        = VTRAN2_TEST_1.DBG
(ascii) velocity output file   = VTRAN2_TEST_1.VEL
 author  = Joseph F. Kanney
 date    = 2003.09.24
 title   = vtran2 test 1
 format  = (448e16.8)
 iscrn   =    0
 ncolmf  =   10
 nrowmf  =   15
 jshftx  =    3
 ishfty  =    7
 ncx     =    4
 ncy     =    3
 dx      = 0.1000E+01
 dy      = 0.2000E+01
 dz      = 0.2000E+01
Using input format ( 1) = (448e16.8)
VTRAN >> Reading budget file
VTRAN >> Processing velocities
VTRAN >> Writing velocity transfer file
VTRAN >> Writing ascii velocity output file
VTRAN >> Cleaning up
VTRAN >> Normal Completion
```

Figure A.5 VTRAN2_TEST_1.DBG

A.3.2 VTRAN2 Verification Test Case 2

In this test we specify a synthetic volume flux field on the 10x15 mesh such that the modulus of the velocity component equals the row number and the fractional part equals the column number. Thus the cell number is embedded in the value of the flux component. We then specify $dx = dy = dz = 1$ in the VTRAN2 command file. In this way, we can visually inspect the velocity file to verify that the correct row and column indices are extracted.

The command file (VTRAN2_TEST_2.CMD), and the budget file (VTRAN2_TEST_2.BUD) are shown in, Figure A.6 and Figure A.7, respectively. Running VTRAN2 with these input files produces the ASCII velocity file (VTRAN2_TEST_2.VEL) and the diagnostic file (VTRAN2_TEST_2.DBG) show in, Figure A.8 and Figure A.9, respectively. We note from the velocity component values that the correct translation of indices between the two meshes has been effected.

```
* author
Joseph F. Kanney
* date
2003.09.24
* title
vtran2 test 2
* input format type
(448e16.8)
* iscrn > 0 will print to screen, otherwise to dbg file
0
* ncol nrow
10 15
* jshftx ishfty ncx ncy
3 7 4 3
* dx dy dz (3e10.3)
 1.000E+00 1.000E+00 1.000E+00
```

Figure A.6 VTRAN2_TEST_2.CMD

```
0.10100000E+01 0.10200000E+01 0.10300000E+01 0.10400000E+01 0.10500000E+01 0.10599999E+01 0.10700001E+01 0.10800000E+01 0.10900000E+01 0.11000000E+01
0.20100000E+01 0.20200000E+01 0.20300000E+01 0.20400000E+01 0.20500000E+01 0.20599999E+01 0.20699999E+01 0.20799999E+01 0.20899999E+01 0.20999999E+01
0.30100000E+01 0.30200000E+01 0.30300000E+01 0.30400000E+01 0.30500000E+01 0.30599999E+01 0.30699999E+01 0.30799999E+01 0.30899999E+01 0.30999999E+01
0.40100002E+01 0.40200000E+01 0.40300002E+01 0.40400000E+01 0.40500002E+01 0.40599999E+01 0.40700002E+01 0.40799999E+01 0.40900002E+01 0.40999999E+01
0.50100002E+01 0.50200000E+01 0.50300002E+01 0.50400000E+01 0.50500002E+01 0.50599999E+01 0.50700002E+01 0.50799999E+01 0.50900002E+01 0.50999999E+01
0.60100002E+01 0.60200000E+01 0.60300002E+01 0.60400000E+01 0.60500002E+01 0.60599999E+01 0.60700002E+01 0.60799999E+01 0.60900002E+01 0.60999999E+01
0.70100002E+01 0.70200000E+01 0.70300002E+01 0.70400000E+01 0.70500002E+01 0.70599999E+01 0.70700002E+01 0.70799999E+01 0.70900002E+01 0.70999999E+01
0.80100002E+01 0.80200005E+01 0.80299997E+01 0.80400000E+01 0.80500002E+01 0.80600004E+01 0.80699997E+01 0.80799999E+01 0.80900002E+01 0.81000004E+01
0.90100002E+01 0.90200005E+01 0.90299997E+01 0.90400000E+01 0.90500002E+01 0.90600004E+01 0.90699997E+01 0.90799999E+01 0.90900002E+01 0.91000004E+01
0.10010000E+02 0.10020000E+02 0.10030000E+02 0.10040000E+02 0.10050000E+02 0.10060000E+02 0.10070000E+02 0.10080000E+02 0.10090000E+02 0.10100000E+02
0.11010000E+02 0.11020000E+02 0.11030000E+02 0.11040000E+02 0.11050000E+02 0.11060000E+02 0.11070000E+02 0.11080000E+02 0.11090000E+02 0.11100000E+02
0.12010000E+02 0.12020000E+02 0.12030000E+02 0.12040000E+02 0.12050000E+02 0.12060000E+02 0.12070000E+02 0.12080000E+02 0.12090000E+02 0.12100000E+02
0.13010000E+02 0.13020000E+02 0.13030000E+02 0.13040000E+02 0.13050000E+02 0.13060000E+02 0.13070000E+02 0.13080000E+02 0.13090000E+02 0.13100000E+02
0.14010000E+02 0.14020000E+02 0.14030000E+02 0.14040000E+02 0.14050000E+02 0.14060000E+02 0.14070000E+02 0.14080000E+02 0.14090000E+02 0.14100000E+02
0.15010000E+02 0.15020000E+02 0.15030000E+02 0.15040000E+02 0.15050000E+02 0.15060000E+02 0.15070000E+02 0.15080000E+02 0.15090000E+02 0.15100000E+02

0.10100000E+01 0.10200000E+01 0.10300000E+01 0.10400000E+01 0.10500000E+01 0.10599999E+01 0.10700001E+01 0.10800000E+01 0.10900000E+01 0.11000000E+01
0.20100000E+01 0.20200000E+01 0.20300000E+01 0.20400000E+01 0.20500000E+01 0.20599999E+01 0.20699999E+01 0.20799999E+01 0.20899999E+01 0.20999999E+01
0.30100000E+01 0.30200000E+01 0.30300000E+01 0.30400000E+01 0.30500000E+01 0.30599999E+01 0.30699999E+01 0.30799999E+01 0.30899999E+01 0.30999999E+01
0.40100002E+01 0.40200000E+01 0.40300002E+01 0.40400000E+01 0.40500002E+01 0.40599999E+01 0.40700002E+01 0.40799999E+01 0.40900002E+01 0.40999999E+01
0.50100002E+01 0.50200000E+01 0.50300002E+01 0.50400000E+01 0.50500002E+01 0.50599999E+01 0.50700002E+01 0.50799999E+01 0.50900002E+01 0.50999999E+01
0.60100002E+01 0.60200000E+01 0.60300002E+01 0.60400000E+01 0.60500002E+01 0.60599999E+01 0.60700002E+01 0.60799999E+01 0.60900002E+01 0.60999999E+01
0.70100002E+01 0.70200000E+01 0.70300002E+01 0.70400000E+01 0.70500002E+01 0.70599999E+01 0.70700002E+01 0.70799999E+01 0.70900002E+01 0.70999999E+01
0.80100002E+01 0.80200005E+01 0.80299997E+01 0.80400000E+01 0.80500002E+01 0.80600004E+01 0.80699997E+01 0.80799999E+01 0.80900002E+01 0.81000004E+01
0.90100002E+01 0.90200005E+01 0.90299997E+01 0.90400000E+01 0.90500002E+01 0.90600004E+01 0.90699997E+01 0.90799999E+01 0.90900002E+01 0.91000004E+01
0.10010000E+02 0.10020000E+02 0.10030000E+02 0.10040000E+02 0.10050000E+02 0.10060000E+02 0.10070000E+02 0.10080000E+02 0.10090000E+02 0.10100000E+02
0.11010000E+02 0.11020000E+02 0.11030000E+02 0.11040000E+02 0.11050000E+02 0.11060000E+02 0.11070000E+02 0.11080000E+02 0.11090000E+02 0.11100000E+02
0.12010000E+02 0.12020000E+02 0.12030000E+02 0.12040000E+02 0.12050000E+02 0.12060000E+02 0.12070000E+02 0.12080000E+02 0.12090000E+02 0.12100000E+02
0.13010000E+02 0.13020000E+02 0.13030000E+02 0.13040000E+02 0.13050000E+02 0.13060000E+02 0.13070000E+02 0.13080000E+02 0.13090000E+02 0.13100000E+02
0.14010000E+02 0.14020000E+02 0.14030000E+02 0.14040000E+02 0.14050000E+02 0.14060000E+02 0.14070000E+02 0.14080000E+02 0.14090000E+02 0.14100000E+02
0.15010000E+02 0.15020000E+02 0.15030000E+02 0.15040000E+02 0.15050000E+02 0.15060000E+02 0.15070000E+02 0.15080000E+02 0.15090000E+02 0.15100000E+02
```

Figure A.7 VTRAN2_TEST_2.BUD

```
  4    3  0.00000000E+00
0.00000000E+00 0.80299997E+01 0.80400000E+01 0.80500002E+01 0.80600004E+01 0.80699997E+01
0.00000000E+00 0.70300002E+01 0.70400000E+01 0.70500002E+01 0.70599999E+01 0.70700002E+01
0.00000000E+00 0.60300002E+01 0.60400000E+01 0.60500002E+01 0.60599999E+01 0.60700002E+01
0.00000000E+00 0.50300002E+01 0.50400000E+01 0.50500002E+01 0.50599999E+01 0.50700002E+01
0.00000000E+00 0.40300002E+01 0.40400000E+01 0.40500002E+01 0.40599999E+01 0.40700002E+01
0.00000000E+00 0.00000000E+00 0.00000000E+00 0.00000000E+00 0.00000000E+00 0.00000000E+00
-0.70300002E+01 -0.70400000E+01 -0.70500002E+01 -0.70599999E+01 -0.70700002E+01 -0.70799999E+01
-0.60300002E+01 -0.60400000E+01 -0.60500002E+01 -0.60599999E+01 -0.60700002E+01 -0.60799999E+01
-0.50300002E+01 -0.50400000E+01 -0.50500002E+01 -0.50599999E+01 -0.50700002E+01 -0.50799999E+01
-0.40300002E+01 -0.40400000E+01 -0.40500002E+01 -0.40599999E+01 -0.40700002E+01 -0.40799999E+01
```

Figure A.8 VTRAN2_TEST_2.VEL

```
command file                 = VTRAN2_TEST_2.CMD
budget file                  = VTRAN2_TEST_2.BUD
(binary) velocity transfer file = VTRAN2_TEST_2.TRN
diagnostic/debug file        = VTRAN2_TEST_2.DBG
(ascii) velocity output file   = VTRAN2_TEST_2.VEL
 author   = Joseph F. Kanney
 date     = 2003.09.24
 title    = vtran2 test 2
 format   = (448e16.8)
 iscm     =    0
 ncolmf   =   10
 nrowmf   =   15
 jshftx   =    3
 ishfty   =    7
 ncx      =    4
 ncy      =    3
 dx       = 0.1000E+01
 dy       = 0.1000E+01
 dz       = 0.1000E+01
Using input format ( 1) = (448e16.8)
VTRAN >> Reading budget file
VTRAN >> Processing velocities
VTRAN >> Writing velocity transfer file
VTRAN >> Writing ascii velocity output file
VTRAN >> Cleaning up
VTRAN >> Normal Completion
```

Figure A.9 VTRAN2_TEST_2.DBG

Chavez, Mario Joseph

From: Stein, Joshua Stephenson
Sent: Wednesday, October 19, 2005 3:13 PM
To: Chavez, Mario Joseph
Cc: Kanney, Joseph F; Kessel, David S
Subject: Signature Authority

Attachments: PABC_CFT_DRC_Tech_JSS-1019-2005.doc

Mario,

I have reviewed the report entitled: "Analysis Report for the CRA-2004 PABC Culebra Flow and Transport Calculations " and have given my comments (DRC) to author Joe Kanney. He has responded to all my comments and I am satisfied with his responses. In my absence, I grant signature you, Mario Chavez, signature authority for the report and DRC. I am attaching the final DRC.

Thanks,
Josh

Joshua S Stein Ph.D.
P.O. Box 5800 MS 0076
Sandia National Laboratories
Albuquerque, NM 87185-0776
Tel: 505-845-0936
Fax: 505-284-4002
Email: jsstein@sandia.gov

PABC_CFT_DRC_Te
ch_JSS-1019-200...

Chavez, Mario Joseph

From: Kanney, Joseph F
Sent: Wednesday, October 19, 2005 3:38 PM
To: Lowry, Thomas Stephen
Cc: Chavez, Mario Joseph
Subject: CRA-2004 PABC Culebra Report Signature Authority

Tom,

We've had a slight change of plans. EPA is making an announcement tomorrow starting the 45-day clock for the stakeholders' comment period on the CRA.
So we need to submit the Culebra Report and the PABC Summary Report today. Josh, Mario, and Dave have completed their reviews of the Culebra report.

Since you are traveling, I will sign the Culebra Report for you. When you get back, please respond to this email with a statement that it's OK for me to sign for you. Copy Mario on that email.

Thanks!

-- Joe

Joseph F. Kanney
Sandia National Laboratories
Carlsbad Programs Group
4100 National Parks Highway
Carlsbad, NM 88220
(505) 234-0033 (Carlsbad, NM)
(505) 284-2731 (Albuquerque, NM)
jfkanne@sandia.gov